



Establishing a readout for validating genetic interactions of *C. elegans*
PINK-1, LRK-1 and SGK-1 and their putative roles in regulating
endomembrane trafficking

written by:

Dipak Gangurde

Albert-Ludwigs-Universität Freiburg

Director:

Prof. Dr. Ralf Baumeister

Institut für Biologie 3

Bioinformatik und Molekulargenetik

Albert-Ludwigs-Universität Freiburg

Co-Director

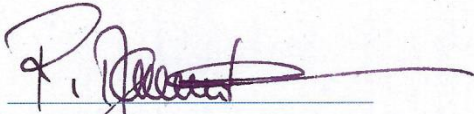
Dr. Sergio Simonetta

Technology center CITES

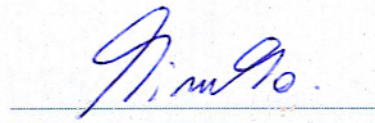
Sunchales, Argentina



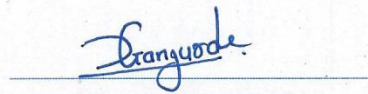
July 2013 – May 2015



Prof. Dr. Ralf Baumeister
Director



Dr. Sergio Simonetta
Co-Director



Dipak Gangurde
Student

Acknowledgement

I would like to take this opportunity to convey my sincere thanks to Prof. Dr. Ralf Baumeister, for allowing me to do my Master Thesis work in his lab. He has always been a great inspiration and motivation for me during this work. I enjoyed his supervision which is always with full of good advises and suggestions.

I would also like to thank Dr. Sergio Simonetta for co-directing my thesis work.

I want to thank Yijian Yan for his guidance and help in understanding necessary details of my project. All the lab members deserve a big thank you for discussing every detail and concern during our lab seminars. For excellent technical assistance Ruth Jähne deserve a thank you. Special thanks to my team mates Tim, Lena and Claudio for their support and spending good times. “Muchas gracias” to my IMBS amigos for sharing nice memories in Buenos Aires and Freiburg, special thanks to Ana Valreria for her Spanish lessons and translation.

Last I would like to thank my brother Bhushan and my parents for their continuous love and support.

Abstract

Endomembrane trafficking (ET) is required for maintaining cell homeostasis in eukaryotes. Endocytic recycling, endomembrane vesicular transport, autophagy, mitophagy are considered important aspects of ET process. LRRK2/LRK-1, PINK1/PINK-1, two genes associated with hereditary Parkinson's Disease, and SGK1/SGK-1, in distinct experimental settings, have been suggested to play either direct or indirect roles in regulating these processes. Previous work of my lab had indicated that these genes and their encoded proteins may be mechanistically linked. In addition, *C. elegans* PINK-1 and LRK-1 have been shown to function antagonistically in stress response and neurite outgrowth and also interaction between SGK-1 and hLRRK2/CeLRK-1 has been suggested in controlling cytoskeletal dynamics which may affect endocytosis and intracellular cell sorting. Our hypothesis is that PINK1, LRRK2, and SGK1 may share a common function in ET. Currently available readouts for the function of these genes do not relate to ET. Studying genetic interaction of these genes in *C. elegans* requires screenable phenotype associated with ET, and this was the focus of my master project.

In this work with mutant analysis and pharmacological studies I have found several new phenotypic readouts using *pink-1* mutant animals. Vacuole phenotype observed in *pink-1* animals was found to be rescued by loss of *lrk-1* in consistency with the antagonistic function of PINK-1 and LRK-1, although present results suggest that this vacuole phenotype may be independent of ET perturbations. In another readout, modulation of RAB-10 marker protein (*rab-10::gfp*) in the intestinal cells of *pink-1* animals suggested the potential role of PINK-1 in controlling transport of early endosomes during endomembrane trafficking. Furthermore I have also used the vacuole phenotype in SGK-1 transgene for an RNAi test to study putative interaction between LRK-1, PINK-1 and SGK-1, resulting in the identification of several modulators of this phenotype. Moreover *lrk-1* downregulation was sufficient to reduce the levels of transgenic SGK-1 expression, suppressing its phenotypic consequences. This data further support the existence of a mechanistic connection between LRK-1 and SGK-1.

Resumen

El tráfico endomembranoso (TE) es necesario para el mantener la homeostasis celular en eucariontes. El reciclaje endocítico, el transporte vesicular endomembranoso, la autofagia y mitofagia se consideran aspectos importantes en el proceso de TE. Y se ha propuesto que LRRK2/LRK-1, PINK1/PINK-1, genes asociados a la enfermedad de Parkinson hereditaria; y SGK1/SGK-1 desempeñan un rol directo o indirecto en la regulación de este proceso en distintas condiciones experimentales. Trabajos previos realizados en mi grupo han demostrado que estos genes y las proteínas que codifican podrían estar implicadas en mismo mecanismo de interacción. Por otra parte se demostró que PINK-1 y LRK-1 en *C. elegans* funcionan antagónicamente en respuesta al estrés y en el crecimiento de neuritas, también se ha propuesto que la interacción entre SGK-1 and hLRRK2/CeLRK-1 participa en el control de la dinámica del citoesqueleto que a su vez afecta la endocitosis y clasificación celular interna. Nuestra hipótesis es que PINK1, LRRK2 y SGK1 pueden compartir una función común en el TE. Las lecturas disponibles hasta ahora para la función de estos genes no se relacionan con TE. El estudio de la interacción genética de estos genes en *C. elegans* requiere fenotipos detectables asociados con TE, por lo tanto este fue el principal foco de mi proyecto de maestría.

En este trabajo mediante el análisis de mutantes y estudios farmacológicos encontré nuevas lecturas de *pink-1* mutado animal. Se halló que el fenotipo vacuola observado en *pink-1* animal puede ser rescatado por la pérdida de función de *lrk-1* que es consistente con la función antagónica de PINK-1 y LRK-1, aunque resultados aquí presentados mostraron que el fenotipo vacuola podría ser independiente de las perturbaciones de TE. En otra lectura, la modulación de la proteína marcadora RAB-10 en *pink-1* animal sugiere que PINK-1 tiene un rol potencial en el control del transporte de los endosomas tempranos durante el tráfico endomembranoso. Además también he utilizado el fenotipo vacuola ya identificado en el transgén SGK-1 para una prueba de RNAi y poder estudiar la interacción putativa entre LRK-1, PINK-1 y SGK-1 donde se identificaron varios moduladores del fenotipo. La supresión de *lrk-1* fue suficiente para reducir los niveles de expresión del SGK-1 transgénico, suprimiendo su fenotipo. Estos datos soportan la existencia de un mecanismo de conexión entre LRK-1 y SGK-1.

Abbreviations

::	fused to
°C	degree Celsius
µg	microgram
µM	micro molar
3'	3 prime
5'	5 prime
6-OHDA	6- Hydroxydopamine
ATP	Adenosine triphosphate
BLAST	Basic Local Alignment Research Tool
bp	base pairs
BR	Laboratory strain ID
<i>C. elegans</i>	<i>Caenorhabditis elegans</i>
cDNA	complementary DNA
CeLRK-1	<i>C. elegans</i> LRK-1
CGC	Caenorhabditis Genetics Center
COPI/II	Coat protein complex I/II
COR	C-terminal of ROC
DA neurons	dopaminergic neurons
DIC	Differential Interference Contrast microscopy
DMSO	Dimethyl sulfoxide
dNTP	deoxy-nucleotide tri-phosphate
DTC	distal tip cell
<i>E. coli</i>	<i>Escherichia coli</i>
e.g.	for example
ER	endoplasmic reticulum
ET	endomembrane trafficking
ETC	electron transport chain
Ex	extrachromosomal transgene
F1/2/3	first/second/third generation
GAP	GTPase-activating proteins
GEF	Guanine nucleotide exchange factor
GFP	Green Fluorescent Protein
hLRRK2	human LRRK2
hsp	heat shock protein
IS	Integrated strain
L1/2/3/4	larval stage
LB	Liquid Broth
LRRK2	Leucine-rich repeat kinase 2
MAP	Mitogen-activated protein
mg	milligram
mM	mill molar
MPTP	1-methyl-4-phenyl-1,2,3,6-tetrahydropyridine

n	number
NGM	Nematode Growth Medium
P0	Parental generation
PCR	polymerase chain reaction
PD	Parkinson's disease
PQ	Paraquat
RB	Laboratory oligonucleotide ID
RNAi	RNA interference
ROC	Ras of complex protein
ROS	Reactive oxygen species
S.E.M.	Standard error of the mean
SW-PCR	Single Worm Polymerase Chain Reaction
TGN	Trans Golgi network
WT	wild type

Content

Acknowledgement.....	i
Abstract	ii
Abbreviations.....	iv
1. Introduction	1
1.1 Endomembrane trafficking pathway	1
1.2 Parkinson’s Disease (PD)	2
1.2.1 Parkinson’s Disease and ET	3
1.3 Leucine Rich Repeat Kinase 2 (LRRK2)	3
1.3.1 LRRK2 function in ET	4
1.4 PTEN-induced Kinase 1 (PINK1)	6
1.4.1 PINK1 function in ET	7
1.5 Serum and Glucocorticoid Inducible Kinase (SGK)	8
1.5.1 SGK1 function in ET	9
1.6 <i>C. elegans</i> as a model organism to study ET	11
1.6.1 Defects related to ET	12
1.7 Genetic interaction between PINK1/PINK-1, LRRK2/LRK-1 and SGK1/SGK-1	14
1.7.1 PINK-1 and LRK-1 act antagonistically	14
1.7.2 SGK-1 regulates hLRRK2/CeLRK-1 mediated DTC migration defect	15
1.8 Paraquat induces reactive oxygen species (ROS) in pink-1 mutant	16
2. Hypothesis and Aims	17
2.1 Phenotypic readouts in pink-1 and lrk-1 mutants	17
2.1.1 Pharmacological approach to find ET defect	17
2.2 Characterization of ET phenotype using RAB-10::GFP marker strain	18
2.3 RNAi test for modulators of SGK-1 induced ET associated phenotype	18
2.4 Epistatic analysis	20
3. Materials and Methods	22
3.1 Materials	22
3.1.1 <i>C. elegans</i> strains	22
3.1.2 Bacteria strains	23
3.1.3 Oligonucleotides	23
3.1.4 Buffers and solutions	24
3.1.5 Media	24
3.1.6 Chemical compounds	25
3.1.7 Software’s	25
3.1.8 Equipment	25
3.1.9 Transgenic strains	26
3.2 Methods	26
3.2.1 Maintenance of <i>C. elegans</i>	26
3.2.2 Decontamination of <i>C. elegans</i>	26
3.2.3 Synchronization of <i>C. elegans</i> population	27
3.2.4 RNA interference assay	27

3.2.5	Crosses	28
3.2.5.1	Generation of Males by heat shock	38
3.2.5.2	Scheme for cross between <i>lrk-1(tm1898)</i> and <i>byIs207[sgk-1::gfp]</i>	29
3.2.6	Genotyping	30
3.2.6.1	Worm lysis	31
3.2.6.2	Polymerase chain reaction	31
3.2.7	DNA sequencing	32
3.2.8	Paraquat stress assay	32
3.2.9	Microscopy	34
3.2.10	Image Analysis	34
3.2.11	Statistical analysis	35
3.2.12	Bioinformatics	35
4.	Results	36
4.1	Phenotypic analysis of <i>pink-1</i> , <i>lrk-1</i> and their functionally related genes	36
4.2	<i>pink-1</i> animals shows a phenotypic change in intestine and hypodermis	37
4.2.1	Vacuole phenotype in <i>pink-1</i> suppressed by <i>lrk-1</i> loss of function	40
4.3	Generation <i>rab-10::gfp</i> reporter strain for characterization of phenotype by <i>pink-1</i>	41
4.4	Intracellular accumulation of RAB-10::GFP in <i>pink-1(tm1779)</i>	43
4.5	RNAi test for modulators of SGK-1 induced vacuole phenotype	45
4.6	Generation of reporter strain <i>lrk-1(tm1898);sgk-1::gfp(+)</i>	47
4.6.1	<i>lrk-1</i> downregulation suppresses SGK-1::GFP vacuole phenotype	48
4.6.2	<i>lrk-1</i> downregulation alters the SGK-1::GFP intensity	49
5.	Discussion	52
5.1	Phenotypic alterations in PD related genes	52
5.2	Antagonistic behavior of PINK-1 and LRK-1	53
5.3	Phenotypic change in the <i>pink-1</i> worms may related to ET defect	53
5.4	RNAi downregulation modulating SGK-1 induced vacuole phenotype	54
5.5	Mechanistic link between LRK-1 and SGK-1 regulating ET	56
6.	Conclusion	58
	References	60

1. Introduction

Membrane trafficking is the process by which proteins and other macromolecules are distributed throughout the cell, and released to or internalized from the extracellular space. It employs membrane-bound small vesicles and larger intracellular organelles, including the endoplasmic reticulum (ER), mitochondria, the Golgi complex, endosomes, lysosomes, and autophagosomes (Fig 1) (Mukherjee, Ghosh et al. 1997).

1.1 Endomembrane trafficking pathways:

Various transmembrane proteins and secretory proteins are synthesized in ER and transported in the form of COPII coated vesicles to the Golgi through ER exit sites (Bonifacino and Glick). These cargos are then sorted and then delivered to their destination such as plasma membrane, endosomes and lysosomes via trans Golgi network (TGN) or recycled from Golgi to ER via COPI mediated retrograde transport.

In another pathway, cell surface proteins along with some extracellular macromolecules internalized through the process called endocytosis. Endocytosis of these cargos took place either through clatherin dependent or clatherin independent mechanism (Brodsky, Chen et al. , Mayor and Pagano). Internalized cargos are then transported to endosomes, where they get sorted either to lysosome for their degradation or recycled to plasma membrane via recycling endosome compartment (REC), or may be transported to the TGN via retrograde transport mechanism (Grant and Donaldson , Seaman).

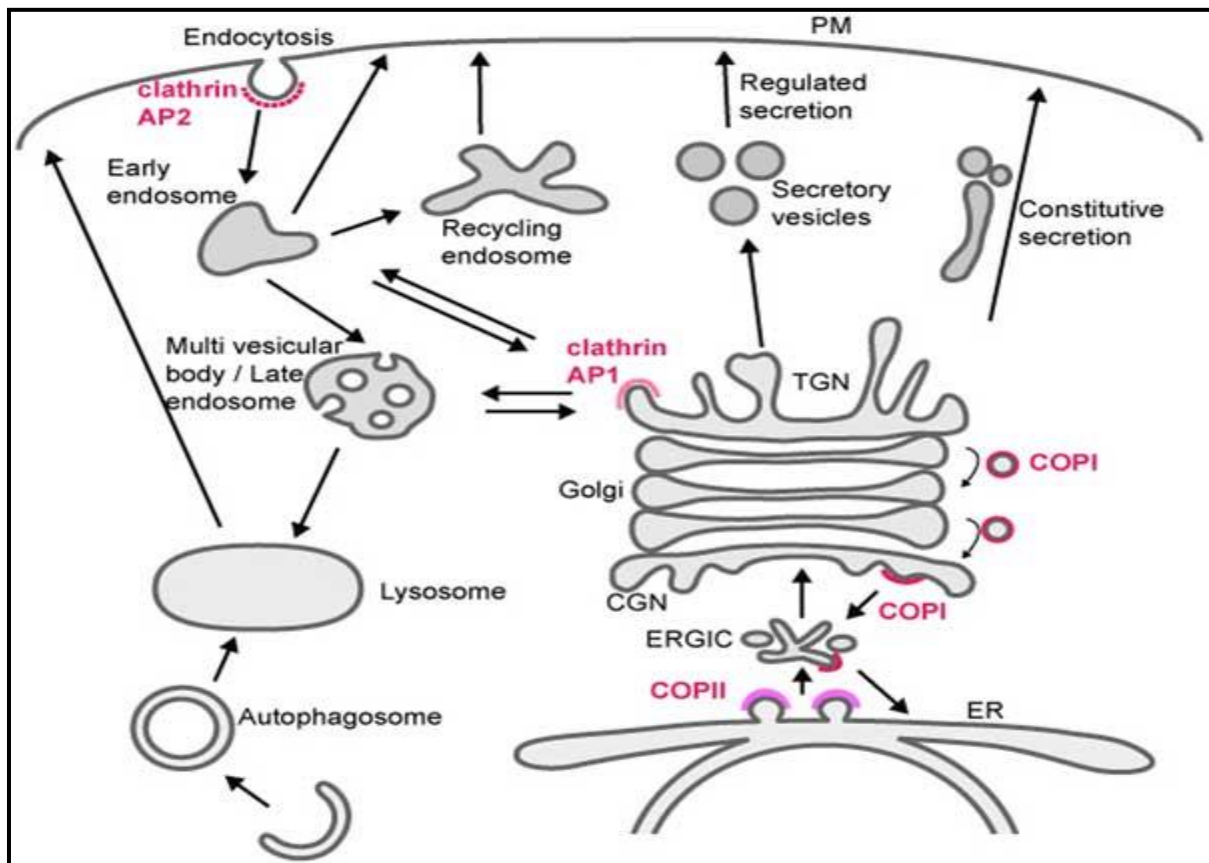


Fig 1. Endomembrane trafficking pathways: Transport is mediated by budding and fission of transport carriers (vesicles or tubules), fusion of organelles or maturation of organelles. Budding of some proteins and representative coat proteins are indicated. Adapted from (Mukherjee, Ghosh et al. 1997).

On the other hand, large particles like apoptotic cell bodies, cytoplasmic organelles and other macromolecules reach to lysosomes for their degradation via know mechanism like phagocytosis, autophagy or mitophagy, where these cytoplasmic cargos are encircled by distinct double membranes and then fused with lysosomes (Sato and Sato) and will eventually be digested for recycling.

1.2 Parkinson's Disease (PD)

Parkinson's disease is the second most common age related neurodegenerative movement disorder characterized by resting tremor, slowness of movement, muscular rigidity and postural instability. The neuropathological hallmarks of PD include progressive degeneration of dopaminergic neurons in the substantia nigra pars compacta, and the presence of intraneuronal cytoplasmic inclusions called Lewy bodies in surviving neurons, which are rich in α -synuclein (Halliday, Klenerman et al.). The majority of PD cases appear to be idiopathic and probably reflect a complex interaction between age, genetic predisposition and environmental factors (Lang and Lozano 1998). Despite lot of research, the

molecular and cellular mechanisms underlying the pathogenesis of Parkinson's disease (PD) have largely remained unknown. Recent advances in genetic studies suggested that mutation in several genes have been linked to familial forms of PD, including mutations in LRRK2 (leucine-rich repeat kinase 2), SNCA (α synuclein), PARK2 (parkin), PINK1 (phosphatase and tensin homologue deleted on chromosome 10-induced putative kinase 1), PARK7 (DJ-1), and GBA (acid b-glucosidase) (Singleton, Farrer et al. 2013). A major task ahead is to validate the molecular mechanism by which these genes cause clinical and pathological characteristics leading to development of PD and studying mechanistic role of these genes in regulating ET is one of the prime object of this study.

1.2.1 Parkinson's disease and ET

ET as a complex process involving various trafficking steps, have been implicated in several neurodegenerative and neurodevelopmental disease such as PD. Genetic mutation and polymorphism leading to subtle alteration in endomembrane trafficking has been shown to have association with development of late onset familial PD, which strongly suggest ET is an important aspect in this disease (MacLeod, Rhinn et al. 2013, Gomez-Suaga, Rivero-Rios et al. 2014, Perrett, Alexopoulou et al. 2015). Although precise role of α -syn and LRRK2 in pathogenesis of PD is remain to be unclear, α -Syn mutations have been reported to modify synaptic vesicle kinetics (Abeliovich, Schmitz et al. 2000) as well as trafficking to the Golgi apparatus in a variety of model systems (Cooper, Gitler et al. 2006, Thayanidhi, Helm et al. 2010), whereas LRRK2 mutations are implicated in effective lysosomal protein degradation and macroautophagy in which cytosolic proteins and protein aggregates delivers to lysosomes for degradation (Dodson, Zhang et al. 2012), Heo, 2010; MacLeod, 2006]. Recent discovery have also identifies rare autosomal dominant familial PD mutation in *VPS35* (Vilarino-Guell, Wider et al. 2011, Zimprich, Benet-Pages et al. 2011), which encodes a component of the retromer complex that guides protein sorting from the endosome-lysosome degradation pathway retrogradely to the Golgi apparatus (Seaman, McCaffery et al. 1998, Bonifacino and Hurley 2008, Skinner and Seaman 2009), suggests that defective protein sorting in vesicular compartments while membrane trafficking process may play a role in PD.

1.3 Leucine Rich Repeat Kinase 2 (LRRK2):

LRRK2 is 285 kDa multidomain protein coded by 51 exons, belongs to the ROCO family of proteins and contains six discrete domains including ankyrin repeats (ANK) at the N-terminus, followed by leucine rich repeats (LRR), a (Miro-like) GTPase ROC (Ras in complex proteins) domain, the COR (C-terminal of Roc) domain in the central region, a serine-threonine kinase domain, and a WD40 protein interaction domain at the C-terminal end (Fig 2) (Bosgraaf and Van Haastert 2003, Mata, Wedemeyer et al. 2006).

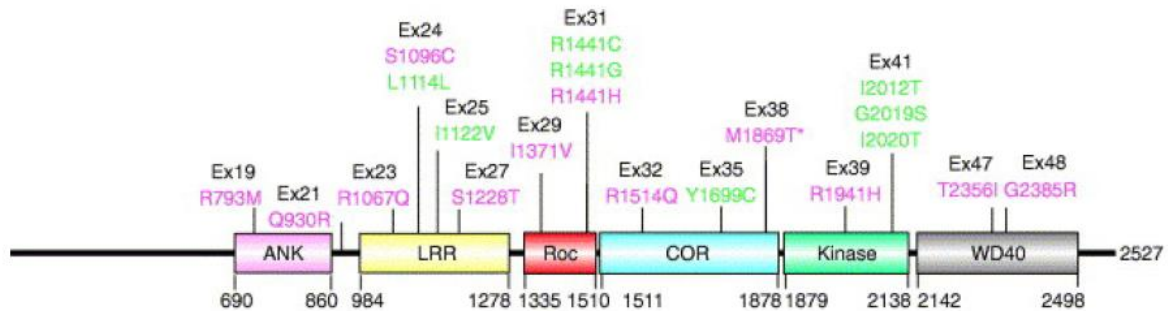


Fig 2: Domain structure and pathogenic mutations of human LRRK2. The 2527 aa protein LRRK2 consists of six discrete domains including the ankyrin repeat region (ANK), leucine-rich repeat domain (LRR), the Ras of complex (ROC) GTPase with a C-terminal of Ras (COR) domain, a serine/threonine kinase and WD40 repeats. The position of all putative pathogenic aa substitutions is indicated in magenta; point mutations associated with familial forms of PD are shown in green. The corresponding exon numbers are depicted in black. Fig adapted from (Mata, Wedemeyer et al. 2006).

LRRK2 has been identified as a gene responsible for PARK-8 linked autosomal dominant inherited familial PD (Paisan-Ruiz, Jain et al. 2004). *LRRK2* mutations were found in 3 to 5% of familial and 1 to 3% of sporadic PD cases (Khan, Jain et al. 2005) (Di Fonzo, Rohe et al. 2005), (Gilks, Abou-Sleiman et al. 2005), (Ozelius, Senthil et al. 2006). Within or close to all domains of *LRRK2*, point mutations such as I1122V in the LRR domain, R1441C/Y1699C in the GTPase domain, or G2019S/I2020T in the kinase domain (Farrer, Stone et al. 2005, Greggio, Jain et al. 2006, Mata, Wedemeyer et al. 2006) have already been reported. Of these, the most frequent mutation is G2019S found in the activation loop of the kinase domain (Aasly, Toft et al. 2005). Expression of mutant *LRRK2* with either reduced or increased kinase activity has been suggested to cause loss of dopaminergic neurons which consequently leads to the development of Parkinsonism (Greggio, Jain et al. 2006, Iaccarino, Crosio et al. 2007, Jaleel, Nichols et al. 2007).

1.3.1 *LRRK2* function in ET

Physiological role of *LRRK2* is still unclear. However, presence of multiple functional motifs suggest a contribution to various processes (Bosgraaf and Van Haastert 2003, Thomas and Beal 2007). The similarity of the *LRRK2* GTPase domain to Ras-GTPases, as well as the association of *LRRK2* with vesicular structures, implicate an important role of this protein in the biogenesis and/or regulation of vesicular transport (Biskup, Moore et al. 2006, Guo, Gandhi et al. 2007).

LRRK2 has been studied in the context of ET, where researchers showed that *LRRK2* co-localized consistently to the Golgi apparatus and Golgi-associated

vesicles, ER, lysosomes and mitochondria and to a significantly lesser degree, to vesicle markers such as synaptotagmin (Biskup, Moore et al. 2006). Analysis of LRRK2 in presynaptic and postsynaptic region showed that silencing of LRRK2 alters synaptic transmission (Fig 3)(Piccoli, Condliffe et al. 2011). It has been shown that excitatory postsynaptic current in postsynaptic neurons connected to silenced LRRK2- presynaptic neurons increase two-fold compared to controls (Piccoli, Condliffe et al. 2011). This suggested that LRRK2 might modulate synaptic vesicle trafficking and distribution, and, therefore, regulates dynamics between vesicle pools inside the pre- and post-synaptic terminals (Piccoli, Condliffe et al. 2011).

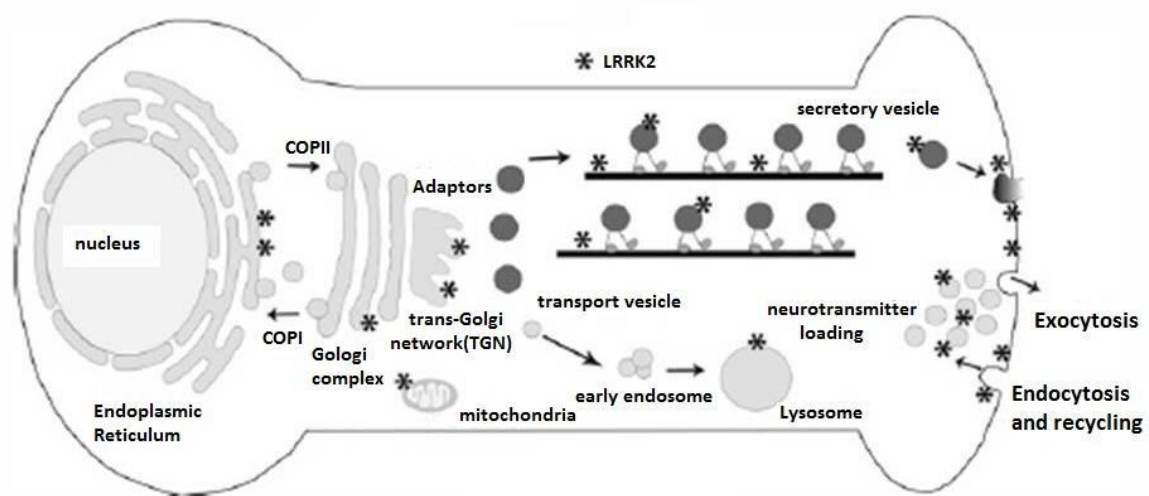


Fig 3: LRRK2 localization in different cellular districts affecting vesicle trafficking
LRRK2 (indicated by asterisks) localizes with the ER, Golgi complex, synaptic vesicles and lipid rafts and may be involved in both anterograde and retrograde transport, regulating vesicle generation, motility, secretion and endocytosis. Moreover, LRRK2 also co-localizes with lysosomes that are generated by the addition of hydrolytic enzymes to early endosomes from the Golgi apparatus. Thus, membrane trafficking regulates different aspects of neuronal physiology ranging from neurotransmitter or neurotrophic factor release, insertion of cell membrane components and organelle biogenesis. Adapted from (Sanna, Del Giudice et al. 2012)).

LRRK2 has also been shown to interact with GTPase RAB5b, a key regulator of early endocytic vesicular trafficking (Shin, Jeong et al. 2008). Both proteins co-localize in synaptic vesicles. Alteration of LRRK2 expression either by overexpression or knockdown of endogenous LRRK2 in primary neuronal cells impairs presynaptic vesicle endocytosis. This defect was rescued by co-expression of functional Rab5b protein (Shin, Jeong et al. 2008).

PD associated *LRRK2* mutations are also implicated in defective transport of cytosolic proteins and proteins aggregates to the lysosome for their degradation (MacLeod, Dowman et al. 2006), (Dodson, Zhang et al. 2012). LRRK2 has been

shown to interact with RAB7L1 to modify intraneuronal protein sorting and Parkinson's disease risk (MacLeod, Rhinn et al. 2013). Defects in *RAB-71-LRRK2* pathway leads to abnormal lysosomal structure and defective retromer complex function that normally links the endolysosomal protein degradation system with Golgi apparatus (Seaman, McCaffery et al. 1998, Bonifacino and Hurley 2008).

Caenorhabditis elegans LRK-1, the orthologue of mammalian LRRK2, has also been shown to be required for transport and sorting of synaptic vesicle (SV) proteins to the axons (Sakaguchi-Nakashima, Meir et al.). Loss of *lrk-1* leads to aberrant localization of SV proteins to presynaptic and dendritic endings in neurons (Fig 4) (Sakaguchi-Nakashima, Meir et al. 2007). Whereas, in wild type, the synaptic vesicles strictly localize to axonal regions, in the absence of *lrk-1* they are also found in dendritic endings. In this case it has been suggested that *C. elegans* LRK-1 protein functions in the TGN to exclude SV proteins from dendrite specific transport (Sakaguchi-Nakashima, Meir et al. 2007).

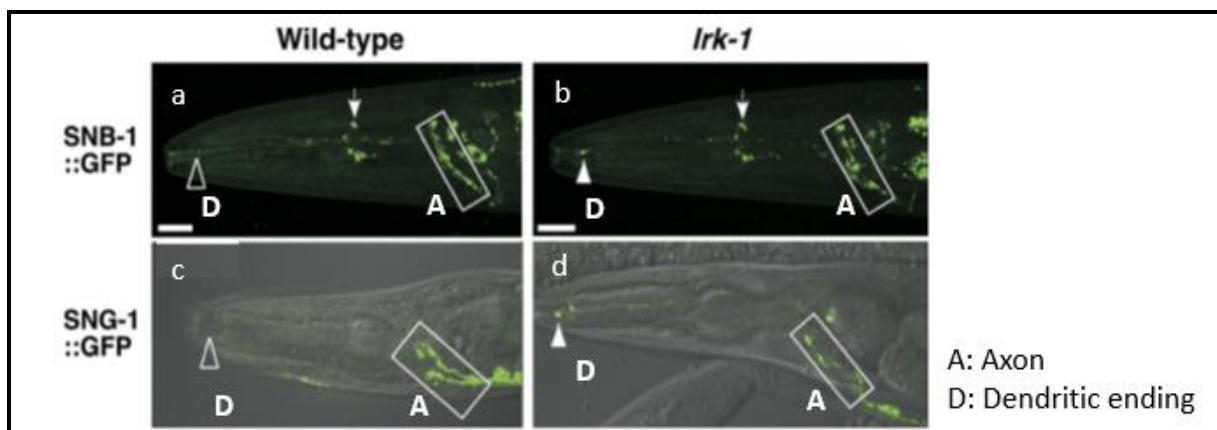


Fig 4: The effect of *lrk-1* mutation on localization of SV proteins. Localization of SV proteins in adult amphid sensory neurons (a-d): In *lrk-1(km17)* mutants, SNB-1::GFP (b), SNG-1::GFP (d) were mislocalized to the dendritic endings of these neurons. Dendritic endings (D) and axonal process of neurons indicated by arrowheads and squares respectively. Positions of SNB-1::GFP and endogenous SNB-1 are indicated by arrows. Adapted from (Sakaguchi-Nakashima, Meir et al. 2007).

1.4 PTEN-induced Kinase 1 (PINK1)

PINK1 encodes a 581 aa protein with a putative serine/threonine kinase domain and a mitochondrial targeting sequence (MTS) at the N-terminus (Fig 5) (Nakajima, Nimura et al. 2003, Valente, Abou-Sleiman et al. 2004, Kitada, Pisani et al. 2007). It is found to be transcriptionally activated in carcinoma mouse cell lines by the tumor suppressor PTEN (Unoki and Nakamura 2001, Nakajima, Nimura et al. 2003). PINK1 is the second kinase that was identified in familial form of PD (Valente, Abou-Sleiman et al. 2004).

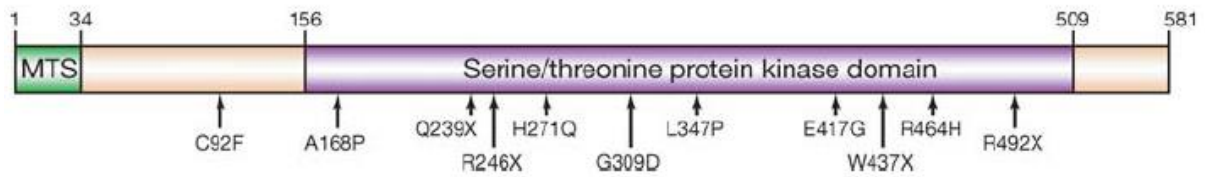


Fig 5: Domain structure and pathogenic mutations of human PINK1. PINK1 is a 581 aa protein, consisting of a mitochondrial targeting sequence (MTS) and a serine/threonine kinase domain. The position of aa missense mutations associated with familial forms of PD are indicated. Fig adapted from (Moore, West et al. 2005).

Various studies proposed mitochondrial localization of PINK1 (Silvestri, Caputo et al. 2005, Muqit, Abou-Sleiman et al. 2006, Pridgeon, Olzmann et al. 2007). However, recent studies have shown that a fraction of PINK1 can also be found in the cytoplasm (Beilina, Van Der Brug et al. 2005, Gandhi, Muqit et al. 2006, Takatori, Ito et al. 2008, Weihofen, Ostaszewski et al. 2008, Zhou, Huang et al. 2011). More than 25 missense mutation in PINK1 have been identified in PD patients, affecting either protein stability, localization or kinase activity. The kinase domain harbors most of these PD associated missense mutation that lead to reduction or complete loss of enzymatic activity (Fig 5) (Bonifati, Rohe et al. 2005, Ibanez, Lesage et al. 2006). However, both the physiological function of PINK1 and its relationship to PD is still under debate. PINK1 function has been studied in various model organisms, where downregulation of *PINK1* in *D. melanogaster* was shown to be associated with apoptotic muscle degeneration, probably caused by defects in mitochondrial function and morphology (Clark, Dodson et al. 2006, Park, Lee et al. 2006, Yang, Gehrke et al. 2006). Also, human PINK1 was found to prevent apoptosis by inhibition of cytochrome c release (Petit, Kawarai et al. 2005, Sim, Lio et al. 2006, Haque, Thomas et al. 2008). In addition, PINK1 and another Parkinson's related gene, PARKIN, have been implicated in a shared pathway regulating mitochondrial function in *M. Drosophila* to mediate degradation of dysfunctional mitochondria upon stress (Greene, Whitworth et al. 2003).

1.4.1 PINK1 function in ET

In a distinct pathway different from canonical mitophagy, PINK1 has been suggested to function in membrane vesicular trafficking pathways to regulate mitochondrial quality control. Oxidative stress induced formation of mitochondrial-derived-vesicles (MDVs) have been shown to target lysosomes for their degradation (Fig 6) (Soubannier, McLelland et al. 2012). Formation of MDVs is required to remove damaged proteins from mitochondria and transport them to lysosomes for their degradation. PINK1 and PARKIN have been demonstrated to be involved in the generation of these MDVs and, upon induction of oxidative stress, contribute to maintaining mitochondrial integrity by extracting damaged mitochondrial components. Loss of PINK1 and PARKIN impairs biogenesis of

MDVs and the ability of mitochondria to selectively degrade oxidized and damaged proteins. It has been proposed that, the resulting mitochondrial dysfunction may contribute to Parkinson's disease (McLelland, Soubannier et al.).

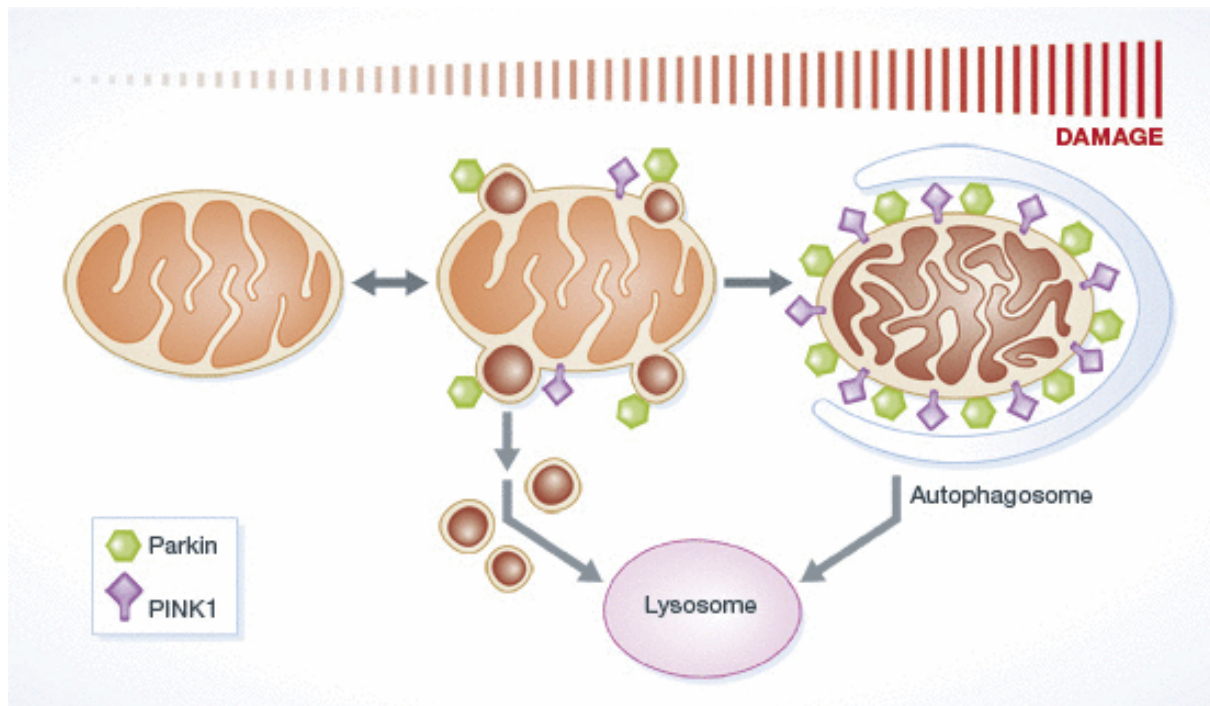


Fig 6: Rapid lysosomal targeting of oxidized mitochondrial proteins via mitochondria-derived vesicles constitutes an additional, mitophagy-independent quality control role for Parkin and PINK1, two proteins responsible for familial forms of Parkinson's disease. Adapted from (McLelland, Soubannier et al. 2014).

1.5 Serum and Glucocorticoid Inducible Kinase (SGK)

SGK is a member of the AGC family of Ser/Thr kinases, and was originally identified as an early induced gene in *Con8hd6* rat mammary tumor cell line when exposed to serum and/or glucocorticoids (Webster, Goya et al. 1993). In a second set of experiments, SGK was identified as a kinase that was upregulated upon exposure of cells to osmotic stress (Waldegger, Barth et al.) Three closely related isoforms exist for human and mouse SGK, referred to as SGK1, SGK2 and SGK3. They share up to 80% of aa sequence identity in their catalytic domain and have been shown to have overlapping function (Kobayashi and Cohen 1999, Kobayashi, Deak et al. 1999, Liu, Yang et al. 2000). The *C. elegans* genome contains only one gene coding for a SGK homologue, referred to as SGK-1, which shares 60% of aa sequence identity to the human SGK protein (Hertweck, Gobel et al. 2004). SGK isoforms displays domain organization similar to other Ser/Thr kinases family homologues (Lang, Bohmer et al. 2006, Kannan, Haste et al. 2007). They contain an N-terminal domain with one or several lipid-binding motifs, an S/T kinase domain in the central part, and a C-terminal X domain characterized by a consensus hydrophobic sequence (Fig 7).

In addition to glucocorticoids, several factors stimulate the transcription of SGK, including p53 tumor suppressor protein (Maiyar, Huang et al. 1996), transforming growth factor- β (TGF- β) (Waldegger, Klingel et al. 1999), platelet-derived growth factor (PDGF) (Alliston, Maiyar et al. 1997), follicle stimulating hormone (FSH) (Gonzalez-Robayna, Falender et al. 2000), and the peroxisome proliferator-activated receptor γ (PPAR γ) (Hong, Lockhart et al. 2003). Also, it has been shown that transcription of SGK is induced upon several environmental and intracellular stress (Waldegger, Barth et al. 1997, Bell, Leong et al. 2000, Leong, Maiyar et al. 2003, Iwata, Nomoto et al. 2004). At the posttranscriptional level, SGK1 is activated by phosphorylation at two highly conserved residue Thr266 in the activation loop of the kinase domain and Ser422 in the hydrophobic motif at the C-terminus (Kobayashi, Deak et al. 1999, Park, Leong et al. 1999, Hong, Lockhart et al. 2003).

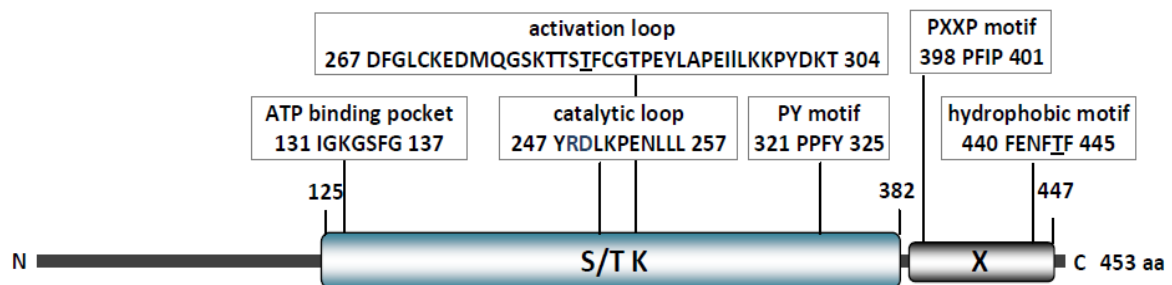


Fig 7: Schematic diagram of the *C. elegans* SGK-1. The conserved regions are accentuated in boxes. Numbers correspond to the amino acid (aa) region of *C. elegans* SGK-1. Underlined aa refers to the putative phosphorylation site; S, serine; T, threonine; K, kinase domain; X, X domain.

Pathophysiological role of SGK has been studied widely. High levels of SGK has been linked to various neurodegenerative diseases including Parkinson's disease (Schoenebeck, Bader et al. 2005, Stichel, Schoenebeck et al. 2005) and ischemic injury of the brain (Nishida, Nagata et al. 2004). In addition, ischemic injury of the brain (Nishida et al., 2004) have been linked with high levels of SGK. Elevated SGK levels have also been observed in fibrosing tissues of pancreas and liver (Klingel, Warntges et al. 2000, Fillon, Klingel et al. 2002), hypertension and increased body weight (Dieter, Palmada et al. 2004).

1.5.1 SGK1 function in ET

SGK 1 regulates various membrane transporters, ion channels and carriers. Na⁺/H⁺ exchanger 3 (NHE3/NHX3) is a transporter of Na⁺ in the human intestine and its activation is mediated by SGK1 through interacting with NHE regulating factor 2 (NHEFR2) (Yun 2003). It has been shown that NHE3 and one of the isoforms of huSGK (SGK3) colocalized in recycling endosomes, whereas SGK1 and SGK2 were diffusely distributed (Yun 2003).

Previous research in membrane trafficking shown that Ypk1, the yeast orthologue of human SGK1, affect fatty acid uptake and maintain energy homeostasis through regulating endocytosis which is one of the main aspects of membrane vesicular trafficking (Jacquier and Schneiter 2010). Cells lacking Ypk1 activity failed to grow under fatty acid auxotrophic condition and showed impaired uptake activity (Fig 8). It has been shown that Ypk1 is specifically required for the internalization step during endocytosis which is involved in the uptake of fatty acids (Jacquier and Schneiter 2010).

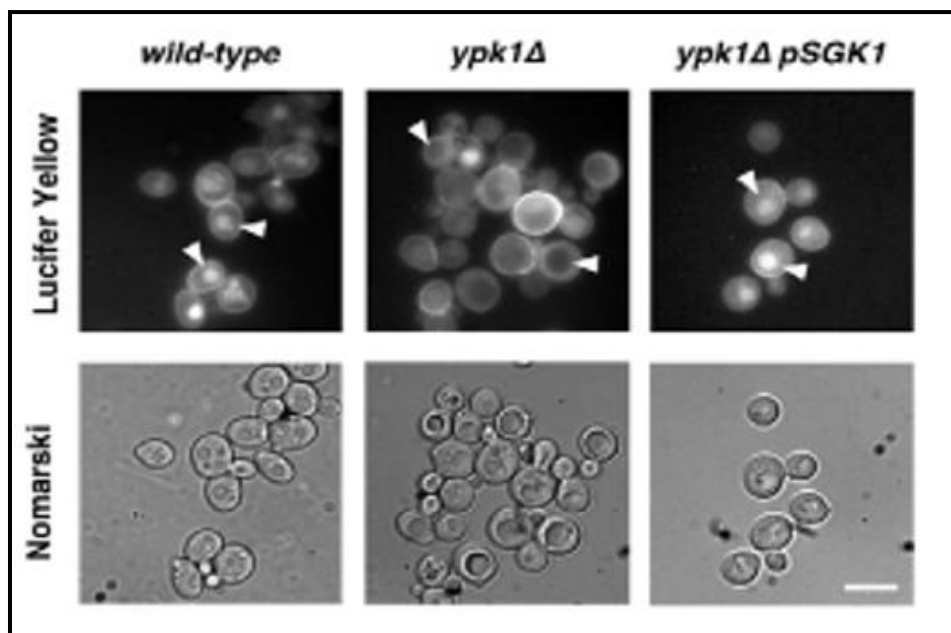


Fig 8: The fatty-acid-uptake defect of *ypk1Δ* mutant cells is rescued by human Sgk1. Sgk1 rescues the defect in fluid-phase endocytosis of *ypk1Δ* mutant cells. Cells of the indicated genotype were incubated with Lucifer Yellow for 60 minutes and examined by fluorescence microscopy. Uptake and transport to the vacuole of the fluidphase marker is indicated by arrowheads. Scale bar: 5μm. Adapted from (Jacquier and Schneiter 2010).

In addition, our lab has recently hypothesized that SGK-1, the *C. elegans* orthologue of mammalian SGKs, negatively regulates membrane trafficking in the intestine [Yijian Yan, unpublished work]. In this context, transgenic expression of SGK-1 was sufficient to generate large vacuoles in the intestine of the respective animals, which is considered to be an indicator of impaired membrane trafficking in intestinal cells [Yijian Yan unpublished work].

1.6 *C. elegans* as a model organism to study ET

Studies in *Caenorhabditis elegans* have revealed diverse roles of membrane trafficking in physiology and development and have also provided molecular insights into the fundamental mechanisms that direct cargo sorting, vesicle budding, membrane fission and fusion (Grant and Sato). Many of these studies have identified novel mechanisms regulating various steps in ET which can predict mechanisms of ET in mammals. Endocytosis, one of the main aspect of ET, has been studied extensively in *C. elegans* in non-polarized cells such as oocytes, coelomocytes, and polarized cells, such as neurons and epithelial cells and the intestine.

One of the genetic screen to study ET found eleven genes by using a receptor mediated endocytosis (RME) assay, where oocytes fail to uptake a intestinally secreted yolk protein YP170A (Grant and Hirsh 1999, Balklava, Pant et al. 2007). YP170::GFP adult hermaphrodites displayed bright fluorescent oocytes, bright embryos in uterus, bright intestine and dim pseudocoelom (body cavity), however worms defective in uptake showed dim or dark oocytes and embryos and the body cavity was filled with fluorescent YP170::GFP (Grant and Hirsh 1999, Balklava, Pant et al. 2007). This phenotype could be a result of defect in endocytosis, recycling or cell surface delivery of yolk receptor (RME-2) in oocytes (Balklava, Pant et al. 2007).

In another test for ET regulators, a coelomocyte uptake defective (CUP) assay identified 14 gene mutants that failed to endocytose green fluorescence protein (GFP) (Fares and Greenwald 2001). Polarized epithelium of intestine and neurons were also used in studies focusing on basolateral recycling mechanisms, where internalized cargos are recycled from endosomes to plasma membrane via recycling endosome compartment (REC) (Chen, Schweinsberg et al. 2006). The polarized nature of these cells provides an interesting case to study ET since they maintain two distinct plasma membrane domains, the apical and the basolateral membrane of the intestine, and the axonal and dendritic region in neurons.

Rab proteins have been found to be master regulators of ET and each step of membrane transport is thought to require at least one member out of 29 predicted Rab members encoded in the *C. elegans* genome (Pereira-Leal and Seabra 2001). Rabs regulating membrane transport included vesical formation recruitment of cargos during budding transport carriers, movement of vesicle to target membrane and their fission with membranes (Zerial and McBride 2001). Based on these facts, several markers associated with endocytic organelles in the intestine of *C. elegans* have already been established (marker constructs and strains obtained from Barth D. Grant; Table.1).

Table 1.

Organelles	Markers
Basolateral recycling endosomes	GFP-RAB-10, ARF-6-GFP, GFP-RME-1,
Late endosomes	GFP-RAB-7
Apical recycling endosomes	GFP-RAB-11

In previous research using this set of markers, several key regulators of ET have been identified, such as *rme-1* (Grant, Zhang et al.), *rme-6* (Sato, Sato et al.), and *rab-10* (Grant and Sato). GFP tagged RAB-5, an early endosome regulator, has been found to be accumulated in *ced-10* and *ced-12* mutants, where CED-10 and CED-12 has been proposed to regulate endocytic recycling via Rab-5 (Sun, Liu et al.). Abnormal morphology of basolateral recycling endosomes observed in *ced-10* and *ced-12* mutants has also been shown to be marked by another marker GFP::RAB-10, ARF-6::GFP, and GFP::RME-1 (Sun, Liu et al.).

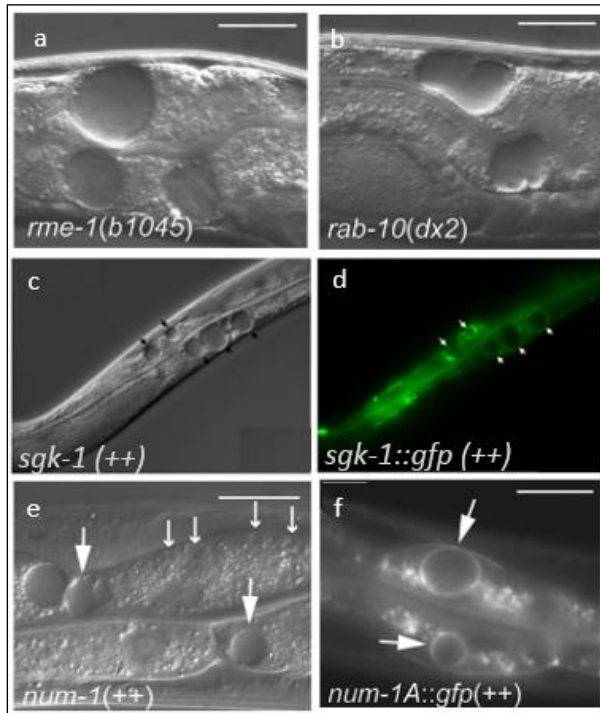
1.6.1 Defects related to ET

Defects in ET may appear in different cells in *C. elegans*. *C. elegans* intestine is a polarized epithelial tube, one cell layer thick (Leung, Hermann et al. 1999), apical surface facing the lumen whereas basolateral surface faces pseudocoelom (body cavity). Normally it consist of 20 enterocytes cells that form nine “donuts like” intestinal rings, maintained for the life of the animal without replacement (McGhee, Sleumer et al. 2007). The hypodermis forms the external surface of *C.elegans*. It consist of multinucleate hypodermal cells forming the single epithelial cell layer. Whereas oocytes are generally considered as non-polarized cells and also studied extensively for ET. Most of the ET mutants studied before shows an obvious phenotypic change in these structures.

Defects may appear as vacuole-like-structures in the intestinal cells, as they were observed in *rme-1* and *rab-10* (Fig.9a and 9b) mutants (Grant, Zhang et al. 2001, Chen, Schweinsberg et al. 2006) and are also induced by a *num-1A::gfp* (Fig.9e & 9f) transgene expressing NUM-1A (Grant and Caplan 2008). Such phenotype is visible even under the dissecting microscope, and has been considered as a consequence of an endocytic recycling defect (Lin, Grant et al. , Chen, Schweinsberg et al. 2006, Grant and Caplan 2008). RAB-10 has been shown to be required for endocytic recycling in the intestine of worm and may regulate transport between basolateral early and recycling endosomes (Chen, Schweinsberg et al. 2006). Also, NUM-1 protein was found localized to basolateral membranes of polarized epithelial cell, including hypodermis and intestine, and *num-1* has been shown to negatively regulate endocytic recycling (Grant and Caplan 2008).

Other defects associated with ET⁻ may resemble phenotype observed in a *rme-1* mutant, identified in the RME screen as described earlier, and have been found in several tissues, like oocytes and embryos, as shown in Fig 10.

A



B

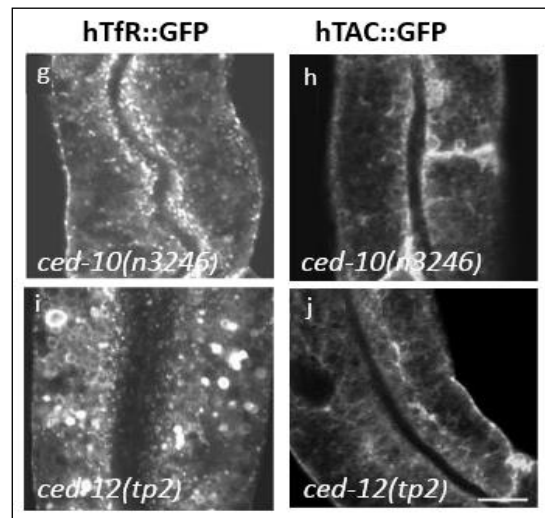


Fig.9 Defects associated with ET⁻ (A):: *rme-1* mutant (a), *rab-10* mutant (b), transgenic expression of *sgk-1* (c) *sgk-1::gfp* (d)[Yijian Yan, unpublished results, reproduced with the permission of the author], and transgenic expression of *num-1* (e) and *num-1A::gfp* (f). (Transgenic expression of *sgk-1::gfp* and *num-1::gfp* resulting in presumably elevated levels of *sgk-1* and *num-1*). (B): Intracellular accumulation of CDE and CIE cargo proteins: intracellular hTfR-GFP and hTAC-GFP accumulates in the intestinal cells of *ced-10* (g & h) and *ced-12* (i & j) respectively.

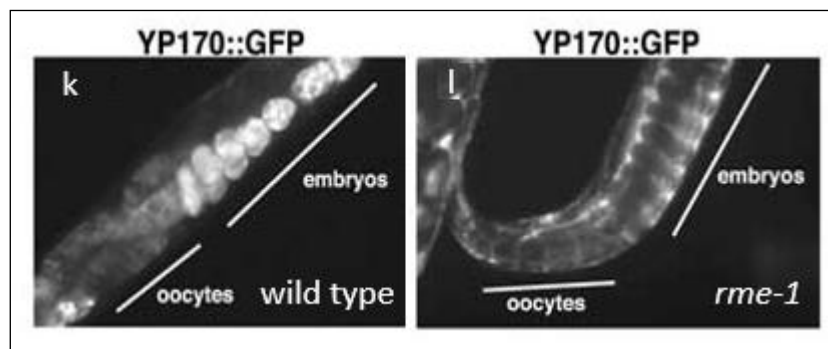


Fig.10 Defects associated with ET⁻ YP170::GFP endocytosis by oocytes. YP170::GFP is synthesized in the intestine and secreted into the body cavity from which it is endocytosed by oocytes. RME-2 is the yolk receptor expressed in oocytes. Fluorescent micrographs of wild-type and typical *rme-1* mutant worms expressing YP170::GFP are shown (Fig 9k & 9l respectively).

In another kind of defect associated with ET, established transmembrane cargo markers in *C. elegans* intestine such as human transferrin receptors (hTfR) and human IL-2 receptor alpha-chain (hTAC), which enter the cell via clatherin dependent (CDE) and clatherin independent endocytosis (CIE), respectively and recycle via recycling endosomes, have been shown to accumulate abnormally inside the cells in ET mutants. Such accumulation of cargo protein markers has been found in *ced-10* (Fig 9g & 9h) and *ced-12* (Fig 9i & 9j) mutants (Sun, Liu et al. 2012). In this context, CED-10 has been proposed to regulate endocytic recycling through RAB-5 GAP TBC-2 (Sun, Liu et al. 2012).

Recently Yijian Yan from our lab has found that a SGK-1::GFP transgene, presumably increasing SGK-1 levels, leads to formation of large vacuole-like-structures (VLS) in the intestinal cells of the worm (Fig.9) [Yijian Yan, unpublished data]. This striking phenotype in the intestine resembles the phenotype explained above in ET. GFP staining of the outer layer of these vacuole structures strongly indicate SGK-1 localization and its role in biogenesis of these vacuoles [Yijian Yan, unpublished data]. Current research is focusing on identifying the nature of these vacuoles and the exact step of ET affected.

1.7 Genetic interactions between PINK-1, LRK-1 and SGK-1

1.7.1 PINK-1 and LRK-1 act antagonistically

Published data from our lab proposes a model that in *C. elegans* PINK-1 and LRK-1 have antagonistic functions (Fig 11). While loss of *pink-1* results in increased sensitivity to the oxidative stressor Paraquat, and leads to axonal outgrowth defects of the canal-associated neurons, downregulation of *lrk-1* suppresses all phenotypic aspects caused by loss of *pink-1* function. Conversely, the hypersensitivity of *lrk-1* mutants to the endoplasmic reticulum stressor tunicamycin was reduced in the absence of *pink-1* (Samann, Hegermann et al. 2009).

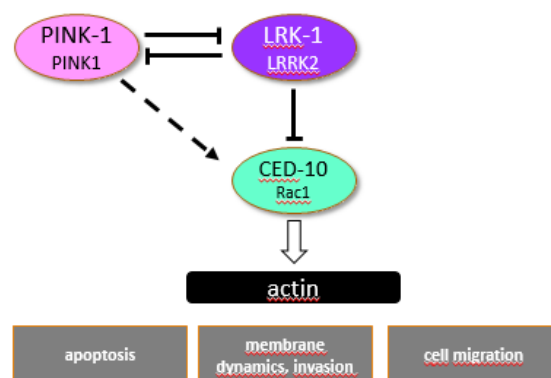


Fig 11: Model for *C. elegans* PINK-1 and LRK-1 showing antagonistic function. It was suggested that PINK-1 and LRK-1 both together might control a small RhoGTPase CED-10 which is a major regulator of actin cytoskeleton. Through modulation of cytoskeleton, they might affect engulfment during apoptosis, invasion and intracellular membrane dynamics and cell migration (J. Sämman, unpublished data).

In addition to stress response and neurite outgrowth showing antagonistic function, PINK-1 and LRK-1 has been studied by using various readouts associated with cell engulfment, membrane dynamics and distal tip cell (DTC) migration defect [Julia Säman, unpublished data].

1.7.2 SGK-1 regulates hLRRK2/CeLRK-1 mediated DTC migration defect

In another *C. elegans* model of a human disease related mutation in LRRK2, G2019S, our lab has recently proposed that human LRRK2 expression in *C. elegans* causes a highly penetrant DTC migration defect (Fig 12) [Xu Huang, unpublished results]. By integrating a functional LRRK2(G2019S) into the worm genome our lab could show that LRRK2 hyperactivity induces an erroneous distal tip cell (DTC) migration defect and has also shown that the effect is caused by hyperactivity of its kinase domain [Xu Huang, unpublished data]. Subsequently, applying RNAi to the above mentioned strain, Dr. Huang conducted a kinase screen, identifying ten possible LRRK2 interactors. Downregulation of these genes significantly reduced the DTC migration defect of *byIs170[LRRK2 (G2019S)]* [Xu Huang, unpublished data].

Out of these 10 genes, downregulation of *sgk-1* showed strong suppression of the DTC migration defect phenotype and also alters the LRRK2 expression [Xu Huang, unpublished data]. It has been shown that hLRRK2/CeLRK-1 negatively regulates Rac1/CED-10, and SGK-1 may in the same pathway as CED-5 to negatively modulate CED-5/CED-10 signaling during cell migration (Fig 10) [Venera Gashaj and Xu Huang, unpublished data].

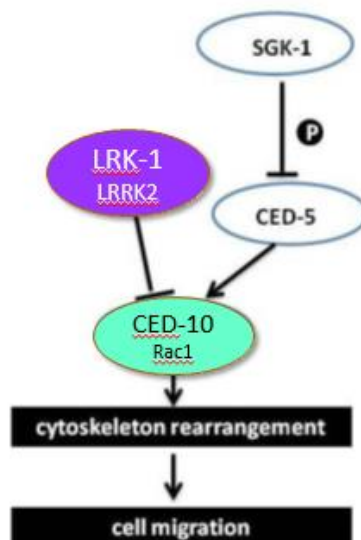


Fig 12: Model of SGK-1 modulates the hLRRK2/CeLRK-1 function via CED-10 in cell migration of *C. elegans*. (Xu. Huang, unpublished data)

From the result of split ubiquitin protein interactor screening performed in our lab, link between DOCK180/CED-5 and SGK-1 has already been suggested

[Dirnberger et.al, unpublished data]. Also it has been shown that *sgk-1*, *ced-5* and *ced-10* functions in a same signaling pathway to mediate DTC migration whereby, it was concluded that *sgk-1* acts upstream of *ced-5* and is epistatic to *ced-10* in regulating DTC migration [Xu Huang unpublished data]. In another set of experiments, it was shown that downregulating *sgk-1* may affect mutant phenotypes associated with PINK-1 and LRRK2/LRK-1 such as cell engulfment defect [Venera Gashaj, unpublished results].

However currently used read-outs to test the genetic relationships between *pink-1*, *lrk-1* and *sgk-1* suffer from the fact that these readouts are quite difficult to interpret and are subject to variable outcomes. Moreover, the commonly used readout, distal tip cell migration, cannot be easily linked mechanistically to endomembrane trafficking defects. Therefore, a novel read-out would be advantageous that will allow the mechanistic understanding of these genes in endocytosis/endomembrane trafficking.

1.8 Paraquat induces reactive oxygen species (ROS) in *pink-1* mutant

The exposure of an organism to stress conditions can result in a selective and asynchronous activation of the stress response in different tissues (Blake, Udelsman et al. 1991). Several studies have been performed using Paraquat induced ROS, which was hypothesized to either serve as a signaling molecule to initiate the signaling cascade or as an intracellular toxin. Paraquat is an herbicide and its initial site of action is mitochondria, where it interferes with electron transport chain reaction being as an electron acceptor (Tawara, Fukushima et al. 1996). ROS are generated when electrons fails to reach consecutive electron carrier within the electron transport chain ETC, but instead leak from the ETC complexes and are released. In principle, single electron can escape at complex I, II and III of ETC upstream of complex IV, and then radially reduced molecular oxygen to superoxide molecule, which, then, served as an educt for the generation of other ROS damaging cellular components (Cadenas, Boveris et al. 1977, Turrens 2003).

Loss of PINK1 in mammalian cells, mouse, and *D. melanogaster* have already shown to result in vulnerability to oxidative stress and morphological alteration in mitochondrial structure as a consequence of disrupted mitochondrial cristae (Yang, Gehrke et al. 2006). It has been shown that *pink-1* mutant worms have increased sensitivity to Paraquat treatment, and also display altered mitochondrial morphology (Samann, Hegermann et al. 2009). Stress induced effect of Paraquat has been studied by analyzing transcription levels of nuclear encoded mitochondrial chaperon HSP-6 fused to GFP (Runkel, Baumeister et al.). Induction of HSP-6 is a consequence of mitochondrial unfold protein response (UPR^{MI}) triggers to counteract ROS stress.

2.0 Hypothesis & Aims

Knowing the similar phenotypic consequences and their proposed pathways involved of *pink-1*, *lrk-1* and *sgk-1* mutants which suggest a contribution to ET, I hypothesized that PINK1, LRRK2 and SGK1 may be functionally related and may have interacting roles in ET. Since PINK-1 and LRK-1 have already been proposed to behave in antagonistic manner, this antagonicity should also involve ET regulation. Moreover, SGK-1 in such a case could affect both LRK-1 and PINK-1 activities.

2.1 **To analyze phenotypic changes upon perturbation of *pink-1* and *lrk-1***

As a first step towards confirming my hypothesis, I aimed to test whether manipulation of PINK1 and LRRK2/LRK-1 activities causes a phenotype that may be interpreted as an ET perturbation. Using *C. elegans*, I could take advantage of both mutations in the respective genes, as well as RNA interference to down-regulate expression of genes-of-interest. I hypothesize that these perturbations should result in phenotypic aspects related to those described previously for endomembrane transport mutants (see Chapter 2.9.1). Finding such readouts would be advantageous for understanding the mechanistic interplay of these genes and their products. To this end different approaches will be followed to observe such readout.

Most of the ET defect studied so far, such as vacuole in intestine, hypodermis and oocytes (described in chapter 2.6.1) are easily visible under dissecting microscope or using compound microscope, where *C. elegans* transparency eases the study of different tissues of an organism.. Therefore, I want to do a careful microscopic analysis of *pink-1* and *lrk-1* mutants aiming to observe ET associated phenotype mainly in certain tissues like intestine, hypodermis and oocytes. To broaden the power of my investigation I also aim to include genes of functionally linked proteins in this observation such as CED-5/DOCK180, CED-10/RAC1, MIG-2/RhoG, because it has been shown that PINK-1 and LRK-1 antagonistically modulate *C. elegans* RhoG/Rac-GTPases, where PINK-1 functions with MIG-2 and LRK-1 with CED-10 to control axon guidance and cell migration in *C. elegans* [Julia Säman, unpublished data].

2.1.1 **Pharmacological approach to find ET defect**

As stated above, Paraquat (PQ) induces mitochondrial stress (Runkel, Baumeister et al. 2014) by increasing mitochondrial ROS levels (Fukushima, Yamada et al. 1993, Feng, Bussiere et al. 2001, Fukushima, Tanaka et al. 2002). Given the fact that mitochondria are the power houses to produce the energy required by all cells

in an organism, damaged mitochondria may affect the cell integrity and may show some phenotypic abnormalities in different tissues of the worm. *pink-1(tm1779)* has been shown to display increased sensitivity upon exposure to Paraquat accompanied by defect in the mitochondrial integrity (Sämman, Hegermann et al. 2009). Therefore, taking into consideration, the effect of PQ inducing ROS and *pink-1* sensitivity, I will test the effect of Paraquat on *pink-1(tm1779)* mutant worms in order to search for an ET associated defect. In order to do this Paraquat dose response study will be performed with *pink-1(tm1779)* mutants. Dose response study will help to understand correlation between differential concentration of PQ and its induced effect on animals leading to change in phenotypic behavior. If PQ treatment does not show any obvious phenotype resembling ET defect, in this case I aim to test other stress inducers reported already such as heat stress [Julia Säman, unpublished data], MPTP, 6-OHDA and/or rotenone (Ryu, Harding et al. 2002, Holtz and O'Malley 2003) to see their effect on *pink-1* mutant worms.

2.2 Characterization of ET phenotype using RAB-10::GFP marker strain

If *pink-1* mutant phenotype, as hypothesized, alters ET, then such phenotype should be made visible. For this purpose, I will investigate *pink-1* mutant phenotype using RAB-10::GFP marker which can be used to monitor ET abnormalities. As mentioned before Rab proteins are master regulators of ET and each step of membrane transport is thought to require at least one member out of 29 predicted Rab members encoded in the *C. elegans* genome (Pereira-Leal and Seabra 2001). RAB-10 is a key basolateral recycling regulator in the intestine (Chen, Schweinsberg et al. 2006). The RAB-10::GFP protein staining appeared punctated in most tissues. In the intestine, it is localized to distinct cytoplasmic puncta resembling early endosomes that ranged in size from 0.5 to 1.0 μm (Grant, 2005). *rab-10* mutants also show large vacuoles in the intestine which, by using fluid phase markers such as GFP and fluorescent BSA, were identified as basolateral recycling endosomes (Chen, Schweinsberg et al. 2006).

2.3 RNAi test for modulators of *byIs207[sgk-1::gfp]* induced ET associated phenotype

RNA interference (RNAi) provides a powerful approach to manipulate almost any gene in the *C. elegans* genome. RNAi studies have been used to identify and study components of the regulatory network responsible for membrane trafficking (Balklava and Sztul 2013).

Main purpose of this step is to learn whether *pink-1* and *lrk-1* functionally interact or regulate *sgk-1*. For this purpose, I will use a *sgk-1::gfp* transgene which allows me to monitor changes in the expression of *sgk-1*, as well as in the localization of the SGK-1::GFP fusion protein. Previous studies had indicated that the SGK-1

localization may be dynamic, and that SGK-1 preferentially associates with intracellular membranes (see above). I plan to test *sgk-1::gfp* expression and protein localization after RNAi manipulating *pink-1*, *lrk-1* and candidate genes suspected in functional relationships with both. These include for reasons that have been discussed above *ced-5*, *ced-10* and *mig-2*. The *sgk-1::gfp* transgene I use is integrated in the *C. elegans* genome and has been suggested to result in an overexpression of SGK-1. As also discussed above, this transgene results in an vacuole like phenotype as a consequence of a proposed ET defect. Therefore, using this transgene will also allow me to monitor whether any of the PD associated genes is able to positively or negatively modulate this phenotype.

In addition to these experiments, based on already known direct and indirect interactors of SGK1/SGK-1 and genes involved in ET, I have selected several candidates from different signaling pathways that our lab has been implicated in SGK-1 regulation. These include TGF β signaling, NOTCH signaling, Insulin signaling, MAPK signaling and Rho/Rac GTPase signaling pathway. List of selected candidates for RNAi screen are mentioned in table 2. I want to analyze whether their perturbations, as well, can affect *sgk-1* expression, localization, or mutant phenotype, indicating a functional relationship of *sgk-1* with these pathways.

Table 2: List of candidate gene for RNAi screen

Candidate gene	Involved signaling pathway	Known interaction with SGK1/SGK-1 or role in ET
<i>sma-2</i> <i>sma-3</i> <i>sma-4</i> <i>sma-6</i> <i>sma-9</i>	TGF β signaling pathway	SGK1 has been shown to upregulate TGF β activity by phosphorylating and thus inactivating Nedd4L ligase which is require for degradation of Smad2/Smad3 transcription factor (Lang, Bohmer et al.)
<i>lin-12</i> <i>glp-1</i> <i>lag-1</i> <i>lag-2</i>	NOTCH signaling pathway	Elevated levels of NUM-1A protein in <i>C. elegans</i> impaired ET (Grant and Caplan) and in mammals Numb protein has been implicated in regulation of NOTCH signaling pathway (Jan, Y. N. and L. Y. Jan 1998; Le Borgne, R. 2006)
<i>mek-1</i> <i>mek-2</i>	MEK/ERK signaling pathway	SGK1 and ERK co-localize to either nucleus or cytoplasmic compartment in growth factor dependent signaling event (Buse, Maiyar et al.) and SGK1 activating MEK/ERK signaling is required for cell proliferation (Talarmin, Rescan et al.)

<i>akt-1</i> <i>akt-2</i> <i>daf-2</i> <i>pkc-2</i>	Insulin/IGF-1 signaling (IIS) pathway	<i>C. elegans</i> SGK-1 acts in parallel to AKT-1 and AKT-2 homologue of Akt/PKB family members in mammals in regulating longevity through phosphorylation of DAF-16/FOXO
<i>ced-2</i> <i>ced-5</i> <i>ced-10</i>	Rho/Rac GTPase signaling pathway	Split ubiquitin protein interactor screening revealed a link between DOCK180/CED-5 and SGK-1 [Dirnberger et.al, unpublished data], Also it has been shown that <i>sgk-1</i> , <i>ced-5</i> and <i>ced-10</i> functions in a same signaling pathway to mediate DTC migration [Xu Huang unpublished data] where <i>sgk-1</i> acts upstream of <i>ced-5</i> and is epistatic to <i>ced-10</i> . Also CED-10 and CED-12 have been shown to regulate endocytic recycling (Sun, Liu et al. 2012)

2.4 Epistatic analysis of loss of *lrk-1* function in SGK-1::GFP transgenic worms

Downregulation of *sgk-1* alters the distal tip cell migration defect of LRRK2(G2019S), and it was suggested that this occurs via Rho GTPase CED-10 [Xu Huang, unpublished data]. However, a direct mechanistic link between SGK-1 and LRK-1 is still unknown and the only phenotype that, so far, indicated a correlation of *sgk-1* and *lrk-1* function, does not easily explain the mechanism of this genetic interaction or their role in ET.

As stated before, if LRK-1 and SGK-1 both functions in endocytic transport (Yun 2003, Sakaguchi-Nakashima, Meir et al. 2007, Jacquier and Schneiter 2010) they could share a common function in regulating endomembrane trafficking. Therefore, epistatic analysis can be done to reveal whether one mutant affects the phenotype of the respective other mutants positively or negatively. In detail, since overexpression of SGK-1 give rise the formation of large vacuoles in intestinal cell which may be a consequence of ET defect, downregulation of *lrk-1* may increase or decrease this vacuole phenotype, if *lrk-1* is mechanistically linked to *sgk-1*.

Taking into consideration that RNAi downregulation may not be efficient to produce expected downregulation of targeted gene of interest, in addition RNAi (chapter 3.3) I will also test the mutant interactions. *lrk-1* loss of function allele, *tm1898* is a deletion/insertion allele. Previous data from lab has shown that *lrk-1(tm1898)* animals displayed a misdistribution of synaptic vesicles from axonal to dendritic compartments in neuronal cells [J. Säman & U. Schäffer unpublished data] suggesting role of *lrk-1(tm1898)* in vesicle trafficking and transport. As stated before in *C.elegans*, in addition to neuronal cells LRK-1 is also expressed in non

neuronal tissue like intestine, hypodermis, somatic gonad and distal tip cells. Therefore, I aimed at crossing the *byIs207[sgk-1::gfp]* strain with *lrk-1(tm1898)(lf)* loss of function mutant and analyze the resulting phenotype. The VLS phenotype observed in the strain overexpressing SGK-1:GFP is also temperature dependent [Yijian Yan, unpublished work]. Worms cultured at 15°C temperature show 88% +/- 3% of phenotype however at 20°C this phenotype was reduced to 18% +/- 3% [Yijian Yan, unpublished work]. This fact provides me two experimental conditions where I aim to test my hypothesis at two different temperature 15°C and 20°C. Modulation of phenotype at either experimental condition will give a hint in the direction of LRK-1 interaction with SGK-1 in the context of ET. For example such modulation of phenotype may appear as reduced or enhanced number of vacuoles or changes in expression pattern of SGK-1::GFP when compared to *byIs207[sgk-1::gfp]* strain alone.

3.0 Materials & Methods

3.1 Materials

3.1.1 *C. elegans* strains

Table 3: *C. elegans* strains

Strain ID		Genotype	constructed by/received from
	N2	wild type isolate (Bristol)	CGC
BR3755	tm1898	<i>lrk-1(tm1898)</i>	Julia Sämman
BR4623		<i>lrk-1(tm17)</i>	Matsumoto
BR4624		<i>lrk-1(tm41)</i>	Matsumoto
BR3411	tm1779	<i>pink-1(tm1779)</i>	Mitani
BR4360	CF162	<i>mig-2(mu28)</i>	Hengartner lab
BR3969	CB3203	<i>ced-1(e1735)</i>	CGC
BR3574	MT4952	<i>ced-2(n1994)</i>	Hengartner lab
BR3585	MT4962	<i>ced-5(n2002)</i>	Hengartner lab
BR3576	MT4433	<i>ced-6(n1813)</i>	Hengartner lab
BR6944	RT525	<i>pwIs[vha6p::GFP::rab-10; unc-119(+)]</i>	Barth Grant Lab
BR3580	MT4983	<i>ced-7(n1996)</i>	Hengartner lab
BR3579	MT9958	<i>ced-10(n3246)</i>	Hengartner lab
BR3581		<i>ced-12(o_z167)</i>	Hengartner lab
BR3756		<i>lrk-1(tm1898); pink-1(tm1779)</i>	Julia Sämman
BR7005		<i>pink-1(tm1779)II;pwIs[vha-6p::gfp::rab-10;unc-119(+)]</i>	Dipak Gangurde
BR5994		<i>wt;byIs170[Plrk-1::lrrk2(G2019S)::gfp; Punc-</i>	Xu Huang

		<i>122::gfp]</i>	
BR6575		<i>byIs207[sgk-1::gfp]</i>	Tim Wolf
		<i>lrk-1(tm1898); byIs207[sgk-1::gfp]</i>	Dipak Gangurde
BR3840	CB502	<i>sma-2(e502)III</i>	Ekkehard Schulze

CGC: Caenorhabditis Genetics Center

3.1.2 Bacteria strains

Table 4: Bacteria strains

Strain	Genotype	Purpose
OP50	<i>ura-</i>	feeding
HT115(DE3)	<i>F-, mcrA, mcrB, IN(rrnD-rrnE)1, lambda-, rnc14::Tn10(DE3 lysogen:lacUV5 promoter-T7polymerase, RNase III minus)</i>	RNAi feeding

3.1.3 Oligonucleotides

Table 5: Oligonucleotides

Oligo ID	Sequence (5'to 3')	purpose
RB3019	GGAGCCTTTTGTGAGTACGACA	to detect <i>pink-1(tm1779)</i>
RB3020	AGC CTC GGG CTT ATT AAG GA	
	GCATTGAGCTCTTTCAACGCTG	to detect <i>lrk-1(tm1889)</i>
	GCACCAGCGTCGAGAAGAAGCC	

Lyophilized oligonucleotides were purchased from Sigma-Aldrich and stored as 100µM aqueous stock solutions at -20°C.

3.1.4 Buffers and solutions

All buffers and solutions were prepared with deionized (MilliQ™) water and autoclaved prior to usage.

Table 6: Buffers and solutions

Buffers and Solutions	Composition
Nystatin solution	4g Nystatin, 200ml Ethanol, 200ml Ammonium acetate
M9 buffer	3g/l KH ₂ PO ₄ , 6g/l Na ₂ HPO ₄ , 5g/l NaCl (pH 6.0), 1mM MgSO ₄
S Basal buffer	5.85g NaCl, 1g K ₂ HPO ₄ , 6g KH ₂ PO ₄ , 1ml Cholesterol (5mg/ml in ethanol), add H ₂ O to 1 liter
Worm lysis buffer	10 mM Tris, pH 8.2; 50 mM KCl; 2.5 mM MgCl ₂ ; 0.45% NP40; 0.45% Tween 20; 0.01% gelatin; 0.5 mg/ml Proteinase K
bleach solution (2x)	0.5 M KOH; 1-2% NaOCl fixation solution
Freezing buffer(2×)	0.1M Na ₂ Cl, 50mM KH ₂ PO ₄ (pH 6.0), 30% (w/v) glycerol; 1M NaOH, add optional 0.1M MgSO ₄

3.1.5 Media

Media used for culturing *C. elegans* strain are listed below

Table 7: Media

Media	Composition
NGM agar medium	3g/l NaCl, 17g/l Agar, 2.5g/l Bacto peptone, 5mg/ml Cholesterol, 1mM CaCl ₂ , 1mM MgSO ₄ , 5mM KH ₂ PO ₄ (pH 6.0), 20mg/l Nystatin

DYT medium	16 g/l bacto-trypton; 10 g/l yeast extract; 5 g/l NaCl
LB medium	5.85g NaCl, 1g K ₂ HPO ₄ , 6g KH ₂ PO ₄ , 1ml Cholesterol (5mg/ml in ethanol), add H ₂ O to 1 liter

3.1.6 Chemical compounds

Chemical compounds for standard laboratory use and with highest purity were purchased from AppliChem, Carl Roth, Merck, Sigma-Aldrich, and VWR. Compounds used for stress assays are listed below.

Table 8: Chemical compounds

Chemical compound	Distributor (article nr.)
Methyl viologene dichloride Hydrate 98% (Paraquat)	Sigma-Aldrich (856177)
Rotenone ($\geq 95\%$)	Sigma-Aldrich (R8875)
Tunicamycin (batch number: 112 M 4010 V)	Sigma-Aldrich (T7765)

3.1.7 Software's

Table 9: Software's

Product	Distributor
Axio Vision 4.6	Carl Zeiss AG
Contur Electronic Lab Notebook version 4	Scientific & Educational Software
GraphPad Prism 5.0	Contur Software AB
ImageJ v1.43	GraphPad Prism Software Inc
Clone manager 9 (Basic Edition)	Scientific & Educational Software, USA
Microsoft Excel 2003/2007	NIH, Bethesda, MD, USA
Microsoft Power Point 2003	Microsoft Deutschland GmbH
Microsoft Word 2003/2007	Microsoft Deutschland GmbH
NIS-Elements AR 4.0 64-bit	Microsoft Deutschland GmbH

3.1.8 Equipment

Equipment used for microscopy are listed in table.

Table 10: Equipment's

Product	Distributor
AxioCam MRm3 CCD camera	Carl Zeiss AG
AxioCam MRm3_2 CCD camera	Carl Zeiss AG
Axio Imager.Z1 compound microscope	Carl Zeiss AG
Fluorescence Stereomicroscope SZX12	Olympus
Light Stereomicroscope SZX7	Olympus

3.1.9 Transgenic strains

3.1.9.1 BR6944: Genotype - *pwIs[vha6p::GFP::rab-10; unc-119(+)]*

This transgenic strain was kindly provided by Barth D. Grant lab. Constructed by using cDNA sequence of *C. elegans* gene *rab-10* cloned into entry vector pDONR221 and transferred into *vha-6-GFP* vector. This vector was prepared by using promoter region of intestine specific gene *vha-6* cloned into *C. elegans* pPD117.01 vector, followed by *gfp* coded sequence *unc-119* gene of *C. brigassae*.

3.1.9.2 BR6575: Genotype - *byIs207[sgk-1::gfp]*

Constructed in our lab by Tim Wolf. Contains *C.elegans* whole genomic SGK-1 fused with GFP where 3.1 kb region at 5' end was consider as a promoter region. This transgenic line was outcrossed 10 times.

3.2 Methods

3.2.1 Maintenance of *C. elegans*

All *C.elegans* strains were maintained at 15°C or 20°C on NGM (Nematode Growth Medium) plates seeded with *Escherichia coli* OP50 (Brenner 1974) unless otherwise indicated. OP50 bacteria were grown in shaking liquid cultures overnight in DYT medium at 37°C, 180 rpm. NGM agar plates were seeded with grown OP50 and dried overnight at the bench top. For picking worms from plates usually platinum wire pick or eyelash pick was used. Experiments were performed at 20°C unless otherwise indicated.

3.2.2 Decontamination of *C. elegans*

5 µl 2 M sodium/potassium hydroxide plus 5 µl sodium hypochlorite (12%) used as a bleaching solution to get rid of bacterial and fungal contamination. 10 to 15 gravid *C. elegans* adult from contaminated plates were transferred to drop of

bleaching solution on a clean seeded NGM plate. Following day bleaching area was cut off and decontaminated animals were maintained as described.

3.2.3 Synchronization of *C. elegans* population

For all the experiments (except PQ assay) following protocol was adapted to synchronize *C. elegans* population

The appropriate number of gravid adult hermaphrodites (~1,000 worms/large NGM agar plate (Ø 10 cm)) was collected in M9 buffer in 15 ml falcon tubes. After two washing steps (centrifugation at 2000 rpm) worms were resuspended in 4 ml deionized water (MilliQ™) to which 4 ml of 2x bleaching solution (10 ml stock solution: 0.5 ml 5M KOH, 0.2 ml NaOCl (12%), 9.3 ml deionized water (MilliQ™)) were added. Worms were shaken on a vortex mixer for 20-30 min until eggs were freed. Eggs were washed in M9 buffer 4 to 6 times, transferred to fresh falcon tubes and washed for another 2 times. Prepared eggs were kept in 15 ml falcon tubes in M9 buffer for 24 h on a rotation mixer at 15°C. The next day synchronized hatched L1 larvae were placed onto NGM plates seeded with the respective feeding bacteria and maintained as described or used for subsequent experiments.

3.2.3.1 Synchronization of *C.elegans* for Paraquat assay

To avoid the effect of additional stress other than stress applied by PQ, such as effect of bleaching solution, M9 buffer and external stress while following synchronization protocol described above, following protocol was adapted to synchronize *C. elegans* population.

15 to 20 gravid *C. elegans* hermaphrodites were placed on small NGM plate's seeded with OP50 and allow to lay eggs for 3 hours. After 3 hours gravid animals were removed and eggs were allow to hatch at 20°C and maintained as described. In this way I got the synchronized worms with 3 hours of maximum difference in development stage.

3.2.4 RNA interference assay

There are three ways to carry out RNAi in *C. elegans*: injection, soaking, and feeding (Tabara, Grishok et al. 1998, Timmons and Fire 1998). All three can produce efficient gene knockdowns. Two RNAi libraries are available for *C. elegans*, namely Ahringer and ORFeome which provide clones targeting around 87% of currently annotated *C.elegans* genes. For my experiment RNAi by feeding method was performed. Animals were fed with bacteria expressing dsRNA corresponding to coding region of selected genes (chapter 4) to be silence.

RNAi experiments was performed on NGM plates supplied with ampicillin as an antibacterial agent. Prior to RNAi experiment on plates, the single RNAi clones were prepared from the original stocks obtained from available RNAi, confirmed by sequencing and archived as monoclonal bacterial stock in LB medium supplemented with 5% glycerol. From the confirmed clone a 1:50 dilution of the respective RNAi bacterial overnight culture (37°C, 150 rpm) in LB medium supplemented with 12.5 µg/ml tetracycline and 12.5 µg/ml ampicillin was grown in LB medium supplemented with 12.5 µg/ml ampicillin for another 6 h at 37°C, 150 rpm. Bacteria were then seeded on small NGM plates (Ø 3.5 cm) containing 1.0 mM IPTG and 25.0 µg/ml ampicillin. To knockdown a gene, worms were raised on RNAi bacteria starting from L4 stage (gonadogenesis starts at this stage of animals) and progeny of these worms were analyzed for respective experiment. Experiment was performed in triplicate to perform statistical analysis of the effect observed with knockdown of specific gene for respective experiment.

3.2.4.1 RNAi test for SGK-1::GFP induced vacuole phenotype modifiers

Synchronized L4 animals were placed on the NGM plates seeded with *E. coli* bacterial containing plasmids of target candidates and maintain at 15°C and 20°C for respective suppressor and enhancer test of phenotype. Day one adult animals from next progeny, with vacuole phenotype were scored by Nomarski microscope. Significant increased or decreased in number of animals with vacuole phenotype by RNAi compared to animals fed with HT115 *E. coli* with L4440 were calculated as potential regulators of SGK-1::GFP induced vacuole phenotype.

3.2.5 Crosses

Crosses were performed on small NGM agar plates (Ø 3.5 cm) seeded with *E. coli* (OP50) at 20°C. Hermaphrodites of a respective mutant strain were mated with males in a ratio of at least 1:4 in duplicate and singled on two new plates after observing enough eggs. F1 generation from old plates were observed after 2 days for male animals. Mating was considered as successful when in the F1 generation the numbers of males approximately equaled the numbers of hermaphrodites. F2 animals of 8 singled F1 hermaphrodites were preselected for respective mutant identified by a corresponding phenotype and singled. After egg-laying commenced, singled F2 animals were screened for the respective mutation by PCR (chapter). Homozygosity of both required genotype was confirmed in subsequent generations by phenotype analyses and/or PCR.

3.2.5.1 Generation of Males by heat shock

In addition to hermaphrodite (XX) *C.elegans* produces male sex (X0), arise from fusion of null-X gamete and normal X bearing gamete. Null-X gamete is a result of spontaneous non-disjunction of the X chromosome during meiosis in germ cells.

Frequency of this spontaneous non-disjunction is 0.1 to 0.2 % (Ward, Burke et al. 1988[Hodgkin, 1997 #465]).

Males for crossing experiment used in this study were generated by heat shock method (Ward, Burke et al. 1988). NGM plates seeded with OP50 were set up, each containing 6 L4 stage hermaphrodites of respective mutant. Incubated exactly at 30°C, 1st plate for 5 hours, and 2nd for 5.5 hours and 3rd for 6 hours. Progeny of these worms were observed for males and further enriched to get more number of males by crossing with hermaphrodites of respective strain.

3.2.5.2 Scheme for cross between *lrk-1(tm1898)* and *byIs207[sgk-1::gfp]*

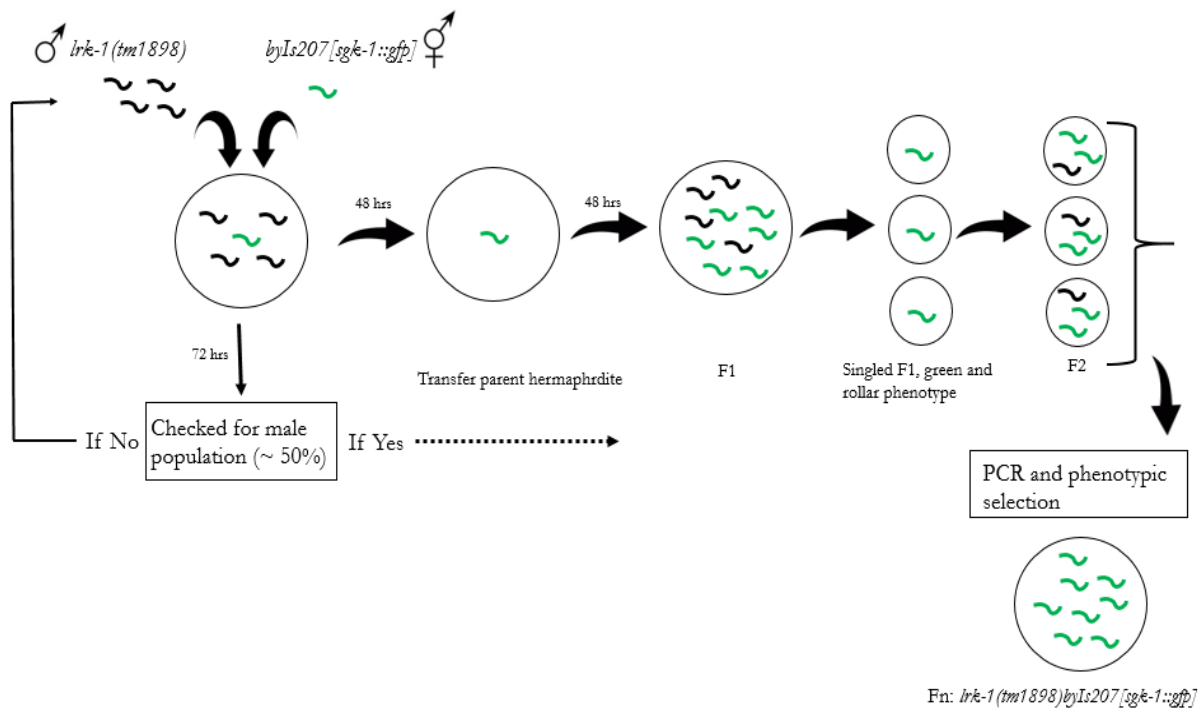
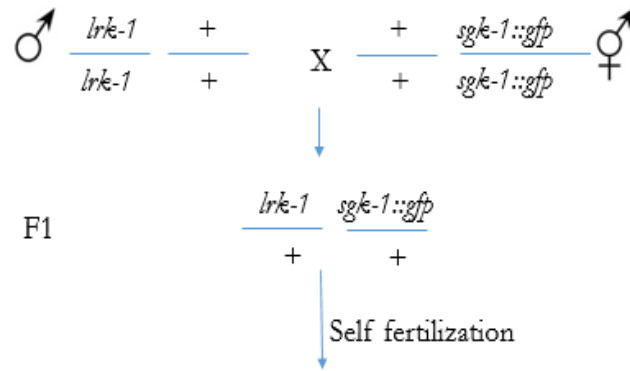


Fig. 13: Schematic representation of cross between *lrk-1(tm1898)* and *byIs207[sgk-1::gfp]*. 4 males of *lrk-1(tm1898)* were crossed with a *byIs207[sgk-1::gfp]* hermaphrodite in duplicate and cultured at 20°C. After 48 hours parent hermaphrodite were transferred to the new plate. 72 hours later the beginning of cross original plate was observed under stereo microscope for male population which was around 50%, indicated cross was successful. In another case when no males were observed on the plate, crossing was repeated. New plate with transferred hermaphrodite were continued to culture at 20°C. 48 hours after 8 F1 worms were singled by selecting roller worms with green fluorescence phenotype. For every generation this selection criteria was maintained until all progeny showed green fluorescence and roller phenotype, which confirms the homozygosity for *sgk-1::gfp* transgene. Singled F1's, after they have laid enough eggs on plate were subjected to PCR to identify the *lrk-1(tm1898)* allele. This genotypic and phenotypic selection carried out for all the successive generation until desired result were obtained.



F2	<i>lrk-1/sgk-1</i>	<i>+/sgk-1</i>	<i>lrk-1/+</i>	<i>+/+</i>
<i>lrk-1/sgk-1</i>	<i>lrk-1/lrk-1; sgk-1/sgk-1</i>	<i>+/lrk-1; sgk-1/sgk-1</i>	<i>lrk-1/lrk-1; sgk-1/+</i>	<i>+/lrk-1; sgk-1/+</i>
<i>+/sgk-1</i>	<i>+/lrk-1; sgk-1/sgk-1</i>	<i>+/+; sgk-1/sgk-1</i>	<i>+/lrk-1; sgk-1/+</i>	<i>+/+; sgk-1/+</i>
<i>lrk-1/+</i>	<i>lrk-1/lrk-1; +/sgk-1</i>	<i>+/lrk-1; sgk-1/+</i>	<i>lrk-1/lrk-1; +/+</i>	<i>+/lrk-1; +/+</i>
<i>+/+</i>	<i>lrk-1/+; sgk-1/+</i>	<i>+/+; sgk-1/+</i>	<i>+/lrk-1; +/+</i>	<i>+/+; +/+</i>

Fig. 14: Genotypic representation of cross between *lrk-1(tm1898)* and *byIs207[sgk-1::gfp]*. F1 generation shows heterozygous genotype which upon self-fertilization produced different genotypic combination. Green cell in the Punnett square represent the desired genotype of expected mutant.

3.2.6 Genotyping

3.2.6.1 Worm lysis

1 worm per 5 μ l worm lyses buffer including 0.5 mg/ml proteinase K was subjected to following mentioned worm lysis program. Genomic DNA contained in the solution was used as template for subsequent polymerase chain reactions (PCRs) for genotyping.

Table 11: Worm lysis program

Worm lysis program	
65°C	60 min
95°C	5.0 min
10°C	infinite

3.2.6.2 Polymerase chain reaction

Genotyping of mutants by PCR is used to detect deletion alleles in respective mutant. Combination of forward and reverse primer were used to flank the deletion region in mutant. Primers used are purchased from Sigma-Aldrich in lyophilized form, dissolved in deionized water and stored as 100 μ M aqueous stock at -20°C. PCR reaction was performed as per the scheme mentioned below and analyzed with standard DNA gel electrophoresis.

Table12: PCR scheme for detection of *lrk-1(tm1898)* allele

Standard PCR mixture contain (20 μ l)	
gDNA template	2.0 μ l (from worm lysis)
10X buffer	2.0 μ l
MgCl ₂ (25 mM)	1.0 μ l
dNTP (2 mM)	1.0 μ l
Primer 1 (10 μ M)	1.0 μ l
Primer 2 (10 μ M)	1.0 μ l
TaqS polymerase	0.2 μ l
Water (deionized)	add up to 20 μ l

PCR program		
95°C	5.0 min	35 cycles
94°C	30 sec	
57°C	30 sec	
72°C	30 sec	
72°C	10 min	
7°C	infinite	

Table 13: PCR scheme for detection of *pink-1(tm1779)* allele

Standard PCR mixture contain (20 μ l)	
gDNA template	2.0 μ l (from worm lysis)
10X buffer with MgCl ₂	2.0 μ l
dNTP (2 mM)	1.0 μ l
Primer 1 (10 μ M)	1.0 μ l
Primer 2 (10 μ M)	1.0 μ l
Polymerase from ROCHE	0.2 μ l
Water (deionized)	add up to 20 μ l

PCR program		
94°C	2.0 min	35 cycles
94°C	30 sec	
57°C	30 sec	
68°C	1.5 min	
72°C	7.0 min	
7°C	infinite	

3.2.7 DNA sequencing

DNA was sequenced at GATC Biotech (www.gatc-biotech.com).

3.2.8 Paraquat stress assay

PQ stress was performed on synchronized worm population being grown from L1 stage on small NGM agar plates (Ø 3.5 cm, agar volume 4 ml) seeded with *E. coli* OP50. Every PQ assay was performed in triplicate with 50 to 60 synchronized worms raised on each plate. For administration of PQ, 200 µl of respective concentration was pipetted onto the plate containing synchronized worms. Stock solution concentration, working solution concentration and final concentration mentioned below (Table). PQ solution was distributed evenly by swirling and plates were dried under a sterile bench protected from light because of the sensitivity of PQ to light.

Table 14: PQ stress assay

stressor	Stock solution	Working solution	Final concentration (200µl)
Paraquat	1 M (aq.)	1mM	0.05mM
	1 M (aq.)	2mM	0.1mM
	1 M (aq.)	5mM	0.25mM
	1 M (aq.)	10mM	0.5mM
	1 M (aq.)	20mM	1.0mM
	1 M (aq.)	40mM	2.0mM
	1 M (aq.)	50mM	2.5mM
	1 M (aq.)	100mM	5.0mM

	1 M (aq.)	200mM	10.0mM
	1 M (aq.)	500mM	25.0mM
	1 M (aq.)	1000mM	50.0mM

aq.: aqueous

Working solution was freshly prepared for each experiment. 200 µl of working solution was distributed to each small plate (4ml).

3.2.8.1 Protocol for the PQ assay

Taking into consideration of previously published results from the lab about effect of PQ on survival rate (7.5 mM, 71.5 +/- 3% survivors), and lethal concentration of 50mM, (Säman 2008[Runkel, 2013 #526]) to know the non-lethal concentration of PQ, which may produce phenotypic change in different tissue, *pink-1(tm1779)* strain was subjected to PQ dose response study. Protocol for developmental stage of worm while treating them with PQ and optimal exposure time to which PQ tested has been adapted and modified from Eva Runkel (Fig 15) [Eva Runkel, unpublished results], whereby treatment of L3 worms and exposure time of one day was sufficient to induce mitochondrial stress (Säman 2008, Runkel, Baumeister et al. 2014).

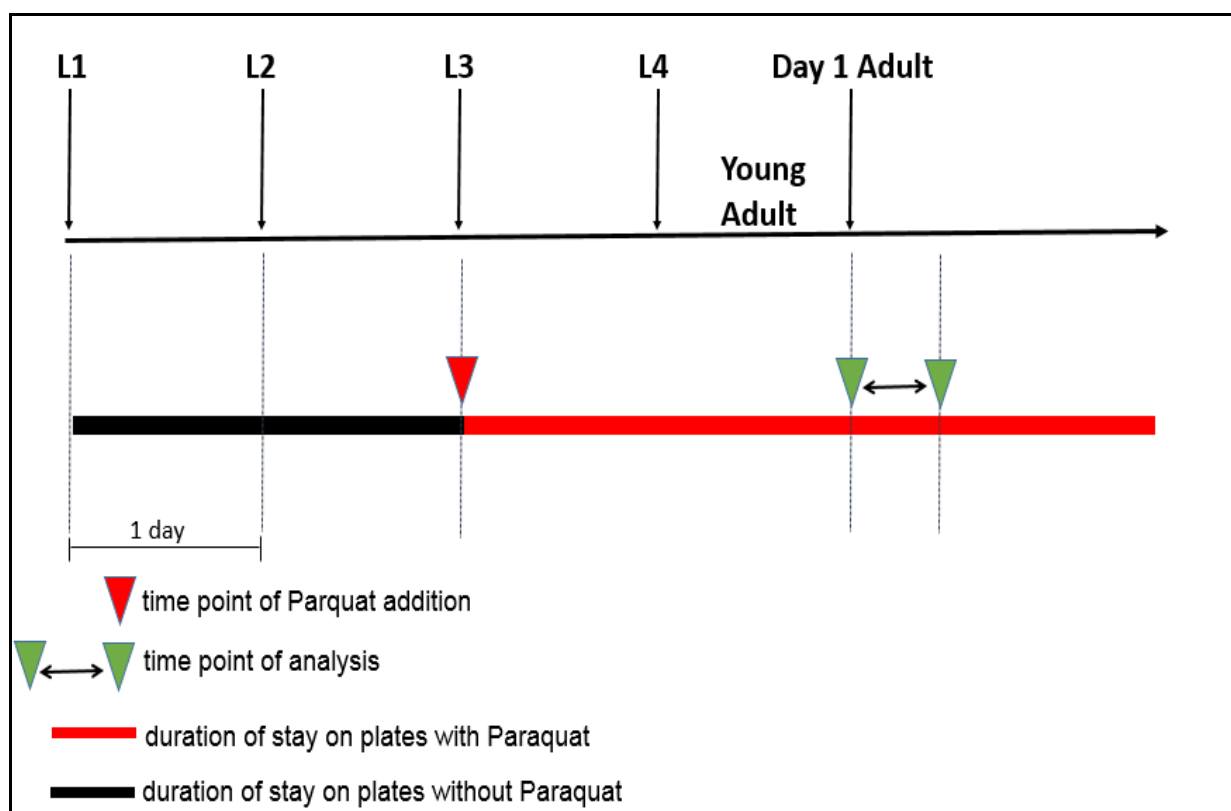


Fig 15: Scheme of the experimental procedures: worms are treated with 2.5 mM PQ at L3 stage and observed after one day for the exert effect.

3.2.9 Microscopy

a. Stereo microscopy:

Live *C. elegans* analyzed for the phenotypic analysis and GFP expression on NGM plates with a stereo microscope (Olympus) using standard GFP filter.

b. Compound microscopy:

C. elegans were immobilized by levamisole (0.5mM); mounted on 2% agarose pad on glass slide and analyzed with an Axio Imager Z1 compound microscope with different objectives (5x, 10x, 20x, 40x). For quantification of GFP expression 10x objective was used, where micrographs were recorded with an AxioCam Mrm3CCD camera.

3.2.10 Image Analysis

a. Fluorescence Intensity:

To quantify the fluorescence intensity of *C. elegans* transgenes, Image J software was used. The relative fluorescence intensity of each whole worm was measured and background fluorescence was subtracted from each (Fig. 16).

b. Body Length:

The body length of animal (anterior to posterior) was measured with Axiovision Vision 4.6 software (Fig. 17).



Fig 16: Fluorescence intensity measurements. The fluorescence intensity of the area of interest, here the whole worm, was measured. The area was marked with the “outline spline tool” which is provided by the Image J software. Shown is the BR7005 worms at adult stage of development, mounted on glass slide and immobilized with 0.5mM levamisole. The background fluorescence intensity was measured for each micrograph (red circle) and subtracted.

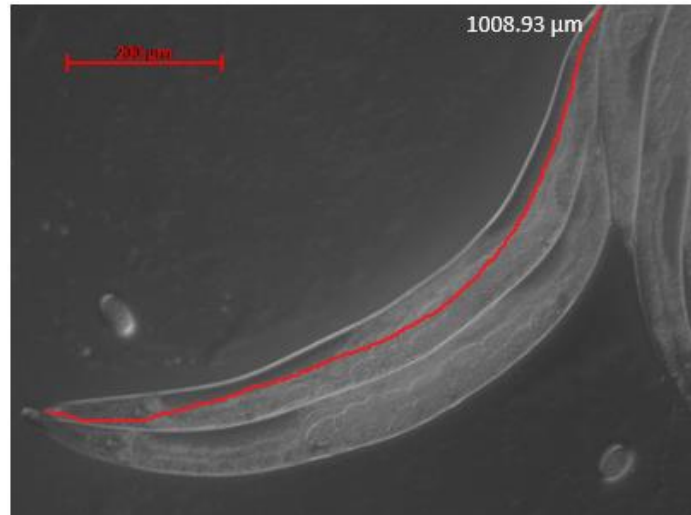


Fig 17: The length of an animal was measured with “curve spline” tool provided by Axiovision software. Shown is wild type worm at adult stage of development mounted on glass slide and immobilized with 0.5mM levamisole.

3.2.11 Statistical analysis

Statistics were performed using GraphPad Prism 4 (GraphPad Software Inc., San Diego, USA). Results are presented as standard error of the mean (\pm SEM) from the analysis of at least 90 worms, performed in triplicate, if not mentioned otherwise. Student’s *t*-test were applied to calculate statistical difference. Differences with $p < 0.05$ were accepted as statistically significant. Asterisks denote the degree of statistical significance. * $p < 0.05$, ** $p < 0.01$ and *** $p < 0.0001$.

3.2.12 Bioinformatics

To find the regions of similarity between sequences and to find gene homologous Basic Local Alignment Search Tool (BLAST) algorithm studies were conducted. Information on *C. elegans* genes, proteins and mutants was retrieved from Wormbase (www.wormbase.org). Clone manager 9 Basic Edition (Scientific & Educational Software, USA) was used to designed and analyze primers.

4 Results

4.1 Phenotypic analysis of *pink-1*, *lrk-1* and their functionally related genes

As a first step towards confirming my hypothesis, I aimed to test whether manipulation of PINK1 and LRRK2/LRK-1 activities causes a phenotype that may be interpreted as an ET perturbation. I used an Axio Imager compound microscope to examine *pink-1(tm1779)*, *lrk-1(tm1898)*, *ced-5(n2002)*, *ced-10(n3246)*, *mig-2(mu28)* mutants. In particular, I looked at intestine, hypodermis and oocyte of these animals from L1 to adult stage of their development. Alteration in the normal structure of these cells upon perturbation of above mentioned genes, specifically which resembles like vacuole structure, was the main focus of this microscopic analysis.

For each set of mutant and developmental stage ranging from L1 to adult, synchronized worms were grown on NGM agar plate at 20°C and around 30 worms were mounted on 3% agarose slides and immobilized by 0.1% of levamisole, and then observed under Axio Imager compound microscope.

For RNAi downregulating targeted genes, synchronized wild type L4 worms were grown at 20°C on RNAi bacteria of gene of interest and their progeny was observed at an adult stage using compound microscope. For negative control wild type L4 worms were grown at 20°C on bacteria containing L4440 empty vector.

Representative wild type intestine, hypodermis and oocytes structure in adult worm is shown in Fig 18 (B, C and D respectively), which was considered as a normal in appearance compare with mutant set of worms.

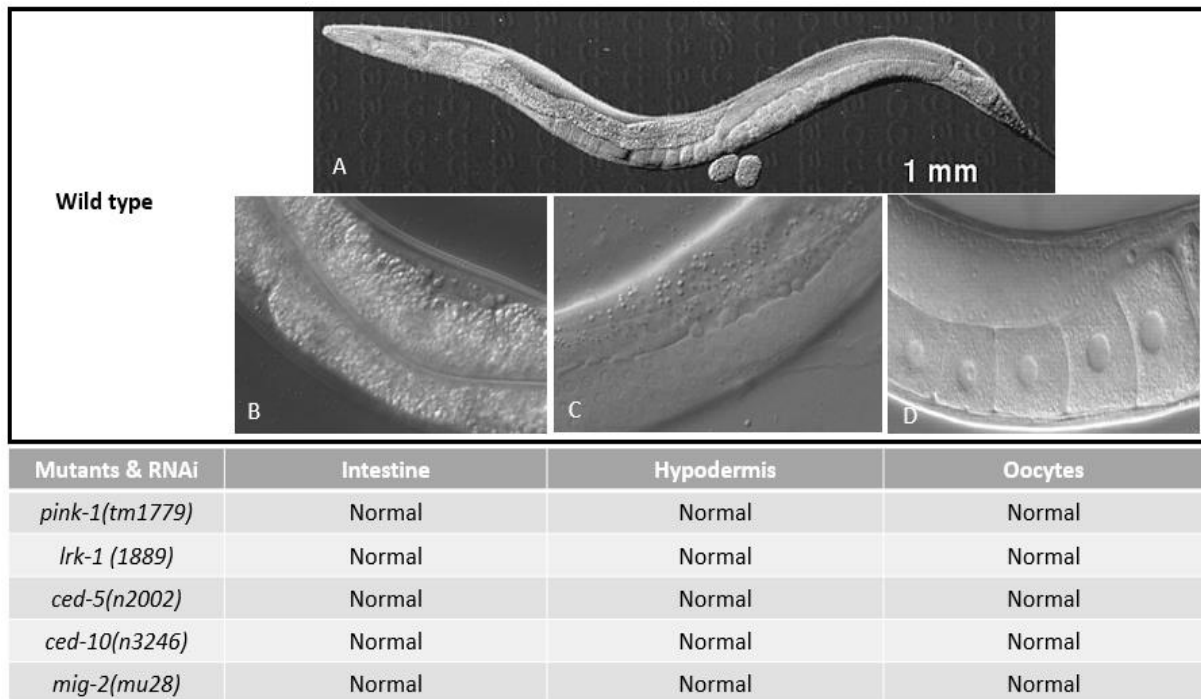


Fig 28: DIC image of adult *C. elegans* whole body (A), intestine (B), hypodermis (C) and oocyte (D) structures.

Table: Represent the microscopic observation result of listed mutants in particular tissues in adult *C. elegans*. *Normal* indicate that tissue and cellular structure observed for ET defect did not show any phenotypic change upon gene perturbation and resembles wild type structure.

In my observation, none of the observed mutant studied for microscopic analysis showed an obvious phenotype resembling an ET defect. Intestinal cells, hypodermal layer and oocytes observed upon perturbation looked similar in appearance when compared with wild type structure (Fig.18B, 20C, 20D).

These results suggest that despite their known role in ET, such an approach is not sufficient to observe phenotypic readout related to ET in the mutants I have tested and, hence, required a different approach.

4.2 *pink-1* mutant animals shows a phenotypic change in intestine and hypodermis

With the purpose of using a sensitized background to discover subtle differences effects in the mutant strains, I decided to induce stress pharmacologically. As described in the hypothesis session, the effect of Paraquat inducing ROS and *pink-1* sensitivity could make a synergic effect.

With this idea in mind, I tested the effect of Paraquat on *pink-1(tm1779)* mutant worms using a “Protocol for developmental stage of worm while treating them with PQ” (see material and methods 3.2.8.1) in order to search for an ET associated defect.

pink-1(tm1779) and wild type worms were subjected at early L3 stage to Paraquat doses ranging from 0 mM PQ to an acutely lethal dose of 50 mM. Visual observation by using compound microscopy of treated worms (0.5 to 2.5 mM) after one day showed phenotypic changes in the intestine and hypodermis of both mutant and wild type worms (Fig 19A). Strong phenotypic alteration appeared as small holes in the intestine and hypodermis of the worm without causing any detrimental effect. Penetrance of the observed phenotype was assessed quantitatively by using a compound microscope. The number of worm with the vacuoles in the intestine and hypodermis was quantified for both wild type and *pink-1(tm1779)* mutants, with or without PQ treatment (Fig. 19B). A significant phenotype was observed after application of a concentration between 0.5 mM to 2.5 mM. To avoid other detrimental effects, 2.5 mM concentration was selected as a non-lethal dose in the *pink-1(tm1779)* mutant strain.

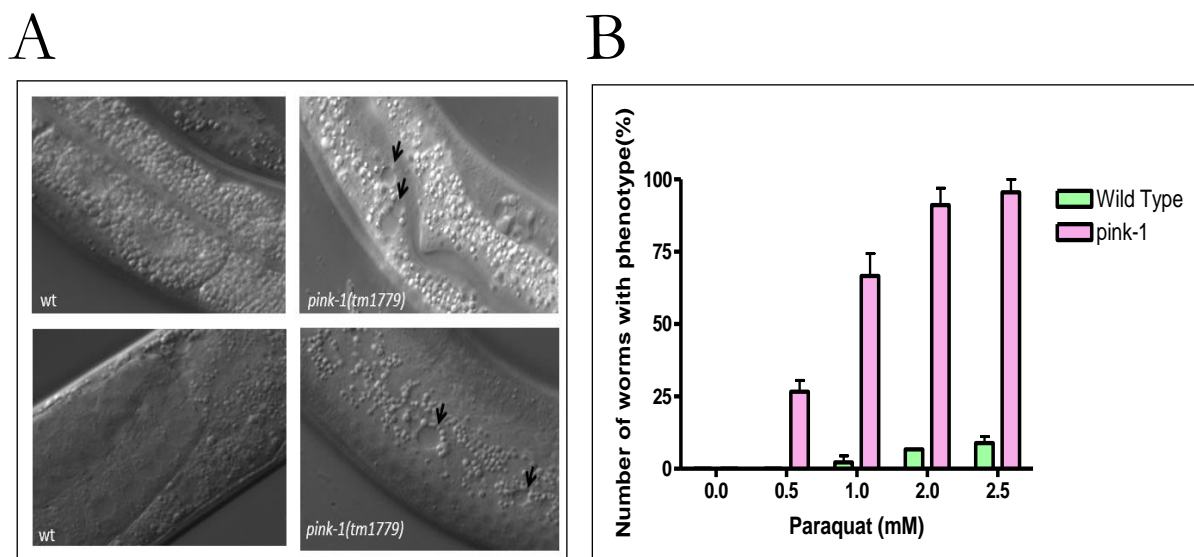


Fig 19: (A) Representative micrographs of observed phenotype in the intestine (upper row) and the hypodermis (lower row) of *pink-1(tm1779)* worms compared to wild type worm treated with 2.5 mM PQ: arrow indicate the formation of vacuoles in the intestine and hypodermis of *pink-1* worms, (B) Quantification of the observed phenotype by using dose response study: wild type and *pink-1(tm1779)* worms exposed to different concentration of PQ ranging from 0.5 mM to 2.5mM for one day at L3 stage. Phenotype was observed with compound microscope at 40X magnification. Exposure of non-lethal 2.0 mM and 2.5 mM PQ showed strongest phenotype in *pink-1* worms. Experiment was performed in triplicate counting approx. 30 worms each time from each strain. Error bar represent SEM.

Table 15: Behaviour of vacuole phenotype at different concentration of Paraquat.

Paraquat concentration (mM)	Genotype	% vacuole phenotype \pm SEM	n
0.0	wild type	0	65
	<i>pink-1(tm1779)</i>	0	62
0.5	wild type	0	78
	<i>pink-1(tm1779)</i>	26.66 \pm 6.66 ^a	84
1.0	wild type	2.23 \pm 2.23	69
	<i>pink-1(tm1779)</i>	66.66 \pm 7.69 ^b	70
2.0	wild type	6.67 \pm 0	75
	<i>pink-1(tm1779)</i>	91.11 \pm 5.87 ^c	80
2.5	wild type	8.89 \pm 2.22	90
	<i>pink-1(tm1779)</i>	95.55 \pm 4.44 ^d	90

P values related to wild type: a,b,c,d: ***P<0.001. All values represented as percentage mean \pm SEM. n: number of worms analyzed after paraquat treatment.

Paraquat treatment also reduced the body length of both *pink-1(tm1779)* and wild type animals, hence effect of 2.5 mM PQ was quantified using compound microscope and with the help of Axio Imager software (Fig. 20).

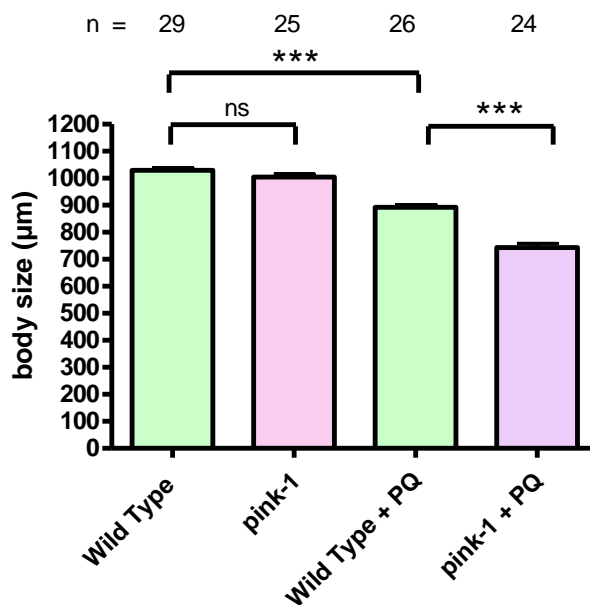


Fig 20: Effect of PQ on the body length of *pink-1(tm1779)* and wild type animal. The length (body size (µm)) of animals treated with 2.5mM PQ at L3 was compared to untreated control animals after one day. The exposure to PQ resulted in reduction in body length of both wild type and *pink-1(1779)* animals.

In summary, a synergistic effect of PQ and *pink-1* mutation was found to lead to phenotypic changes.

4.2.1 PQ induced vacuole phenotype in *pink-1* mutants suppressed by *lrk-1* loss of function mutant

PINK-1 and LRK-1 have already been proposed to act antagonistically, whereby all the phenotypic aspects observed with loss of *lrk-1* are suppressed by *pink-1(lf)* mutation and vice versa (Säman 2008). So I wondered if this newly discovered phenotypic aspects of *pink-1* is also subject to modulation by *lrk-1*.

To investigate whether the vacuole phenotype in *pink-1* is affected by other mutants and upon PQ treatment, *C. elegans pink-1* and *lrk-1* single and double mutants were subjected to 2.5 mM PQ following standard PQ test assay as described before. Loss of function (*lf*) of *lrk-1(tm1889)* (26.66 ± 3.84^b) slightly increased this phenotype with respect to wild type (16.57 ± 1.98) (Fig 21 and Table 16), but this effect was not significant. In contrast, downregulation of *lrk-1(tm1898)* suppressed the vacuole phenotype of *pink-1(tm1779)* significantly (Fig 21).

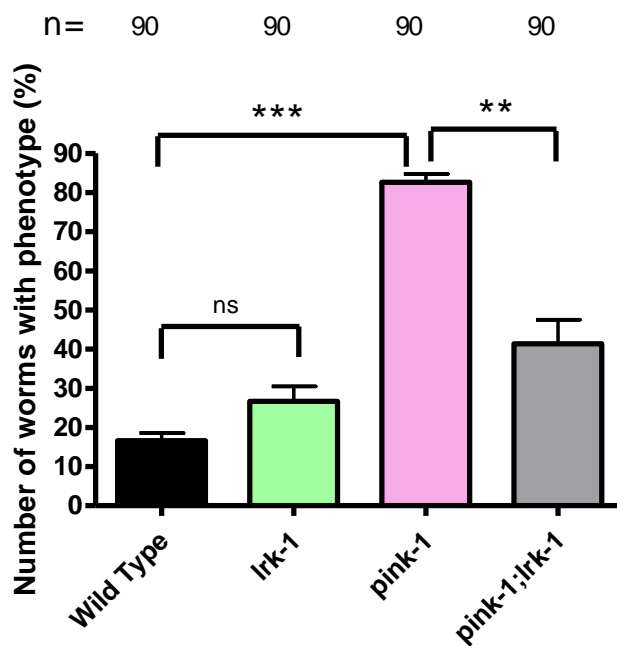


Fig 21: Paraquat induced vacuole phenotype upon loss of *pink-1* was suppressed by deletion of *lrk-1*. Synchronized L3 larval worms grown at 20° on NGM plates were exposed to 2.5 mM PQ for one day and microscopy was performed with day 1 adult worms using compound microscope. Shown is the mean number of worms (percentage) with a phenotype. Total number of worms analyzed are listed above each column (n). P values were calculated by t-test analysis (***P<0.0005, **P<0.0095). Error bar represent SEM.

Table 16: Behavior of observed vacuole phenotype in *pink-1* and *lrk-1* single and double mutant

Genotype	% vacuole phenotype \pm s.e.m.	n
Wild type	16.57 ± 1.98	90
<i>pink-1(tm1779)</i>	82.64 ± 2.04^a	90
<i>lrk-1(tm1889)</i>	26.66 ± 3.84^b	90
<i>pink-1(tm1779);lrk-1(tm1898)</i>	$43.9 \pm 6.08^{c,d}$	90

P values related to wild type: a: ***P<0.0005, b: P=n.s, c: *P<0.0357

P value related to *pink-1(tm1779)*: d: **P<0.0095

n: total number of worms scored for each genotype. (P values calculated using Student's t- test)

The vacuole phenotype observed in *pink-1* mutant was found to be suppressed by *lrk-1* downregulation is consistence with the published results (Sämman, Hegermann et al. 2009).

4.3 Generation of a *rab-10::gfp* reporter strain for characterization of vacuole phenotype by *pink-1*

RAB-10 is a key basolateral recycling endosomes regulator and GFP fusion proteins stain punctate structures in most tissues (Chen, Schweinsberg et al. 2006). In the intestine it is localized to distinct cytoplasmic puncta resembling endosomes (Sim, Lio et al. 2006). If *pink-1* plays a role in ET by regulating transport of MDVs (McLelland, Soubannier et al.), I suspected that vesicles formed in the intestine could be one of the consequences of defects during ET, where *pink-1* may also play a role at endosomal level. This fact led me to cross a *pink-1(tm1779)* strain with transgene BR6944 (kindly provided by Barth D. Grant lab) in which *rab-10* is fused with GFP and intestine specific *vha-6* promoter (for details see Material and Methods).

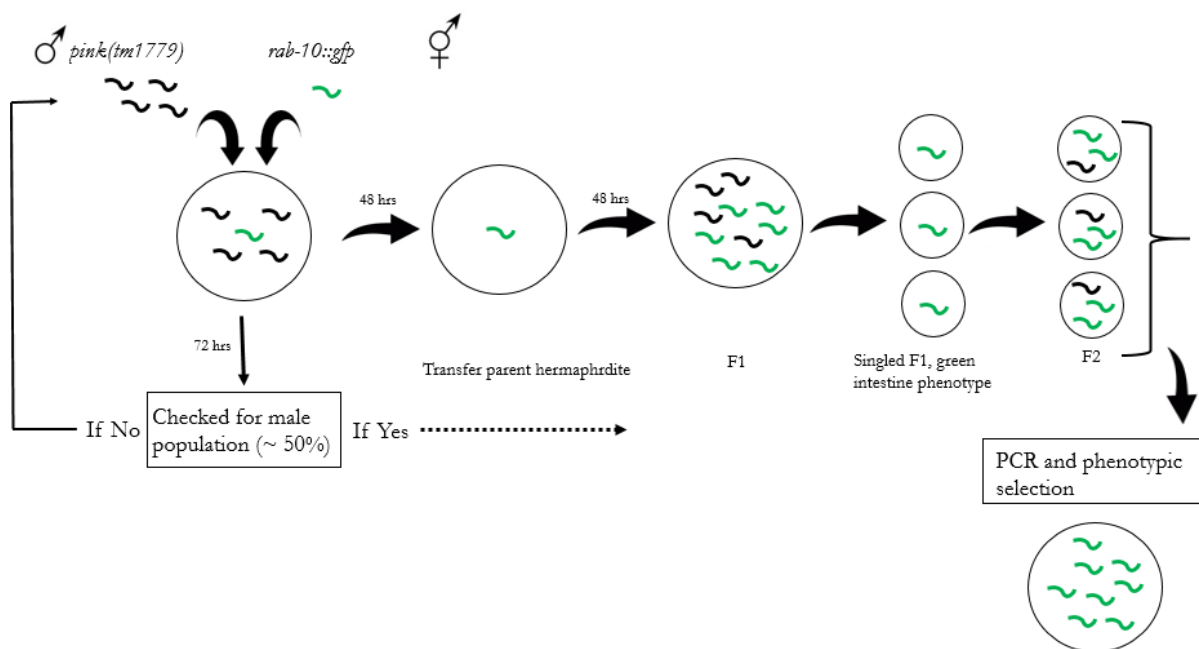
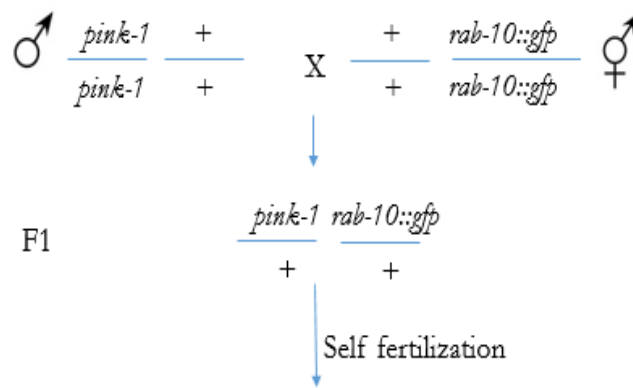


Fig. 22: Schematic representation of cross between *pink-1(tm1779)* and BR6944 which is *rab-10::gfp*. 4 males of *pink-1(tm1779)* were crossed with a *rab-10::gfp* hermaphrodite in duplicate and cultured at 20°C. After 48 hours, F0 parents were transferred to the new plate. 72 hours later the beginning of cross original plate was observed under stereo microscope for male population which was around 50%, indicating that cross was successful. In another case when no males were observed on the plate, the mating was repeated. New plate with transferred hermaphrodite were continued to culture at 20°C. 48 hours after 8 F1 worms were singled by selecting green fluorescent intestinal phenotype. For every generation this selection criteria was maintained until all progeny showed green fluorescence, which confirms the homozygosity for *rab-10::gfp* transgene. Singled F1 animals, after they have laid eggs for, were subjected to PCR to identify the *pink-1(tm1779)* allele. This genotypic and phenotypic selection was carried out for all the successive generation until desired result were obtained.



F2	<i>pink-1/rab-10</i>	<i>+/rab-10</i>	<i>pink-1/+</i>	<i>+/+</i>
<i>pink-1/rab-10</i>	<i>pink-1/pink-1; rab-10/rab-10</i>	<i>+/pink-1; rab-10/rab-10</i>	<i>pink-1/pink-1; rab-10/+</i>	<i>+/pink-1; rab-10/+</i>
<i>+/rab-10</i>	<i>+/pink-1; rab-10/rab-10</i>	<i>+/+; rab-10/rab-10</i>	<i>+/pink-1; rab-10/+</i>	<i>+/+; rab-10/+</i>
<i>pink-1/+</i>	<i>pink-1/pink-1; +/rab-10</i>	<i>+/pink-1; rab-10/+</i>	<i>pink-1/pink-1; +/+</i>	<i>+/pink-1; +/+</i>
<i>+/+</i>	<i>pink-1/+; rab-10/+</i>	<i>+/+; rab-10/+</i>	<i>+/pink-1; +/+</i>	<i>+/+; +/+</i>

Fig. 23: Genotypic representation of cross between *pink-1(tm1779)* and *rab-10::gfp*. F1 generation combination. Green cell in the Punnett square represent the desired genotype of expected mutant.

In order to verify the final resulting strain, I took advantage of the characterization of *pink-1* mutant. The *pink-1(tm1779)* allele harbors a 350 bp deletion elimination transcriptional and translational sites (Fig 24).

pink-1 (EEED8.9)

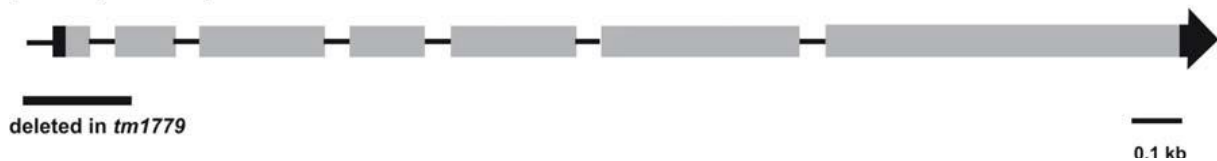


Fig 24: Genomic structure of *pink-1*. Exons and introns are indicated by boxes and lines, respectively. The genomic region that is deleted in the *tm1779* allele is indicated by a bold line.

To identify the *pink-1(tm1779)* genotype in the resulting strain by PCR, oligonucleotide (mentioned in Material and Methods) were designed to amplify the genomic DNA of *pink-1*.

As shown in Figure 25, wild type (wt) and mutant (mt) alleles were distinguished according to the size of their PCR product. Because of the deletion of 350 bp resulting band for *pink-1(tm1779)* was observed shorter (317 bp) compared to wild type (667 bp), verify the homozygous *pink-1(tm1779)* genotype. On the other hand,

BR6944 constitute an integrated *rab-10::gfp* expressed in the intestine, which is a dominant phenotype. By selecting green worm in every generation until it produced 100% progeny with green intestine phenotype confirmed the homozygosity for BR6944.



Fig 25: Identification of *pink-1* (mt) in BR7005 strain by analysis of genomic DNA. The mutant allele bearing a deletion results in a shorter PCR product compare to a wild type (wt) animal: amplified DNA of wt (666 bp) and BR7005 (mt) (317 bp) compared with *pink-1(tm1779)* (317 bp) as a positive control (+). m: 100 bp ladder DNA marker.

4.4 Loss of *pink-1* and PQ induced stress leads to intracellular accumulation of RAB-10::GFP

I used the marker strain BR7005 to test, using the endosomal marker RAB-10::GFP, whether *pink-1* modulates vacuolar structures and/or the aggregation of RAB-10::GFP marked endosomes.

In this assay, BR7005 and *rab-10::gfp* strains were subjected to 2.5 mM PQ treatment according to the standard PQ assay (chapter 3.2.8). 30 synchronized day 1 worms with and without PQ treatment from each group in triplicate were analyzed for *rab-10::gfp* expression pattern, by using an Axio Imager compound microscope. In detail, pictures were taken from each worm with combination of DIC and GFP channels with 40X magnification, keeping the same exposure time and compared among all groups with and without PQ.

In the intestine, RAB-10::GFP localized to distinct cytoplasmic puncta resembling endosomes; when observed with confocal microscope (Fig.26B) (Sun, Liu et al. 2012). Using the Axio Imager compound microscope, *rab-10::gfp* appeared as evenly distributed in the intestine of an animal with very minute punctate structure when analyzed with and without PQ treatment (Fig.26Ac and 26Aa respectively). BR7005 strain without PQ treatment shows no change in expression pattern of RAB-10::GFP (Fig.26A). However, upon PQ treatment I found that RAB-10::GFP was accumulated in the intestinal cells and appeared as more intense punctate structures (Fig.26Ag). I also observed that vacuole structure that arose in *pink-1(tm1779)* after PQ treatment was not labeled by RAB-10::GFP. I further quantify the number of

worms with aggregation of RAB-10::GFP by using compound microscope and also performed statistical analysis using student's *t*-test (Fig.26C).

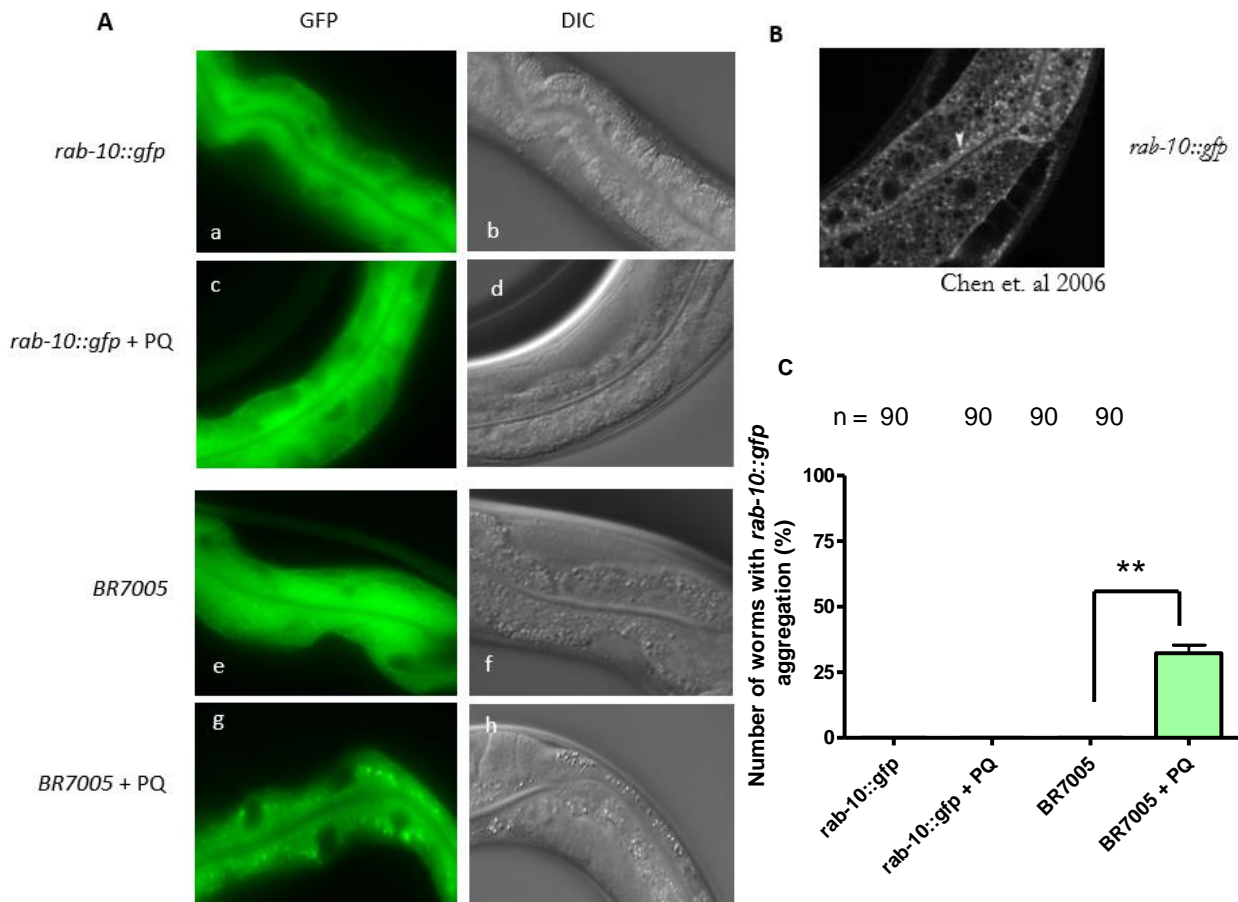


Fig 26: A) Representative micrograph of BR7005 and *rab-10::gfp* with and without 2.5mM PQ treatment. (a-d) GFP and DIC images of live *rab-10::gfp* worm intestine without PQ (a & b) and with PQ (c & d) respectively. (e-h) GFP and DIC images of live BR7005 worm intestine without PQ (e & f) and with PQ (g & h) respectively. BR7005 worms shows intracellular accumulation of *rab-10::gfp* upon PQ treatment (b). B) Confocal image showing expression of RAB-10::GFP in intestine, arrow head represent cytoplasmic puncta (Chen, Schweinsberg et al. 2006). C) Quantification number of worms showing aggregation of *rab-10::gfp* as a punctate structure in the intestinal cells. For PQ treatment L3 worms were treated with 2.5mM PQ and analyzed after 36 hours. Untreated worms were also analyzed at the same time point. Total number of worms analyzed are listed above each column (n). P values were calculated by student's *t*-test analysis (**P<0:0095). Error bar represent SEM.

In summary, RAB-10::GFP marker protein was found to be accumulated in the intestine of the *pink-1* animals suggesting impairment of trafficking of endosomes structure.

4.5 RNAi test for modulators of SGK-1 induced phenotype

The yeast orthologue of SGK, Ypk1, has been shown to affect ET in *S. cerevisiae* by regulating the endocytosis of fatty acids (Jacquier and Schneider 2010). Despite this proposed role in ET, there is no other information available about the mechanism of SGK/Ypk1 function in ET. Since the vacuole phenotype is easy to monitor, I have used this readout to screen for the modulators of SGK-1::GFP vacuole formation defect by RNAi.

I have used RNAi to test if a number of genes linked to PD related mechanisms may affect the vacuole phenotype and may, thus, be implicated in ET. In particular I studied Rho/Rac GTPase pathway mutants [Julia Säman, unpublished data] such as *ced-5*, *ced-10* and *mig-2*.

Also, from known direct or indirect interaction of SGK/SGK-1 with the genes involved in TGF β , MAPK, NOTCH, IIS and Rho/Rac GTPase signaling pathway (Table 2) have been screened to identify modulators of the vacuole phenotype of SGK-1 transgene.

I based my approach on preliminary results of another lab member, Yijian Yan (unpublished data), who showed first that the SGK-1::GFP strain (*byIs207[sgk-1::gfp]*) shows 88% \pm 3% of vacuole phenotype penetrance at 15°C and 20% \pm 3% of penetrance at 20°C observed at day 1 of adult stage of development in *C. elegans*.

This characteristic allowed me to perform the screen for suppression and enhancement of phenotype at 15° and 20° using an RNAi approach. Synchronized L4 worms of *byIs207[sgk-1::gfp]* strain were grown on NGM plates seeded with RNAi bacteria of targeted gene of interest at 15°C and 20°C. Progeny from these worms were analyzed by compound microscope at day 1 adult stage. Number of worms with the vacuole phenotype were quantified and compared with *byIs207[sgk-1::gfp]* worms grown on L4440 bacteria containing empty vector. Modifiers of the vacuole phenotype observed while performing this test are listed in Table 5 with their protein domain composition and function in *C. elegans*.

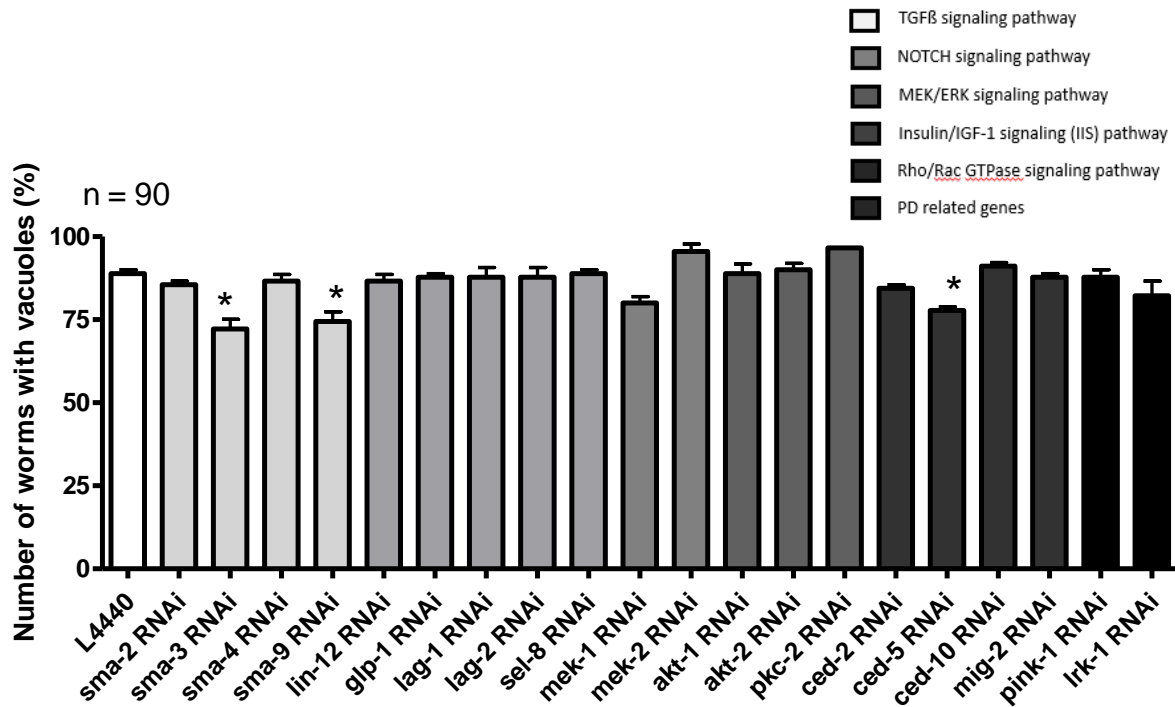


Fig. 27: RNAi of candidate genes for suppression of SGK-1::GFP induced vacuole phenotype. Vacuole phenotype of *IS(SGK-1::GFP)* strain fed with *E.coli* containing empty vector L4440 was scored as control. Suppressor screen were performed at 15° and 30 adult worms from each set of genotype were analyzed under compound microscope. Experiment was performed in triplicate. Total number of animals scored for each genotype is mentioned above (n). Statistical analysis performed by using Student's *t*-test. P values related to *IS(SGK-1::GFP)* fed with L4440 (*P<0.05; **P<0.01, error bar represent SEM).

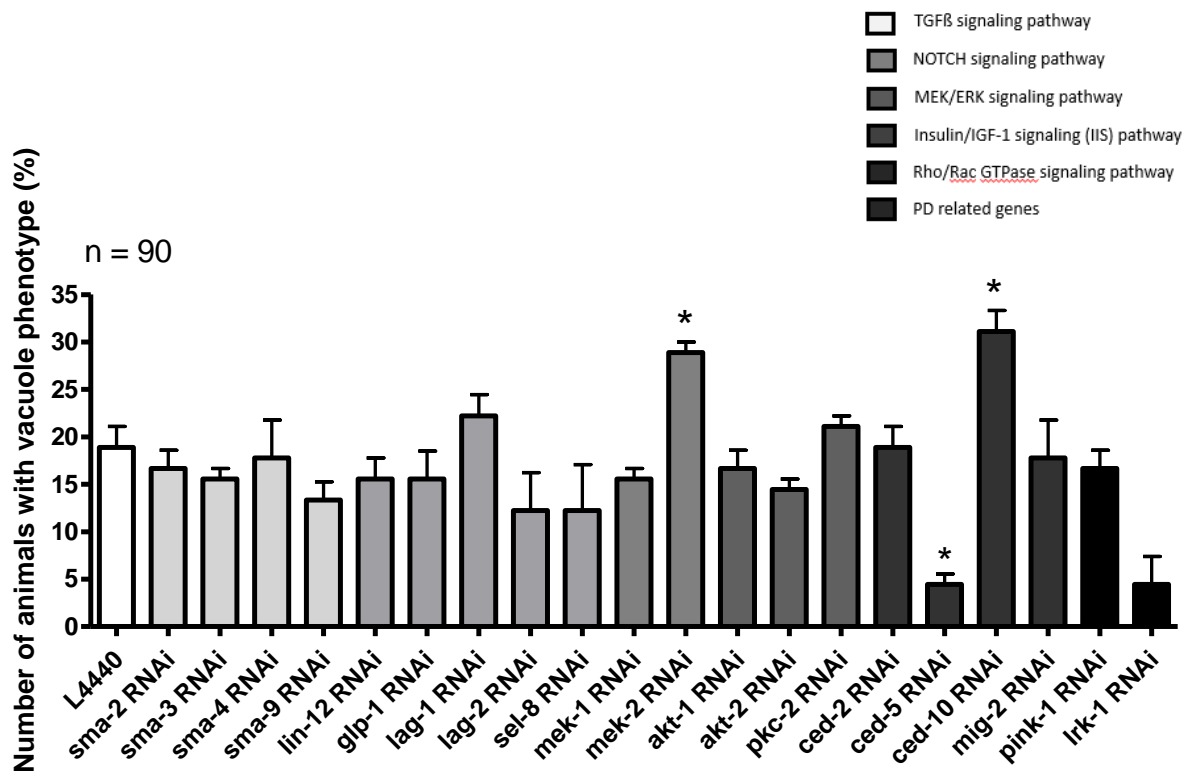


Fig. 28: RNAi of candidate genes for enhancement of SGK-1::GFP induced vacuole phenotype. Vacuole phenotype of *IS(SGK-1::GFP)* strain fed with *E.coli* containing empty vector L4440 was scored as control.

Enhancer screen was performed at 20° and 30 adult worms from each set of genotype were analyzed under compound microscope. Experiment was performed in triplicate. Total number of animals scored for each genotype is mentioned above (n). Statistical analysis performed by using Student's *t*-test. P values related to *IS(SGK-1::GFP)* fed with L4440 (*P<0.05; error bar represent SEM.)

This RNAi test provided a list of potential modifier candidates which need to be further studied for their role in ET or possible interaction with SGK-1.

4.6 Generation of reporter strain *lrk-1(tm1898);sgk-1::gfp(+)*

Although there was no significant effect observed with *lrk-1* RNAi on vacuole phenotype of SGK-1::GFP, its putative role in ET and previously described interaction with SGK-1 (described in chapter 2.7.2) makes it a potential candidate for epistatic study. In order to perform such an epistatic analysis, where I expect that *lrk-1* mutation may affect the SGK-1::GFP induced vacuole phenotype, I crossed *lrk-1(tm1898)* loss of function mutant with the BR6575 *byIs207[sgk-1::gfp]* strain.

lrk-1 allele *tm1898* harbors a 379 bp deletion followed by a 9 bp insertion, leading to an early stop caused by frame shift (Fig. 29). Two characteristic domains of LRK-1, the kinase and the GTPase domain, are removed in *tm1898* by this out-of-frame deletion.

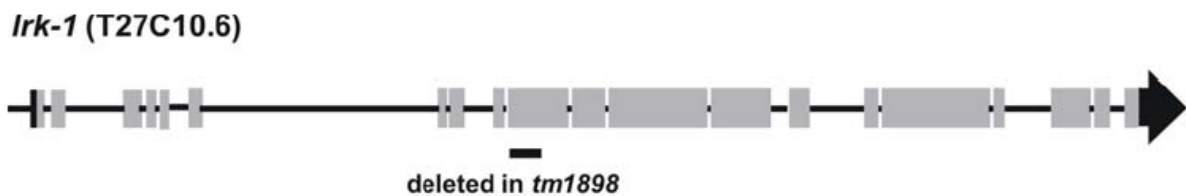


Fig: 29: **Genomic structure of *lrk-1*.** Exons and introns are indicated by boxes and lines, respectively. Bold lines underneath indicate the extent of the deleted region in deletion mutant.

The detailed crossing scheme is explained in the Methods section (chapter 3.2.5). The resulting strain *lrk-1(tm1898);byIs207[sgk-1::gfp]* was analyzed for the homozygosity of *lrk-1(tm1898)* and the transgene. To identify the *lrk-1(tm1898)* homozygous mutant, candidate animals were subjected to genotypic analysis by using PCR. Oligonucleotides were designed (Materials and Methods section) for the amplification of genomic DNA of *lrk-1* to identify and distinguish between wild type (wt) and mutant (mt) allele according to the size of PCR product (Fig. 30).

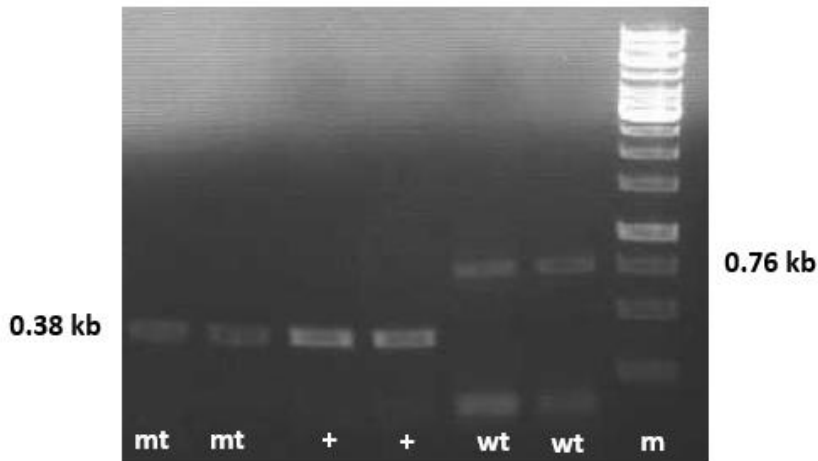


Fig. 30: Identification of *lrk-1(mt)* strain by analysis of genomic DNA. The mutant allele bearing a deletion results in a shorter PCR product compare to a wild type (wt) animal: amplified DNA of wt (762 bp) and mutant (mt) (385 bp) compared with *lrk-1(tm1898)* (385 bp) as a positive control (+). m: 100 bp ladder DNA marker.

Observed band for *lrk-1(tm1898)* allele was shorter (385 bp) than the wild type (762 bp) due to deletion of 379 bp's, confirms the homozygosity of allele *tm1898* in the mutant strain compared with *lrk-1(tm1898)* mutant band (385 bp) used as a positive control. To confirm the homozygous nature of BR6575 in the resulting strain, a phenotypic analysis was performed. BR6575 strain is an integrated transgene of SGK-1 fused with GFP and has a dominant phenotype of both green GFP staining and rolling body due to the integrated co-marker *rol-6*. So while following the crossing scheme, selection of green worm with roller phenotype until all the progeny in successive generation showing this phenotype confirmed the homozygosity for strain BR6575.

4.6.1 *lrk-1* downregulation suppresses the SGK-1::GFP vacuole phenotype

To test the effect of loss of *lrk-1* on the vacuole phenotype of SGK-1::GFP, a new strain *lrk-1(tm1898); byIs207[sgk-1::gfp]* was generated as described above and analyzed. In this analysis, day 1 adult worm were analyzed for the number of vacuoles in the intestine and compared with *byIs207[sgk-1::gfp]* at 15°C. Quantification of number of vacuoles in each worm was performed by using Axio Imager compound microscope. Although RNAi treatment did not affect the phenotype significantly, in this analysis I found that loss of *lrk-1(tm1898)* strongly suppressed the vacuole phenotype in *byIs207[sgk-1::gfp]*(Fig. 31). Average number of vacuoles in *byIs207[sgk-1::gfp]* intestine, when observed under compound microscope with 40X magnification (15.14 ± 0.54) are significantly reduced (2.12 ± 0.05) upon loss of *lrk-1(tm1899)* (table 17).

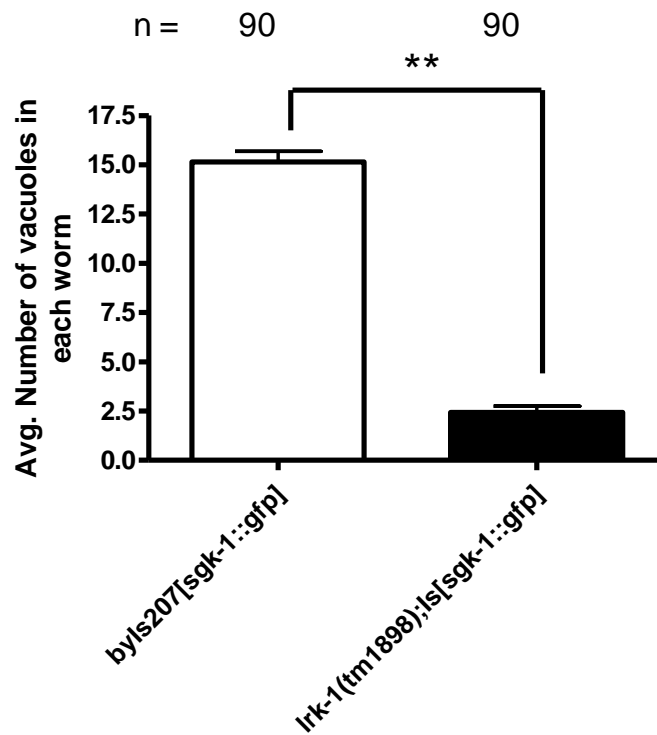


Fig. 31: Loss of *lrk-1* suppress the SGK-1 induced vacuole phenotype. Synchronized day 1 adult worm of *byIs207[sgk-1::gfp]* and *lrk-1(tm1898); byIs207[sgk-1::gfp]* strains were analyzed by using compound microscope 40X magnification. Shown is the average number of vacuoles (mean \pm SEM.) in each strain. Total number of worms analyzed are listed above each column (n). P values were calculated by t-test analysis (**P<0:0095). Error bar represent SEM.

Table 17: Behavior of vacuole phenotype upon loss of *lrk-1(tm1898)*

Genotype	Average number of vacuoles \pm s.e.m.	n
<i>byIs207[sgk-1::gfp]</i>	15.14 \pm 0.54	90
<i>byIs207[sgk-1::gfp];lrk-1(tm1898)</i>	2.12 \pm 0.05*	90

P values related to *byIs207[sgk-1::gfp]*: a: **P<0.0045 (Values are represented as SEM)

P value calculated using Student's *t*-test.

4.6.2 *lrk-1* downregulation alters SGK-1::GFP intensity

Suppression of vacuole phenotype of SGK-1 transgene by loss of *lrk-1(tm1898)*, which is supposed to be an ET defect, suggests a mechanistic role of *lrk-1* in generating vacuoles. However, the exact mechanism of how *lrk-1* interact with *sgk-1* is still an unanswered question.

To study this interaction, first I wanted to know whether *lrk-1* affects the expression level of SGK-1. Therefore, I compared the fluorescence intensity of *lrk-1(tm1898);byIs207[sgk-1::gfp]* with *byIs207[sgk-1::gfp]* alone. In *byIs207[sgk-1::gfp]* transgenic worms SGK-1 fused with GFP expressed specifically in intestine as well

as in head and tail neurons. In intestine it also stains the outer membrane of the vacuoles (Fig 9d).

In order to perform this analysis, more than 20 synchronized day 1 adult worm of each strain grown on NGM plates at 15°C, from three independent groups were analyzed for intestinal GFP expression by using an Axio Imager compound microscope. In detail for each worm pictures were taken by using combination of GFP and DIC channels using 10X magnification, keeping the same exposure time. GFP intensity was measured by using Image J software. Average intensity of GFP in both strains were quantified and statistics were applied using Student's *t*-test (Fig. 32 and table 18).

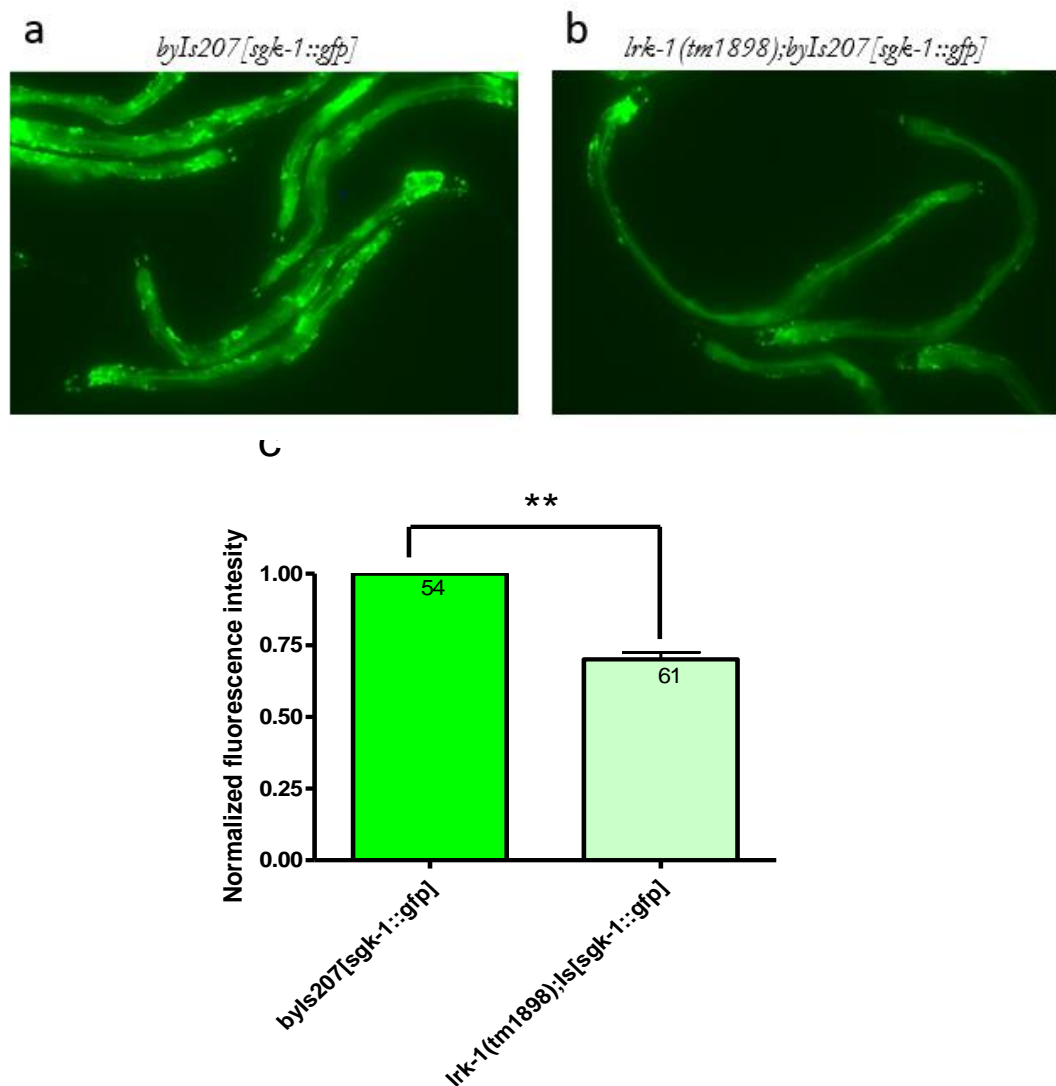


Fig. 32: *lrk-1* downregulation reduce the SGK-1::GFP expression. Representative micrographs (a, b) and corresponding fluorescence intensity quantification (c) shows that loss of *lrk-1(tm1898)* reduced the SGK-1::GFP intensity in *byIs207[sgk-1::gfp]* transgene. Columns represent pooled normalized values of three independent experiments plus standard error of the mean (SEM). Number inside the column indicate number of worm analyzed. ** $p < 0.05$, calculated by student's *t*-test.

Table 18: Fluorescence intensity data summary

Genotype	Average fluorescence intensity \pm SEM	Normalized fluorescence intensity \pm SEM	n
<i>byIs207[sgk-1::gfp]</i>	770 \pm 104.17	1 \pm 0	54
<i>byIs207[sgk-1::gfp];lrk-1(tm1898)</i>	586.54 \pm 32.82	0.69 \pm 0.04*	61

Average intensity of *lrk-1(tm1898); byIs207[sgk-1::gfp]* normalized to average intensity of *byIs207[sgk-1::gfp]*.

P values related to *byIs207[sgk-1::gfp]*: a: **P<0.0068 (Values are represented as SEM)

P value calculated using Student's *t*-test. n: number of worm analyzed.

In summary, I found that *lrk-1(tm1898)* significantly reduced number of vacuoles and also reduces the intensity of SGK-1::GFP staining, which is the consequence either of a reduced *sgk-1* gene expression or mRNA half-life or of a reduced SGK-1 protein stability/half-life. Despite this unresolved ambiguity, my data suggest a mechanistic interaction of SGK-1 and LRK-1 which appears to regulate the vacuole formation phenotype.

5 Discussion

5.1 Phenotypic alterations in PD related genes

Most of the ET defect as described previously are easy to observe even under the light microscope, such as vacuole formation in *rab-10*, *rme-1* mutant (Shi, Liu et al. 2012). Vacuole formation in these mutants is a consequence of impaired trafficking where intracellular organelles like endosomal structures fail to transport either to the lysosomes for their degradation or are recycled via the plasma membrane. It leads to enlargement of these organelles and their intracellular accumulation. As described earlier, PD related genes such as *pink-1* and *lrk-1* were studied to explain their putative role in regulation of endomembrane trafficking. However, obvious readout associated with ET as explained before is missing in these mutants. My results shows that with the help of microscopic analysis, despite their role in ET, *pink-1*, *lrk-1* and their functionally related genes upon perturbation do not shows an obvious ET defect (Fig.19) under standard, non-stress conditions. However, when challenged by e.g. exposure to reactive oxygen species (via application of Paraquat), different phenotypic aspects can be detected.

In order to observe ET defect in PD related genes, a pharmacological approach was adapted, where these mutants were treated with chemical stressors which supposed to induced intracellular stress. Such stress induced studies has been performed previously, where induced stress in the form of ROS served as a signaling molecule. In this work, response of *pink-1(tm1779)* animals to non-lethal concentration of PQ (2.5mM) was analyzed. PQ is known to induce superoxide molecule generation (Bus and Gibson 1984) which in turn triggers mitochondrial stress by increasing mitochondrial ROS levels in wild type animals (Fukushima, Yamada et al. 1993, Fukushima, Tanaka et al. 2002). *pink-1(tm1779)* worms sensitivity to PQ affects their survivor rate and also mitochondrial integrity (Sämman, Hegermann et al. 2009). However such stress induced studies which may leads to ET defect was not been studied before. Upon treatment with 2.5mM PQ, *pink-1(tm1779)*, as well as wild type worms, showed the described phenotypic changes in the intestine and the hypodermis (Fig: 21A). Intestine and hypodermis of treated worms displayed vacuole like structure which may be the consequence of increased intracellular ROS. Dose response study of PQ with observed phenotypic change explained that the penetrance of phenotype increased with increased PQ concentration in both wild type and *pink-1(tm1779)* worms. However, strong penetrance was observed in *pink-1(tm1779)* worms as compared with wild type, indicates synergistic effect of PQ and *pink-1* deletion. This is consistent with the fact that *pink-1* worms compared to wild type are more sensitive to ROS stress (Sämman, Hegermann et al. 2009).

A possible explanation for the strong penetrance of phenotype in *pink-1* mutants could be that the consequences of PQ which is known to alter mitochondrial morphology in *C. elegans* can no longer counteracted by the PINK-1/Parkin axis of mitochondrial stress signaling (Sämman, Hegermann et al. 2009), (Matsuda, Sato et al. 2010, Narendra, Jin et al. 2010, Vives-Bauza, Zhou et al. 2010). In this paradigm PINK1 accumulates on damaged mitochondrial membrane and recruits cytosolic PARKIN, which further triggers whole mitochondrial engulfment through an autophagosome-lysosome pathway, a process called mitophagy (Geisler, Holmstrom et al. 2010, Narendra, Jin et al. 2010). Absence of *pink-1* may affect the degradation of damaged mitochondria which may further affect the cell integrity by affecting intracellular transport pathways and may give rise to aggregation of vacuole structure in different tissues.

5.2 Vacuole phenotype in *pink-1(tm1779)* mutant rescued by *lrk-1(tm1899)* deletion

Antagonistic function of *pink-1* and *lrk-1* was already suggested to regulate stress response and neuronal activities (Sämman, Hegermann et al. 2009 2009). In order to see if the vacuole phenotype observed in *pink-1(tm1779)* deletion mutant upon PQ treatment also is functionally related to this mechanism, the influence of *lrk-1* was tested in this response (Fig. 11). It was found that in *pink-1(tm1779);lrk-1(tm1898)* double mutant the number of worms with vacuole phenotype was significantly reduced compared to *pink-1(tm1779)* mutant alone (Fig. 23). PQ inducing vacuole phenotype was also observed with *lrk-1(tm1898)* single mutant which was not significant when compare to wild type worms. This indicates that *lrk-1*, together with *pink-1*, also affects the vacuole phenotype. However mechanistic link explaining the cause of this phenotype is still unexplained. For that reason further investigation was focused on characterization of the ET phenotype.

5.3 Phenotypic change in the *pink-1* worms may related to ET defect

Next question was, if phenotypic change in the intestine of *pink-1(tm1779)* worms upon induced stress is related to endomembrane trafficking impairment. As describe earlier, defect in ET may sometimes leads to enlargement of intracellular organelles which appeared as a vacuole like structure (Fig. 9). To determine more precisely the nature of these vacuoles, RAB-10 fused with GFP marker was used as a marker of early endosomes in *C. elegans* (Chen, Schweinsberg et al. 2006). I found that vacuoles in the PQ treated *pink-1(tm1779)* worm intestine were not labeled by RAB-10::GFP. However, interestingly accumulation of RAB-10::GFP was observed in the intestinal cells of *pink-1(tm1799)* worms treated with PQ. In this case RAB-10::GFP tried to accumulate mostly along the apical membrane and around the nucleus of an intestinal cells (Fig. 26Ag). Such accumulation was not observed in *pink-*

1(tm1779) mutant worms in absence of PQ treatment. In wild type worms carrying only RAB-10::GFP protein with and without PQ treatment also shows even distribution of RAB-10::GFP without any abnormal intracellular accumulation (Fig. 26A). These results suggest that vacuolar structure observed in *pink-1* worms are not associated with early endosomes since RAB-10::GFP specifically labels early endosomes. However, accumulation of RAB-10::GFP indicates that a combined effect of PQ and *pink-1* deletion may be a cause of altered membrane trafficking. This suggest that the interaction of *pink-1* and *lrk-1* may be more complex than previously expected.

However the role of *pink-1* in ET leading to such a phenotype needs to be dissected carefully. One possible explanation for this accumulation could be the only effect of PQ, which is already been shown to induced mitochondrial stress, and as consequence of damaged mitochondria may affect the trafficking pathway. If this the case I may expect that, increasing PQ concentration should also leads to such phenotype in wild type worms without *pink-1* deletion. In this way one could exclude effect of PQ alone leading to trafficking effect if there is no change with increase PQ concentration on wild type worm. So future investigation should focus on the dissection and analysis of my findings.

5.4 RNAi downregulation of candidate genes affects the SGK-1 induced vacuole phenotype

In recent years, the role of SGK1 in ET was studied using various models systems and different readouts. However mechanistic function through which SGK1 regulates ET is missing. In *C. elegans*, transgenic worms overexpressing SGK-1 was shown to produce a vacuole phenotype in the intestine of these animals which is supposed to be a consequence of ET defect [Yijian. Yan, unpublished data]. So, in another set of experiment I have performed an RNAi studies to investigate if downregulating any of the selected candidate genes (Table 2) could modulate the vacuole phenotype either positively or negatively.

In a first approach to find suppressors of phenotype, an experiment was performed at 15°C, at which SGK-1 transgenes show maximum phenotype [Yijian. Yan, unpublished data]. Candidate genes were selected from different signaling pathways which, as identified previously in my lab, have direct or indirect interaction with SGK1/SGK-1. *sma-3* and *sma-9* encodes Smad proteins and functions as part of the DBL-1/SMA-6 TGFβ related signaling pathway (Savage-Dunn 2001 2000). Whereas SGK1 has been shown to upregulate TGFβ activity (Lang, Bohmer et al. 2006). Smad3 is a transcription factor which is phosphorylated by TGFβ and further ubiquitinated through ligase Nedd4L leading to its degradation (Gao, Alarcon et al. 2009). Interestingly, SGK1 is actually known to phosphorylate, and thus inactivate, Nedd4L ligase leading to upregulation of Smad2/Smad3 (Debonneville, Flores

et al. 2001). If this is the case, downregulating *sma-3* and *sma-9*, through a negative feedback mechanism, may suppress the transgenic SGK-1 function. In my experiment I have found that RNAi downregulation of *sma-3*, *sma-9* significantly suppressed the vacuole phenotype of SGK-1 transgene (Fig. 27), indicating an interaction between SGK-1 and TGF β linked genes controlling generation of vacuole phenotype. However, to support this fact one needs to first analyze whether any RNAi down-regulates SGK-1, since this was shown by me to be sufficient for suppressing vacuole formation (see below).

In a yeast split ubiquitin screen DOCK180, human homologue of CED-5 in *C. elegans* was identified as potential interactor of SGK1 [Dirnberger et.al, unpublished results]. *C. elegans* SGK-1 was also shown to interact with CED-5 through its DHR-2 domain in an immunoprecipitation assay [Gashaj, Qi et.al, unpublished results]. Both findings suggests an interaction between DOCK180/CED-5 and SGK1/SGK-1. CED-5 is also a guanine nucleotide exchange factor (GEF) of Rho GTPase RAC1/CED-10, which in studies performed in our lab has been implicated to function in the same signaling pathway as SGK-1 to regulate DTC migration defect [Xu Huang, unpublished data]. My RNAi data shows downregulation of *ced-5* suppress the vacuole phenotype both at 15°C and 20°C, whereas *ced-10* enhance the vacuole phenotype at 20°C (Fig. 27 & 28). This data is in contrast to already established fact, where CED-10 functions downstream of CED-5 and positively controls phagocytosis and cell migration in *C. elegans* (Reddien and Horvitz 2000). To this end further investigation should be in the direction to collect more genetic data by generating double mutants and analyze the effect if it is consistence with the RNAi data.

In addition I also found that *mek-2* silencing by RNAi increase the vacuole phenotype of SGK-1 when observed at 20°C (Fig. 28). *mek-2* encodes a MAP kinase kinase, and functions in a Ras-mediated signal transduction pathway that regulate several biological processes. Transgenic worms overexpressing SGK-1 produce 20% \pm 3% vacuole phenotype, which was found to be enhanced by 10% upon downregulation of *mek-2*. This data may be in the direction towards already established finding where mammalian SGK1 has been shown to activate MEK/ERK signaling required for cell proliferation, if there exist negative feedback response. In this way one could expect that upon loss of MEK/ERK signaling component, it may affect role of SGK-1 negatively.

Table.19: Summary of effect of RNAi downregulation of gene candidates on vacuole phenotype

<i>C. elegans</i> gene	Homo sapiens homologue	Signaling pathway	Function in <i>C. elegans</i>	RNAi test result
<i>ced-5</i>	DOCK180	Rho/RacGTPase	Cell engulfment stage of programmed cell death	Suppressor
<i>sma-3</i>	SMAD4/6/7	TGF β	Controls body size and male tail sensory ray and spicule formation	Suppressor
<i>sma-9</i>	HIVEP1	TGF β	Regulate body size and male tail patterning and morphogenesis and reproductive aging	Suppressor
<i>mek-2</i>	MAP2K1/MAP2K2	MAPK	Larval development, vulval development, cell migration, meiotic cell cycle progression, olfaction, and pathogen defense	Enhancer
<i>ced-10</i>	RAC1	Rho/RacGTPase	Required for phagocytosis during programmed cell death and for migration of the distal tip cells of the somatic gonad	Enhancer

On the other hand, *pink-1* and *lrk-1* RNAi showed no significant effect on vacuole phenotype at both temperature condition. *lrk-1* silencing decreases the vacuole phenotype at 20°C, however this was not significant (Fig. 27 & 28). In summary, this RNAi test provide a list of potential candidates (Table 19), which needs to be investigated carefully to reveal their possible interaction with SGK-1 and role in ET if any.

5.5 Mechanistic link between LRK-1 and SGK-1 regulating ET

LRRK2/LRK-1 function in vesicular trafficking has been studied in recent years, where both implicated in regulating synaptic vesicular transport (Sakaguchi-Nakashima, Meir et al. 2007, Shin, Jeong et al. 2008, Sanna, Del Giudice et al. 2012). Whereas SGK1 regulating ET has been shown in *S. cerevisiae*, in which Ypk1 a yeast orthologue of SGK1 controls the endocytosis of fatty acids. In *C. elegans*, *lrk-1* and *sgk-1* expressed broadly. Recently, our lab has shown that SGK-1 overexpression leads to a vacuole formation in the intestine which has been predicated to be a consequence of endomembrane trafficking impairment [Yijian Yan, unpublished results]. Mechanistic role of *lrk-1* interacting with *sgk-1* has also been suggested previously, where they both together controls the cell migration through modulation of actin cytoskeleton [Xu Huang, unpublished results]. My findings shows that elimination of *lrk-1(tm1898)* suppress the SGK-1 induced vacuole phenotype significantly and also reduced the expression levels of SGK-1::GFP (Fig.31 & 32). LRRK2 co-localization with endosomal marker Rab7 and with lysosomal marker LAMP2 suggested it's function in the endo-lysosomal pathway in ET (Higashi, Moore et al. 2009 2009), whereas SGK-1 role in regulating ET is still under investigation to understand the exact pathway of trafficking influenced by it. Also there is not

enough evidence which can show direct interaction between *lrk-1* and *sgk-1*. Based on my observations, *lrk-1* deletion tends to compensate SGK-1 induced vacuole formation by reducing its number may suggest that both *lrk-1* and *sgk-1* may share common pathway to regulate mechanistically the trafficking of these vesicle like structure.

6 Conclusion

In this work, I have used different approaches to establish a readout that can explain genetic interaction between PINK-1, LRK-1 and SGK-1 in regulating endomembrane trafficking. Although most of the readouts in ET mutants used by previous researchers were easy to observe with light microscope, it is not the case with *pink-1* and *lrk-1* mutants despite their putative role in ET. Based on mutant analysis and pharmacological studies I have found that the synergistic effect of *pink-1* deletion and Paraquat treatment leads to phenotypic changes in *C. elegans*. The most obvious readout I observed in *pink-1* animals was vacuole formation in the intestine and hypodermis. In an attempt to characterize this phenotype by using RAB-10::GFP early endosome marker, I found that vacuoles observed in the intestine did not stain with RAB-10, and, thus, may not be an early endosome related structure. However such finding does not exclude the possibility of ET impairment leading to appearance of these vacuoles. To understand the membrane source of these vacuole like structure in the context of ET, further investigations need to be followed by using other available endocytic markers (for example those listed in Table 1).

Another phenotype I observed in *pink-1* animals was aggregation of RAB-10::GFP in the intestine. Rab modulations recently has been emerged as a general principle of membrane trafficking (Hutagalung and Novick 2011). RAB-10 as an early endosome marker normally appeared as cytoplasmic punctate structure distributed evenly in the intestine. Aggregation of such punctate structure upon loss of *pink-1* suggest that transport of early endosomes, their maturation into late endosome, or their participation in the recycling endosome may be impaired. PINK1 role in ET especially in the neuronal system has been explained previously, where impaired mitochondrial transport in absence of *PINK1* is one of the cause in development of Parkinson's disease. My findings suggesting potential role of PINK-1 in *C. elegance* intestinal cells regulating ET may provide a model to study genes related to PD in more detail.

I also used vacuole phenotype in SGK-1 transgenic worms to better understand the interaction between LRK-1, PINK-1 and SGK-1. Epistatic analysis suggested that *lrk-1* downregulation suppressed the SGK-1 induced vacuole phenotype and also reduced SGK-1 levels. This strong phenotypic alteration suggest a mechanistic role of both LRK-1 and SGK-1 in controlling vacuole formation which may be the consequence of an ET impairment. During this study I also found some other modulators of vacuole phenotype (Table 19) which are associated with different signaling pathways. This list of potential candidate needs to be studied for their interaction with SGK-1.

In summary, during this work I have found a new readout in *pink-1* mutant which may suggest a potential role of PINK-1 in ET and also showed that

LRK-1 and SGK-1 may share common function in regulation of ET associated phenotype. Future work will be directed to understand the nature of new phenotype observed in *pink-1* animals and to test PINK-1, LRK-1 and SGK-1 model for this readout.

References

- Aasly, J. O., M. Toft, I. Fernandez-Mata, J. Kachergus, M. Hulihan, L. R. White and M. Farrer (2005). "Clinical features of LRRK2-associated Parkinson's disease in central Norway." Ann Neurol **57**(5): 762-765.
- Abeliovich, A., Y. Schmitz, I. Farinas, D. Choi-Lundberg, W. H. Ho, P. E. Castillo, N. Shinsky, J. M. Verdugo, M. Armanini, A. Ryan, M. Hynes, H. Phillips, D. Sulzer and A. Rosenthal (2000). "Mice lacking alpha-synuclein display functional deficits in the nigrostriatal dopamine system." Neuron **25**(1): 239-252.
- Alliston, T. N., A. C. Maiyar, P. Buse, G. L. Firestone and J. S. Richards (1997). "Follicle stimulating hormone-regulated expression of serum/glucocorticoid-inducible kinase in rat ovarian granulosa cells: a functional role for the Sp1 family in promoter activity." Mol Endocrinol **11**(13): 1934-1949.
- Balklava, Z., S. Pant, H. Fares and B. D. Grant (2007). "Genome-wide analysis identifies a general requirement for polarity proteins in endocytic traffic." Nat Cell Biol **9**(9): 1066-1073.
- Balklava, Z. and E. Sztul (2013). "Studying Membrane Trafficking in the Worm *C. elegans* by RNA Interference." Methods for Analysis of Golgi Complex Function **118**: 51-68.
- Beilina, A., M. Van Der Brug, R. Ahmad, S. Kesavapany, D. W. Miller, G. A. Petsko and M. R. Cookson (2005). "Mutations in PTEN-induced putative kinase 1 associated with recessive parkinsonism have differential effects on protein stability." Proceedings of the National Academy of Sciences of the United States of America **102**(16): 5703-5708.
- Bell, L. M., M. L. L. Leong, B. Kim, E. Wang, J. Park, B. A. Hemmings and G. L. Firestone (2000). "Hyperosmotic stress stimulates promoter activity and regulates cellular utilization of the serum- and glucocorticoid-inducible protein kinase (Sgk) by a p38 MAPK-dependent pathway." Journal of Biological Chemistry **275**(33): 25262-25272.
- Biskup, S., D. J. Moore, F. Celsi, S. Higashi, A. B. West, S. A. Andrabi, K. Kurkinen, S. W. Yu, J. M. Savitt, H. J. Waldvogel, R. L. M. Faull, P. C. Emson, R. Torp, O. P. Ottersen, T. M. Dawson and V. L. Dawson (2006). "Localization of LRRK2 to membranous and vesicular structures in mammalian brain." Annals of Neurology **60**(5): 557-569.
- Blake, M. J., R. Udelsman, G. J. Feulner, D. D. Norton and N. J. Holbrook (1991). "Stress-Induced Heat-Shock Protein-70 Expression in Adrenal-Cortex - an Adrenocorticotrophic Hormone-Sensitive, Age-Dependent Response." Proceedings of the National Academy of Sciences of the United States of America **88**(21): 9873-9877.
- Bonifacino, J. S. and B. S. Glick (2004). "The mechanisms of vesicle budding and fusion." Cell **116**(2): 153-166.

Bonifacino, J. S. and J. H. Hurley (2008). "Retromer." Current Opinion in Cell Biology **20**(4): 427-436.

Bonifati, V., C. F. Rohe, G. J. Breedveld, E. Fabrizio, M. De Mari, C. Tassorelli, A. Tavella, R. Marconi, D. J. Nicholl, H. F. Chien, E. Fincati, G. Abbruzzese, P. Marini, A. De Gaetano, M. W. Horstink, J. A. Maat-Kievit, C. Sampaio, A. Antonini, F. Stocchi, P. Montagna, V. Toni, M. Guidi, A. Dalla Libera, M. Tinazzi, F. De Pandis, G. Fabbrini, S. Goldwurm, A. de Klein, E. Barbosa, L. Lopiano, E. Martignoni, P. Lamberti, N. Vanacore, G. Mecco, B. A. Oostra and I. P. Networks (2005). "Early-onset parkinsonism associated with PINK1 mutations - Frequency, genotypes, and phenotypes." Neurology **65**(1): 87-95.

Bosgraaf, L. and P. J. M. Van Haastert (2003). "Roc, a Ras/GTPase domain in complex proteins." Biochimica Et Biophysica Acta-Molecular Cell Research **1643**(1-3): 5-10.

Brenner, S. (1974). "The genetics of *Caenorhabditis elegans*." Genetics **77**(1): 71-94.

Brodsky, F. M., C. Y. Chen, C. Knuehl, M. C. Towler and D. E. Wakeham (2001). "Biological basket weaving: formation and function of clathrin-coated vesicles." Annu Rev Cell Dev Biol **17**: 517-568.

Bus, J. S. and J. E. Gibson (1984). "Paraquat - Model for Oxidant-Initiated Toxicity." Environmental Health Perspectives **55**(Apr): 37-46.

Buse, P., A. C. Maiyar, K. L. Failor, S. Tran, M. L. Leong and G. L. Firestone (2007). "The stimulus-dependent co-localization of serum- and glucocorticoid-regulated protein kinase (Sgk) and Erk/MAPK in mammary tumor cells involves the mutual interaction with the importin-alpha nuclear import protein." Exp Cell Res **313**(15): 3261-3275.

Cadenas, E., A. Boveris, C. I. Ragan and A. O. M. Stoppani (1977). "Production of Superoxide Radicals and Hydrogen-Peroxide by Nadh-Ubiquinone Reductase and Ubiquinol-Cytochrome C Reductase from Beef-Heart Mitochondria." Archives of Biochemistry and Biophysics **180**(2): 248-257.

Chen, C. C., P. J. Schweinsberg, S. Vashist, D. P. Mareiniss, E. J. Lambie and B. D. Grant (2006). "RAB-10 is required for endocytic recycling in the *Caenorhabditis elegans* intestine." Mol Biol Cell **17**(3): 1286-1297.

Chen, C. C. H., P. J. Schweinsberg, S. Vashist, D. P. Mareiniss, E. J. Lambie and B. D. Grant (2006). "RAB-10 is required for endocytic recycling in the *Caenorhabditis elegans* intestine." Molecular Biology of the Cell **17**(3): 1286-1297.

Clark, I. E., M. W. Dodson, C. G. Jiang, J. H. Cao, J. R. Huh, J. H. Seol, S. J. Yoo, B. A. Hay and M. Guo (2006). "*Drosophila pink1* is required for mitochondrial function and interacts genetically with parkin." Nature **441**(7097): 1162-1166.

Cooper, A. A., A. D. Gitler, A. Cashikar, C. M. Haynes, K. J. Hill, B. Bhullar, K. Liu, K. Xu, K. E. Strathearn, F. Liu, S. Cao, K. A. Caldwell, G. A. Caldwell, G. Marsischky, R. D. Kolodner, J. Labaer, J. C. Rochet, N. M. Bonini and S. Lindquist (2006). "Alpha-

synuclein blocks ER-Golgi traffic and Rab1 rescues neuron loss in Parkinson's models." Science **313**(5785): 324-328.

Debonneville, C., S. Y. Flores, E. Kamynina, P. J. Plant, C. Tauxe, M. A. Thomas, C. Munster, A. Chraïbi, J. H. Pratt, J. D. Horisberger, D. Pearce, J. Loffing and O. Staub (2001). "Phosphorylation of Nedd4-2 by Sgk1 regulates epithelial Na⁺ channel cell surface expression." Embo Journal **20**(24): 7052-7059.

Di Fonzo, A., C. F. Rohe, R. J. Ferreira, H. F. Chien, L. Vacca, F. Stocchi, L. Guedes, E. Fabrizio, M. Manfredi, N. Vanacore, S. Goldwurm, G. Breedveld, C. Sampaio, G. Meco, E. Barbosa, B. A. Oostra, V. Bonifati and I. P. G. Network (2005). "A frequent LRRK2 gene mutation associated with autosomal dominant Parkinson's disease." Lancet **365**(9457): 412-415.

Dieter, M., M. Palmada, J. Rajamanickam, A. Aydin, A. Busjahn, C. Boehmer, F. C. Luft and F. Lang (2004). "Regulation of glucose transporter SGLT1 by ubiquitin ligase Nedd4-2 and kinases SGK1, SGK3, and PKB." Obes Res **12**(5): 862-870.

Dodson, M. W., T. Zhang, C. Jiang, S. Chen and M. Guo (2012). "Roles of the Drosophila LRRK2 homolog in Rab7-dependent lysosomal positioning." Hum Mol Genet **21**(6): 1350-1363.

Fares, H. and I. Greenwald (2001). "Genetic analysis of endocytosis in Caenorhabditis elegans: coelomocyte uptake defective mutants." Genetics **159**(1): 133-145.

Farrer, M., J. Stone, I. F. Mata, S. Lincoln, J. Kachergus, M. Hulihan, K. J. Strain and D. M. Maraganore (2005). "LRRK2 mutations in Parkinson disease." Neurology **65**(5): 738-740.

Feng, J. L., F. Bussiere and S. Hekimi (2001). "Mitochondrial electron transport is a key determinant of life span in Caenorhabditis elegans." Developmental Cell **1**(5): 633-644.

Fillon, S., K. Klingel, S. Warntges, M. Sauter, S. Gabrysch, S. Pestel, V. Tanneur, S. Waldegger, A. Zipfel, R. Viebahn, D. Haussinger, S. Broer, R. Kandolf and F. Lang (2002). "Expression of the serine/threonine kinase hSGK1 in chronic viral hepatitis." Cell Physiol Biochem **12**(1): 47-54.

Fukushima, T., K. Tanaka, H. Lim and M. Moriyama (2002). "Mechanism of cytotoxicity of paraquat." Environ Health Prev Med **7**(3): 89-94.

Fukushima, T., K. Yamada, A. Isobe, K. Shiwaku and Y. Yamane (1993). "Mechanism of Cytotoxicity of Paraquat .1. Nadh Oxidation and Paraquat Radical Formation Via Complex-I." Experimental and Toxicologic Pathology **45**(5-6): 345-349.

Gandhi, S., M. M. K. Muqit, L. Stanyer, D. G. Healy, P. M. Abou-Sleiman, I. Hargreaves, S. Heales, M. Ganguly, L. Parsons, A. J. Lees, D. S. Latchman, J. L. Holton, N. W. Wood and T. Revesz (2006). "PINK1 protein in normal human brain and Parkinson's disease." Brain **129**: 1720-1731.

Gao, S., C. Alarcon, G. Sapkota, S. Rahman, P. Y. Chen, N. Goerner, M. J. Macias, H. Erdjument-Bromage, P. Tempst and J. Massague (2009). "Ubiquitin Ligase Nedd4L Targets Activated Smad2/3 to Limit TGF-beta Signaling." Molecular Cell **36**(3): 457-468.

Geisler, S., K. M. Holmstrom, A. Treis, D. Skujat, S. S. Weber, F. C. Fiesel, P. J. Kahle and W. Springer (2010). "The PINK1/Parkin-mediated mitophagy is compromised by PD-associated mutations." Autophagy **6**(7): 871-878.

Gilks, W. P., P. M. Abou-Sleiman, S. Gandhi, S. Jain, A. Singleton, A. J. Lees, K. Shaw, K. P. Bhatia, V. Bonifati, N. P. Quinn, J. Lynch, D. G. Healy, J. L. Holton, T. Revesz and N. W. Wood (2005). "A common LRRK2 mutation in idiopathic Parkinson's disease." Lancet **365**(9457): 415-416.

Gomez-Suaga, P., P. Rivero-Rios, E. Fdez, M. B. Ramirez, I. Ferrer, A. Aistui, A. L. De Munain and S. Hilfiker (2014). "LRRK2 delays degradative receptor trafficking by impeding late endosomal budding through decreasing Rab7 activity." Human Molecular Genetics **23**(25): 6779-6796.

Gonzalez-Robayna, I. J., A. E. Falender, S. Ochsner, G. L. Firestone and J. S. Richards (2000). "Follicle-stimulating hormone (FSH) stimulates phosphorylation and activation of protein kinase B (PKB/Akt) and serum and glucocorticoid-induced kinase (Sgk): Evidence for A kinase-independent signaling by FSH in granulosa cells." Molecular Endocrinology **14**(8): 1283-1300.

Grant, B. and D. Hirsh (1999). "Receptor-mediated endocytosis in the *Caenorhabditis elegans* oocyte." Mol Biol Cell **10**(12): 4311-4326.

Grant, B., Y. Zhang, M. C. Paupard, S. X. Lin, D. H. Hall and D. Hirsh (2001). "Evidence that RME-1, a conserved *C. elegans* EH-domain protein, functions in endocytic recycling." Nat Cell Biol **3**(6): 573-579.

Grant, B., Y. H. Zhang, M. C. Paupard, S. X. Lin, D. Hall and D. Hirsh (2001). "Evidence that RME-1, a conserved *C. elegans* EH-domain protein, functions in endocytic recycling." Nature Cell Biology **3**(6): 573-579.

Grant, B. D. and S. Caplan (2008). "Mechanisms of EHD/RME-1 protein function in endocytic transport." Traffic **9**(12): 2043-2052.

Grant, B. D. and J. G. Donaldson (2009). "Pathways and mechanisms of endocytic recycling." Nature Reviews Molecular Cell Biology **10**(9): 597-608.

Grant, B. D. and M. Sato (2006). "Intracellular trafficking." WormBook: 1-9.

Greene, J. C., A. J. Whitworth, I. Kuo, L. A. Andrews, M. B. Feany and L. J. Pallanck (2003). "Mitochondrial pathology and apoptotic muscle degeneration in *Drosophila parkin* mutants." Proceedings of the National Academy of Sciences of the United States of America **100**(7): 4078-4083.

Greggio, E., S. Jain, A. Kingsbury, R. Bandopadhyay, P. Lewis, A. Kaganovich, M. P. van der Brug, A. Beilina, J. Blackinton, K. J. Thomas, R. Ahmad, D. W. Miller, S. Kesavapany, A. Singleton, A. Lees, R. J. Harvey, K. Harvey and M. R. Cookson

(2006). "Kinase activity is required for the toxic effects of mutant LRRK2/dardarin." Neurobiology of Disease **23**(2): 329-341.

Guo, L. X., P. N. Gandhi, W. Wang, R. B. Petersen, A. L. Wilson-Delfosse and S. G. Chen (2007). "The Parkinson's disease-associated protein, leucine-rich repeat kinase 2 (LRRK2), is an authentic GTPase that stimulates kinase activity." Experimental Cell Research **313**(16): 3658-3670.

Halliday, J., P. Klenerman and E. Barnes (2011). "Vaccination for hepatitis C virus: closing in on an evasive target." Expert Review of Vaccines **10**(5): 659-672.

Haque, M. E., K. J. Thomas, C. D'Souza, S. Callaghan, T. Kitada, R. S. Slack, P. Fraser, M. R. Cookson, A. Tandon and D. S. Park (2008). "Cytoplasmic Pink1 activity protects neurons from dopaminergic neurotoxin MPTP." Proceedings of the National Academy of Sciences of the United States of America **105**(5): 1716-1721.

Hertweck, M., C. Gobel and R. Baumeister (2004). "C. elegans SGK-1 is the critical component in the Akt/PKB kinase complex to control stress response and life span." Developmental Cell **6**(4): 577-588.

Higashi, S., D. J. Moore, R. Yamamoto, M. Minegishi, K. Sato, T. Togo, O. Katsuse, H. Uchikado, Y. Furukawa, H. Hino, K. Kosaka, P. C. Emson, K. Wada, V. L. Dawson, T. M. Dawson, H. Arai and E. Iseki (2009). "Abnormal localization of leucine-rich repeat kinase 2 to the endosomal-lysosomal compartment in lewy body disease." J Neuropathol Exp Neurol **68**(9): 994-1005.

Holtz, W. A. and K. L. O'Malley (2003). "Parkinsonian mimetics induce aspects of unfolded protein response in death of dopaminergic neurons." Journal of Biological Chemistry **278**(21): 19367-19377.

Hong, G. Z., A. Lockhart, B. Davis, H. Rahmoune, S. Baker, L. Ye, P. Thompson, Y. P. Shou, K. O'Shaughnessy, P. Ronco and J. Brown (2003). "PPAR gamma activation enhances cell surface ENaC alpha via up-regulation of SGK1 in human collecting duct cells." Faseb Journal **17**(11): 1966-+.

Hutagalung, A. H. and P. J. Novick (2011). "Role of Rab GTPases in Membrane Traffic and Cell Physiology." Physiological Reviews **91**(1): 119-149.

Iaccarino, C., C. Crosio, C. Vitale, G. Sanna, M. T. Carrri and P. Barone (2007). "Apoptotic mechanisms in mutant LRRK2-mediated cell death." Human Molecular Genetics **16**(11): 1319-1326.

Ibanez, P., S. Lesage, E. Lohmann, S. Thobois, G. De Michele, M. Borg, Y. Agid, A. Durr, A. Brice and F. P. D. G. Study (2006). "Mutational analysis of the PINK1 gene in early-onset parkinsonism in Europe and North Africa." Brain **129**: 686-694.

Iwata, S., M. Nomoto, H. Morioka and A. Miyata (2004). "Gene expression profiling in the midbrain of striatal 6-hydroxydopamine-injected mice." Synapse **51**(4): 279-286.

Jacquier, N. and R. Schneiter (2010). "Ypk1, the yeast orthologue of the human serum- and glucocorticoid-induced kinase, is required for efficient uptake of fatty acids." Journal of Cell Science **123**(13): 2218-2227.

Jaleel, M., R. J. Nichols, M. Deak, D. G. Campbell, F. Gillardon, A. Knebel and D. R. Alessi (2007). "LRRK2 phosphorylates moesin at threonine-558: characterization of how Parkinson's disease mutants affect kinase activity." Biochemical Journal **405**: 307-317.

Kannan, N., N. Haste, S. S. Taylor and A. F. Neuwald (2007). "The hallmark of AGC kinase functional divergence is its C-terminal tail, a cis-acting regulatory module." Proceedings of the National Academy of Sciences of the United States of America **104**(4): 1272-1277.

Khan, N. L., S. Jain, J. M. Lynch, N. Pavese, P. Abou-Sleiman, J. L. Holton, D. G. Healy, W. P. Gilks, M. G. Sweeney, M. Ganguly, V. Gibbons, S. Gandhi, J. Vaughan, L. H. Eunson, R. Katzenschlager, J. Gayton, G. Lennox, T. Revesz, D. Nicholl, K. P. Bhatia, N. Quinn, D. Brooks, A. J. Lees, M. B. Davis, P. Piccini, A. B. Singleton and N. W. Wood (2005). "Mutations in the gene LRRK2 encoding dardarin (PARK8) cause familial Parkinson's disease: clinical, pathological, olfactory and functional imaging and genetic data." Brain **128**: 2786-2796.

Kitada, T., A. Pisani, D. R. Porter, H. Yamaguchi, A. Tscherter, G. Martella, P. Bonsi, C. Zhang, E. N. Pothos and J. Shen (2007). "Impaired dopamine release and synaptic plasticity in the striatum of PINK1-deficient mice." Proceedings of the National Academy of Sciences of the United States of America **104**(27): 11441-11446.

Klingel, K., S. Warntges, J. Bock, C. A. Wagner, M. Sauter, S. Waldegger, R. Kandolf and F. Lang (2000). "Expression of cell volume-regulated kinase h-sgk in pancreatic tissue." Am J Physiol Gastrointest Liver Physiol **279**(5): G998-G1002.

Kobayashi, T. and P. Cohen (1999). "Activation of serum- and glucocorticoid-regulated protein kinase by agonists that activate phosphatidylinositide 3-kinase is mediated by 3-phosphoinositide-dependent protein kinase-1 (PDK1) and PDK2." Biochemical Journal **339**: 319-328.

Kobayashi, T., M. Deak, N. Morrice and P. Cohen (1999). "Characterization of the structure and regulation of two novel isoforms of serum- and glucocorticoid-induced protein kinase." Biochemical Journal **344**: 189-197.

Lang, A. E. and A. M. Lozano (1998). "Parkinson's disease - Second of two parts." New England Journal of Medicine **339**(16): 1130-1143.

Lang, F., C. Bohmer, M. Palmada, G. Seeböhm, N. Strutz-Seeböhm and V. Vallon (2006). "(Patho)physiological significance of the serum- and glucocorticoid-inducible kinase isoforms." Physiological Reviews **86**(4): 1151-1178.

Leong, M. L., A. C. Maiyar, B. Kim, B. A. O'Keeffe and G. L. Firestone (2003). "Expression of the serum- and glucocorticoid-inducible protein kinase, Sgk, is a cell survival response to multiple types of environmental stress stimuli in mammary epithelial cells." J Biol Chem **278**(8): 5871-5882.

Leung, B., G. J. Hermann and J. R. Priess (1999). "Organogenesis of the *Caenorhabditis elegans* intestine." Dev Biol **216**(1): 114-134.

Lin, S. X., B. Grant, D. Hirsh and F. R. Maxfield (2001). "Rme-1 regulates the distribution and function of the endocytic recycling compartment in mammalian cells." Nat Cell Biol **3**(6): 567-572.

Liu, D., X. H. Yang and S. Y. Zhou (2000). "Identification of CISK, a new member of the SGK kinase family that promotes IL-3-dependent survival." Current Biology **10**(19): 1233-1236.

MacLeod, D., J. Dowman, R. Hammond, T. Leete, K. Inoue and A. Abeliovich (2006). "The familial Parkinsonism gene LRRK2 regulates neurite process morphology." Neuron **52**(4): 587-593.

MacLeod, D. A., H. Rhinn, T. Kuwahara, A. Zolin, G. Di Paolo, B. D. MacCabe, K. S. Marder, L. S. Honig, L. N. Clark, S. A. Small and A. Abeliovich (2013). "RAB7L1 Interacts with LRRK2 to Modify Intraneuronal Protein Sorting and Parkinson's Disease Risk." Neuron **77**(3): 425-439.

MacLeod, D. A., H. Rhinn, T. Kuwahara, A. Zolin, G. Di Paolo, B. D. McCabe, K. S. Marder, L. S. Honig, L. N. Clark, S. A. Small and A. Abeliovich (2013). "RAB7L1 Interacts with LRRK2 to Modify Intraneuronal Protein Sorting and Parkinson's Disease Risk (vol 77, pg 425, 2013)." Neuron **79**(1): 202-203.

Maiyar, A. C., A. J. Huang, P. T. Phu, H. H. Cha and G. L. Firestone (1996). "p53 stimulates promoter activity of the sgk serum/glucocorticoid-inducible serine/threonine protein kinase gene in rodent mammary epithelial cells." Journal of Biological Chemistry **271**(21): 12414-12422.

Mata, I. F., W. J. Wedemeyer, M. J. Farrer, J. P. Taylor and K. A. Gallo (2006). "LRRK2 in Parkinson's disease: protein domains and functional insights." Trends in Neurosciences **29**(5): 286-293.

Matsuda, N., S. Sato, K. Shiba, K. Okatsu, K. Saisho, C. A. Gautier, Y. Sou, S. Saiki, S. Kawajiri, F. Sato, M. Kimura, M. Komatsu, N. Hattori and K. Tanaka (2010). "PINK1 stabilized by mitochondrial depolarization recruits Parkin to damaged mitochondria and activates latent Parkin for mitophagy." Journal of Cell Biology **189**(2): 211-221.

Mayor, S. and R. E. Pagano (2007). "Pathways of clathrin-independent endocytosis." Nature Reviews Molecular Cell Biology **8**(8): 603-612.

McGhee, J. D., M. C. Sleumer, M. Bilenky, K. Wong, S. J. McKay, B. Goszczynski, H. Tian, N. D. Krich, J. Khattra, R. A. Holt, D. L. Baillie, Y. Kohara, M. A. Marra, S. J. Jones, D. G. Moerman and A. G. Robertson (2007). "The ELT-2 GATA-factor and the global regulation of transcription in the *C. elegans* intestine." Dev Biol **302**(2): 627-645.

McLelland, G. L., V. Soubannier, C. X. Chen, H. M. McBride and E. A. Fon (2014). "Parkin and PINK1 function in a vesicular trafficking pathway regulating mitochondrial quality control." Embo Journal **33**(4): 282-295.

Moore, D. J., A. B. West, V. L. Dawson and T. M. Dawson (2005). "Molecular pathophysiology of Parkinson's disease." Annual Review of Neuroscience **28**: 57-87.

Mukherjee, S., R. N. Ghosh and F. R. Maxfield (1997). "Endocytosis." Physiol Rev **77**(3): 759-803.

Muqit, M. M. K., P. M. Abou-Sleiman, A. T. Saurin, K. Harvey, S. Gandhi, E. Deas, S. Eaton, M. D. P. Smith, K. Venner, A. Matilla, D. G. Healy, W. P. Gilks, A. J. Lees, J. Holton, T. Revesz, P. J. Parker, R. J. Harvey, N. W. Wood and D. S. Latchman (2006). "Altered cleavage and localization of PINK1 to aggresomes in the presence of proteasomal stress." Journal of Neurochemistry **98**(1): 156-169.

Nakajima, T., T. Nimura, K. Yamaguchi, T. Ando, M. Itoh, T. Yoshimoto and R. Shirane (2003). "The impact of stereotactic pallidal surgery on the dopamine D(2) receptor in Parkinson disease: a positron emission tomography study." Journal of Neurosurgery **98**(1): 57-63.

Narendra, D. P., S. M. Jin, A. Tanaka, D. F. Suen, C. A. Gautier, J. Shen, M. R. Cookson and R. J. Youle (2010). "PINK1 Is Selectively Stabilized on Impaired Mitochondria to Activate Parkin." Plos Biology **8**(1).

Nishida, Y., T. Nagata, Y. Takahashi, M. Sugahara-Kobayashi, A. Murata and S. Asai (2004). "Alteration of serum/glucocorticoid regulated kinase-1 (sgk-1) gene expression in rat hippocampus after transient global ischemia." Brain Res Mol Brain Res **123**(1-2): 121-125.

Ozelius, L. J., G. Senthil, R. Saunders-Pullman, E. Ohmann, A. Deligtisch, M. Tagliati, A. L. Hunt, C. Klein, B. Henick, S. M. Hailpern, R. B. Lipton, J. Soto-Valencia, N. Risch and S. B. Bressman (2006). "LRRK2 G2019S as a cause of Parkinson's disease in Ashkenazi Jews." New England Journal of Medicine **354**(4): 424-425.

Paisan-Ruiz, C., S. Jain, E. W. Evans, W. P. Gilks, J. Simon, M. van der Brug, A. L. de Munain, S. Aparicio, A. M. Gil, N. Khan, J. Johnson, J. R. Martinez, D. Nicholl, I. M. Carrera, A. S. Pena, R. de Silva, A. Lees, J. F. Marti-Masso, J. Perez-Tur, N. W. Wood and A. B. Singleton (2004). "Cloning of the gene containing mutations that cause PARK8-linked Parkinson's disease." Neuron **44**(4): 595-600.

Park, J., S. B. Lee, S. Lee, Y. Kim, S. Song, S. Kim, E. Bae, J. Kim, M. H. Shong, J. M. Kim and J. K. Chung (2006). "Mitochondrial dysfunction in Drosophila PINK1 mutants is complemented by parkin." Nature **441**(7097): 1157-1161.

Park, J., M. L. L. Leong, P. Buse, A. C. Maiyar, G. L. Firestone and B. A. Hemmings (1999). "Serum and glucocorticoid-inducible kinase (SGK) is a target of the PI 3-kinase-stimulated signaling pathway." Embo Journal **18**(11): 3024-3033.

Pereira-Leal, J. B. and M. C. Seabra (2001). "Evolution of the Rab family of small GTP-binding proteins." J Mol Biol **313**(4): 889-901.

Perrett, R. M., Z. Alexopoulou and G. K. Tofaris (2015). "The endosomal pathway in Parkinson's disease." Mol Cell Neurosci.

Petit, A., T. Kawarai, E. Paitel, N. Sanjo, M. Maj, M. Scheid, F. S. Chen, Y. J. Gu, H. Hasegawa, S. Salehi-Rad, L. Wang, E. Rogaeva, P. Fraser, B. Robinson, P. St George-Hyslop and A. Tandon (2005). "Wild-type PINK1 prevents basal and induced

neuronal apoptosis, a protective effect abrogated by Parkinson disease-related mutations." Journal of Biological Chemistry **280**(40): 34025-34032.

Piccoli, G., S. B. Condliffe, M. Bauer, F. Giesert, K. Boldt, S. De Astis, A. Meixner, H. Sarioglu, D. M. Vogt-Weisenhorn, W. Wurst, C. J. Gloeckner, M. Matteoli, C. Sala and M. Ueffing (2011). "LRRK2 Controls Synaptic Vesicle Storage and Mobilization within the Recycling Pool." Journal of Neuroscience **31**(6): 2225-2237.

Pridgeon, J. W., J. A. Olzmann, L. S. Chin and L. Li (2007). "PINK1 protects against oxidative stress by phosphorylating mitochondrial chaperone TRAP1." Plos Biology **5**(7): 1494-1503.

Reddien, P. W. and H. R. Horvitz (2000). "CED-2/CrklI and CED-10/Rac control phagocytosis and cell migration in *Caenorhabditis elegans*." Nat Cell Biol **2**(3): 131-136.

Runkel, E. D., R. Baumeister and E. Schulze (2014). "Mitochondrial stress: Balancing friend and foe." Experimental Gerontology **56**: 194-201.

Ryu, E. J., H. P. Harding, J. M. Angelastro, O. V. Vitolo, D. Ron and L. A. Greene (2002). "Endoplasmic reticulum stress and the unfolded protein response in cellular models of Parkinson's disease." J Neurosci **22**(24): 10690-10698.

Sakaguchi-Nakashima, A., J. Y. Meir, Y. Jin, K. Matsumoto and N. Hisamoto (2007). "LRK-1, a *C. elegans* PARK8-Related kinase, regulates axonal-dendritic polarity of SV proteins." Current Biology **17**(7): 592-598.

Säman, J. (2008). LRK-1 and PINK-1 are antagonistically coupled to RhoG / Rac-GTPases in *Caenorhabditis elegans*. PhD thesis, ALBERT LUDWIGS UNIVERSITY OF FREIBURG.

Samann, J., J. Hegermann, E. von Gromoff, S. Eimer, R. Baumeister and E. Schmidt (2009). "*Caenorhabditis elegans* LRK-1 and PINK-1 act antagonistically in stress response and neurite outgrowth." J Biol Chem **284**(24): 16482-16491.

Sämann, J., J. Hegermann, E. von Gromoff, S. Eimer, R. Baumeister and E. Schmidt (2009). "*Caenorhabditis elegans* LRK-1 and PINK-1 Act Antagonistically in Stress Response and Neurite Outgrowth." Journal of Biological Chemistry **284**(24): 16482-16491.

Sanna, G., M. G. Del Giudice, C. Crosio and C. Iaccarino (2012). "LRRK2 and vesicle trafficking." Biochem Soc Trans **40**(5): 1117-1122.

Sato, M. and K. Sato (2013). "Dynamic Regulation of Autophagy and Endocytosis for Cell Remodeling During Early Development." Traffic **14**(5): 479-486.

Sato, M., K. Sato, P. Fonarev, C. J. Huang, W. Liou and B. D. Grant (2005). "*Caenorhabditis elegans* RME-6 is a novel regulator of RAB-5 at the clathrin-coated pit." Nature Cell Biology **7**(6): 559-U557.

Savage-Dunn, C. (2001). "Targets of TGF beta-related signaling in *Caenorhabditis elegans*." Cytokine & Growth Factor Reviews **12**(4): 305-312.

- Schoenebeck, B., V. Bader, X. R. Zhu, B. Schmitz, H. Lubbert and C. C. Stichel (2005). "Sgk1, a cell survival response in neurodegenerative diseases." Mol Cell Neurosci **30**(2): 249-264.
- Seaman, M. N. J. (2012). "The retromer complex - endosomal protein recycling and beyond." Journal of Cell Science **125**(20): 4693-4702.
- Seaman, M. N. J., J. M. McCaffery and S. D. Emr (1998). "A membrane coat complex essential for endosome-to-Golgi retrograde transport in yeast." Journal of Cell Biology **142**(3): 665-681.
- Shi, A., O. Liu, S. Koenig, R. Banerjee, C. C. Chen, S. Eimer and B. D. Grant (2012). "RAB-10-GTPase-mediated regulation of endosomal phosphatidylinositol-4,5-bisphosphate." Proc Natl Acad Sci U S A **109**(35): E2306-2315.
- Shin, N., H. Jeong, J. Kwon, H. Y. Heo, J. J. Kwon, H. J. Yun, C. H. Kim, B. S. Han, Y. Tong, J. Shen, T. Hatano, N. Hattori, K. S. Kim, S. Chang and W. Seol (2008). "LRRK2 regulates synaptic vesicle endocytosis." Exp Cell Res **314**(10): 2055-2065.
- Silvestri, L., V. Caputo, E. Bellacchio, L. Atorino, B. Dallapiccola, E. M. Valente and G. Casari (2005). "Mitochondrial import and enzymatic activity of PINK1 mutants associated to recessive parkinsonism." Human Molecular Genetics **14**(22): 3477-3492.
- Sim, C. H., D. S. S. Lio, S. S. Mok, C. L. Masters, A. F. Hill, J. G. Culvenor and H. C. Cheng (2006). "C-terminal truncation and Parkinson's disease-associated mutations down-regulate the protein serine/threonine kinase activity of PTEN-induced kinase-1." Human Molecular Genetics **15**(21): 3251-3262.
- Singleton, A. B., M. J. Farrer and V. Bonifati (2013). "The Genetics of Parkinson's Disease: Progress and Therapeutic Implications." Movement Disorders **28**(1): 14-23.
- Skinner, C. F. and M. N. J. Seaman (2009). "The Role of Retromer in Neurodegenerative Disease." Intracellular Traffic and Neurodegenerative Disorders: 125-140.
- Soubannier, V., G. L. McLelland, R. Zunino, E. Braschi, P. Rippstein, E. A. Fon and H. M. McBride (2012). "A Vesicular Transport Pathway Shuttles Cargo from Mitochondria to Lysosomes." Current Biology **22**(2): 135-141.
- Stichel, C. C., B. Schoenebeck, M. Foguet, B. Siebertz, V. Bader, X. R. Zhu and H. Lubbert (2005). "sgk1, a member of an RNA cluster associated with cell death in a model of Parkinson's disease." Eur J Neurosci **21**(2): 301-316.
- Sun, L., O. Liu, J. Desai, F. Karbassi, M. A. Sylvain, A. B. Shi, Z. Zhou, C. E. Rocheleau and B. D. Grant (2012). "CED-10/Rac1 Regulates Endocytic Recycling through the RAB-5 GAP TBC-2." Plos Genetics **8**(7).
- Tabara, H., A. Grishok and C. C. Mello (1998). "RNAi in C-elegans: Soaking in the genome sequence." Science **282**(5388): 430-431.

Takatori, S., G. Ito and T. Iwatsubo (2008). "Cytoplasmic localization and proteasomal degradation of N-terminally cleaved form of PINK1." Neuroscience Letters **430**(1): 13-17.

Talarmin, H., C. Rescan, S. Cariou, D. Glaise, G. Zanninelli, M. Bilodeau, P. Loyer, C. Guguen-Guillouzo and G. Baffet (1999). "The mitogen-activated protein kinase kinase/extracellular signal-regulated kinase cascade activation is a key signalling pathway involved in the regulation of G(1) phase progression in proliferating hepatocytes." Mol Cell Biol **19**(9): 6003-6011.

Tawara, T., T. Fukushima, N. Hojo, A. Isobe, K. Shiwaku, T. Setogawa and Y. Yamane (1996). "Effects of paraquat on mitochondrial electron transport system and catecholamine contents in rat brain." Archives of Toxicology **70**(9): 585-589.

Thayanidhi, N., J. R. Helm, D. C. Nycz, M. Bentley, Y. Liang and J. C. Hay (2010). "Alpha-synuclein delays endoplasmic reticulum (ER)-to-Golgi transport in mammalian cells by antagonizing ER/Golgi SNAREs." Mol Biol Cell **21**(11): 1850-1863.

Thomas, B. and M. F. Beal (2007). "Parkinson's disease." Human Molecular Genetics **16**: R183-R194.

Timmons, L. and A. Fire (1998). "Specific interference by ingested dsRNA." Nature **395**(6705): 854-854.

Turrens, J. F. (2003). "Mitochondrial formation of reactive oxygen species." Journal of Physiology-London **552**(2): 335-344.

Unoki, M. and Y. Nakamura (2001). "Growth-suppressive effects of BPOZ and EGR2, two genes involved in the PTEN signaling pathway." Oncogene **20**(33): 4457-4465.

Valente, E. M., P. M. Abou-Sleiman, V. Caputo, M. M. K. Muqit, K. Harvey, S. Gispert, Z. Ali, D. Del Turco, A. R. Bentivoglio, D. G. Healy, A. Albanese, R. Nussbaum, R. Gonzalez-Maldonado, T. Deller, S. Salvi, P. Cortelli, W. P. Gilks, D. S. Latchman, R. J. Harvey, B. Dallapiccola, G. Auburger and N. W. Wood (2004). "Hereditary early-onset Parkinson's disease caused by mutations in PINK1." Science **304**(5674): 1158-1160.

Vilarino-Guell, C., C. Wider, O. A. Ross, J. C. Dachselt, J. M. Kachergus, S. J. Lincoln, A. I. Soto-Ortolaza, S. A. Cobb, G. J. Wilhoite, J. A. Bacon, B. Behrouz, H. L. Melrose, E. Hentati, A. Puschmann, D. M. Evans, E. Conibear, W. W. Wasserman, J. O. Aasly, P. R. Burkhard, R. Djaldetti, J. Ghika, F. Hentati, A. Krygowska-Wajs, T. Lynch, E. Melamed, A. Rajput, A. H. Rajput, A. Solida, R. M. Wu, R. J. Uitti, Z. K. Wszolek, F. Vingerhoets and M. J. Farrer (2011). "VPS35 mutations in Parkinson disease." Am J Hum Genet **89**(1): 162-167.

Vives-Bauza, C., C. Zhou, Y. Huang, M. Cui, R. L. A. de Vries, J. Kim, J. May, M. A. Tocilescu, W. C. Liu, H. S. Ko, J. Magrane, D. J. Moore, V. L. Dawson, R. Grailhe, T. M. Dawson, C. J. Li, K. Tieu and S. Przedborski (2010). "PINK1-dependent recruitment of Parkin to mitochondria in mitophagy." Proceedings of the National Academy of Sciences of the United States of America **107**(1): 378-383.

- Waldegger, S., P. Barth, G. Raber and F. Lang (1997). "Cloning and characterization of a putative human serine/threonine protein kinase transcriptionally modified during anisotonic and isotonic alterations of cell volume." Proceedings of the National Academy of Sciences of the United States of America **94**(9): 4440-4445.
- Waldegger, S., K. Klingel, P. Barth, M. Sauter, M. Lanzendorfer, R. Kandolf and F. Lang (1999). "h-sgk serine-threonine protein kinase gene as transcriptional target of transforming growth factor beta in human intestine." Gastroenterology **116**(5): 1081-1088.
- Ward, S., D. J. Burke, J. E. Sulston, A. R. Coulson, D. G. Albertson, D. Ammons, M. Klass and E. Hogan (1988). "Genomic organization of major sperm protein genes and pseudogenes in the nematode *Caenorhabditis elegans*." J Mol Biol **199**(1): 1-13.
- Webster, M. K., L. Goya, Y. Ge, A. C. Maiyar and G. L. Firestone (1993). "Characterization of sgk, a novel member of the serine/threonine protein kinase gene family which is transcriptionally induced by glucocorticoids and serum." Mol Cell Biol **13**(4): 2031-2040.
- Weihofen, A., B. Ostaszewski, Y. Minami and D. J. Selkoe (2008). "Pink1 Parkinson mutations, the Cdc37/Hsp90 chaperones and Parkin all influence the maturation or subcellular distribution of Pink1." Human Molecular Genetics **17**(4): 602-616.
- Yang, Y. F., S. Gehrke, Y. Imai, Z. N. Huang, Y. Ouyang, J. W. Wang, L. C. Yang, M. F. Beal, H. Vogel and B. W. Lu (2006). "Mitochondrial pathology and muscle and dopaminergic neuron degeneration caused inactivation of *Drosophila* Pink1 is rescued by by Parkin." Proceedings of the National Academy of Sciences of the United States of America **103**(28): 10793-10798.
- Yun, C. C. (2003). "Concerted roles of SGK1 and the Na⁺/H⁺ exchanger regulatory factor 2 (NHERF2) in regulation of NHE3." Cell Physiol Biochem **13**(1): 29-40.
- Zerial, M. and H. McBride (2001). "Rab proteins as membrane organizers." Nat Rev Mol Cell Biol **2**(2): 107-117.
- Zhou, J. X., Y. Huang, J. P. Anderson, W. P. Gai, X. M. Wang and G. M. Halliday (2011). "Changes in the solubility and phosphorylation of alpha-synuclein over the course of Parkinson's disease." Movement Disorders **26**: S32-S32.
- Zimprich, A., A. Benet-Pages, W. Struhal, E. Graf, S. H. Eck, M. N. Offman, D. Haubenberger, S. Spielberger, E. C. Schulte, P. Lichtner, S. C. Rossle, N. Klopp, E. Wolf, K. Seppi, W. Pirker, S. Presslauer, B. Mollenhauer, R. Katzenschlager, T. Foki, C. Hotzy, E. Reinthaler, A. Harutyunyan, R. Kralovics, A. Peters, F. Zimprich, T. Brucke, W. Poewe, E. Auff, C. Trenkwalder, B. Rost, G. Ransmayr, J. Winkelmann, T. Meitinger and T. M. Strom (2011). "A mutation in VPS35, encoding a subunit of the retromer complex, causes late-onset Parkinson disease." Am J Hum Genet **89**(1): 168-175.